IGF-1-MEDIATED REINFORCEMENT OF THE BLOOD BRAIN BARRIER DURING ISCHEMIA-REPERFUSION IN MIDDLE-AGED FEMALE RATS

A Dissertation

by

ANDRE JOHNSON

Submitted to the Office of Graduate and Professional Studies of
Texas A&M University
in partial fulfillment of the requirements for the degree of

DOCTOR OF PHILOSOPHY

Chair of Committee,	Farida Sohrabji
Committee Members,	Jane Welsh
	Brad White
	Jianrong Li
Head of Program,	Warren Zimmer

May 2019

Major Subject: Medical Sciences

ABSTRACT

Nearly three quarters of all strokes occur in people over 65, and within this older group, strokes are more common and more severe in women than men. Added to this disease burden, is the lack of suitable therapies for stroke patients. My research focused on identifying a stroke therapy that is effective for older female stroke patients. Middle-aged female rats were used as a model system to understand disparities in stroke outcomes in middle-aged postmenopausal women. Our laboratory has shown previously that post-stroke Insulin like growth factor (IGF)-I treatment reduces blood brain barrier permeability and decreases infarct volumes in middle aged female rats. In three major experiments, this dissertation tested the hypothesis that IGF-1 acts on the endothelium to reduce neuroinflammation and improve recovery. Through Experiment 1, we found that IGF-1 treatment provided by intracerebroventricular injection, decreased extravasation of CD4+ cells into the ischemic hemisphere. Similarly, IGF-1 reduced protein transfer across a monolayer of brain microvessel endothelial cells derived from middle aged females, further implicating this cell type as the locus of IGF-1 action. Experiment 2 showed that IGF-1 stabilized the actin cytoskeleleton and adhesion of endothelial cells exposed to OGD and preserved microvessel diameter and length in vivo after stroke. Both in vivo and in vitro, IGF-1's effects were reversed with concurrent exposure to the IGFR antagonist JB-1. Additionally, while IGF-1 treatment improved microvessel morphology in early acute phase of stroke, sensory-motor behavior was improved during both the early and late acute phase of stroke. Experiment 3 tested the novel hypothesis

that IGF-1 secreted by astrocytes is neuroprotective. With age, astrocyte derived IGF-1 decreases, and by using IGF-1 gene transfer targeted to astrocytes, we found reduced stroke-induced sensory motor impairment and decreased blood brain barrier permeability, without affecting infarct volumes. Collectively, these data support and suggest that the aging endothelium and astrocyte interaction may be critical for post stroke recovery.

DEDICATION

I would like to dedicate this work to four women who have given me much more than one word can contain, but I will audaciously try:

To my mother, LaRonda Rue Alford—for life.

To my grandmother, Leola Alford—for love.

To my aunt, Theresa Alford-Moore—for hope.

To my mentor, Farida Sohrabji—for guidance.

ACKNOWLEDGEMENTS

I would like to thank my committee chair, Dr. Sohrabji, and my committee members, Dr. Welsh, Dr. White, and Dr. Li for their guidance and support throughout the course of this research.

Thanks also go to my friends and colleagues and the department faculty and staff for making my time at Texas A&M University a great experience.

Finally, thanks to my mother and my aunt for their encouragement and to my husband for his patience and love.

CONTRIBUTORS AND FUNDING SOURCES

Contributors

This work was supervised by a dissertation committee consisting of Professor Farida Sohrabji of the Department of Neuroscience and Experimental Therapeutics, Professor Jane Welsh of the Department of Veterinary Integrative Biosciences, Assistant Professor Jianrong Li of the Department of Veterinary Integrative Biosciences, and Associate Professor Brad White of the Department of Neuroscience and Experimental Therapeutics.

Assistance with data analysis for all studies was provided by Professor Farida Sohrabji. In the first study which was published in 2016, Chanell Dawson and Tiffany Heard provided technical assistance, and Professor Robert Alaniz assisted with experimental design. In the second study which was published in 2019, laboratory technicians Ms. Tiffany Heard, Mr. Victor Cardenas and Ms. Jessica Lee provided technical assistance and surgical and cell culture expertise was provided by Professor Shameena Bake. Professor Homa Khosravian assisted with experimental design in the second study as well. In the third study, which was published in 2017, surgical assistance was provided by Professor Shameena Bake. In addition, Graduate student Nihal Salem provided expert assistance with qRT-PCR. Graduate students Miriam Aceves and Mabel Terminal provided assistance with flow studies, and Post-doctoral fellow Min-Jung Park provided assistance with statistical analysis of cytokines.

All other work conducted for this dissertation was completed by the student independently.

Funding Sources

Graduate study was supported by a fellowship from Texas A&M University M.D./Ph.D program and a NS074895 from the NIH and a discovery grant.

TABLE OF CONTENTS

Page

LIST OF FIGURES

Page

LIST OF TABLES

Page

1. INTRODUCTION: STROKE

Stroke is a classically defined as a neurological deficient and/or dysfunction of vascular origin attributed to the acute focal injury of central nervous system (CNS) (Goldstein, Bertels, & Davis, 1989). In 2013, the American Heart Association expanded the definition to include acute injuries to the CNS caused by vascular deficiencies and/or dysfunctions that do not present clinically (Sacco et al., 2013). Center of Disease Control categorizes strokes into three types, ischemic, hemorrhage, and transient ischemic attack, with ischemic and hemorrhage being the most commonly documented (Go et al., 2014). For strokes that do present clinically, the common symptoms are dysphasia (difficulty swallowing), dysarthria (motor speech disorders), hemianopia (defective vision), weakness, ataxia (lack of muscle control), sensory loss, neglect, and, at worst, death (van der Worp & van Gijn, 2007). Ischemic stroke presents most commonly and occurs when the blood study to CNS is interrupted, temporarily or permanently, depriving cells of nutrients and oxygen (Hinkle & Guanci, 2007). This interruption leads to a cascade of cellular responses, including excretion of toxic excitatory amino acids, free-radical formation, and harmful inflammation (van der Worp & van Gijn, 2007). These events are thought to lead to CNS injury and death.

Ischemic stroke is a multifactorial disease, having both genetic and environment etiologies. Anatomically, the most appreciated causes of ischemic stroke are due to thrombi (obstruction of a blood vessel by a blood clots forming locally) and emboli (obstruction due to an embolus, unattached mass, from elsewhere in the body) occluding

small and large arteries (Hinkle & Guanci, 2007). The middle cerebral artery (MCA), the largest branch of the internal carotid artery, is the largest cerebral artery and the most commonly affected artery in stroke syndromes (Adams et al., 1996; Grotta, 1988). After onset, a central core, an area of low perfusion and high nutrition deprivation, develops and is surrounded by another area of higher perfusion and less metabolic disturbance known as the ischemia penumbra (Hinkle & Guanci, 2007). The size of infarction, tissue death, depends on the level of perfusion within the central core and penumbra and any perfusion changes that occur during recovery as the penumbra incorporates into the central core. The size and location of infarction has direct consequence on clinical outcomes and recovery. Overall, thirty-day case fatality rates for ischemic stroke generally range between 10 and 17% (Hinkle & Guanci, 2007). The survival and prognosis for stroke varies significantly with unmodifiable factors, such as income, race, age, and sex (Go et al., 2014).

1.1. The Burden of Stroke in the United States

Stroke is a fourth leading of death in the United States (U.S.). Though the stroke mortality rate decreased by 35% between 2001 and 2011 (Mozaffarian et. al., 2015; Rasmussen, 2015), stroke stills exacts a catastrophic toll on U.S. families and is a substantial U.S. financial health burden. Stroke causes approximately 1 out of every 20 deaths in the U.S. (Mozaffarian et. al., 2015) On average, every 4 minutes, 6 people in the U.S. will have a stroke, and of those 6 individuals, at least 1 of them will die (Mozaffarian et. al., 2015). It is projected that 1 in every 4 people in the U.S. will have a stroke in their lifetime (Sachdeva, Saeed, Jani, & Razak, 2016). For stroke survivors,

there is an almost certain chance of disability (Ovbiagele et al., 2013), and care is expensive. Immediate direct costs for non–nursing home stroke care constitute >10.7% of the Medicare budget and >1.7% of overall national health expenditures. However, the long-term care, which many patient require, including nursing home care costs more, and indirect costs of stroke care as premature death and lost productivity are greater than all direct costs combined (Ovbiagele et al., 2013). The emotional and psychological distress on families, care givers, health practitioners, and patients is uncalculatable but immense, and all these costs are projected to increase as the U.S. population ages (Sachdeva et al., 2016).

1.2. Unmodifiable Disparities in Stroke: Age; Sex; Race & Income

Young people rarely gets strokes (Onorato et al., 2003). Although the incidence of young stroke is increasing (Swerdel et al., 2016), adults between the ages of 15-44 only account for less than 10 percent of stroke (George, Tong, Kuklina, & Labarthe, 2011). Young adults (> 40 years old) tend to have better stroke outcomes (Nedeltchev et al., 2005). However, the effects of a young stroke can be long-lasting and debilitating, disrupting an individual's life course in its prime and leading to years of unemployment (M. Lawrence & Kinn, 2012; Maaijwee et al., 2014). As ages increases over 50, stroke outcomes get increase dire, increasing morbidity and mortality, and decreasing long-term quality-of-life. The influence of age is so striking it is used in several predictive models of stroke (Bejot et al., 2012; Counsell, Dennis, McDowall, & Warlow, 2002; Koennecke et al., 2011; Weimar et al., 2004).

Males and females respond differently to stroke depending largely but not solely on age (Lutfiyya, Ng, Asner, & Lipsky, 2009; Turtzo & McCullough, 2008). Women tend to have strokes at older ages compared to men when stroke outcomes are worse (Ahnstedt, McCullough, & Cipolla, 2016). After menopause (~51), women exhibit a sharp increases in stroke risk (Towfighi, Saver, Engelhardt, & Ovbiagele, 2007). Understanding the sex differences in stroke is confounded by age, since women have strokes later in life, however even after controlling for other unmodifiable factor, such as age, comorbidities, and stroke severity, women still have worse post-stroke clinical outcomes (Turtzo & McCullough, 2008).

More women die each year of stroke than men (Girijala, Sohrabji, & Bush, 2016). Overall, stroke is the fourth leading cause of death in U.S, but, for women, it is third; for men, the fifth (Sohrabji, Park, & Mahnke, 2017). Over their lifetime, women have an increased risk for stroke compared to men and women live longer (Dotson & Offner, 2017). Hence, there are more women stroke survivors than men (3.8 of the 6.8 million) (Spychala, Honarpisheh, & McCullough, 2017), and these women stroke survivors are more likely to need extensive care. Women are twice as likely as men to be discharged to long-term care upon hospital discharge, placing a disproportionate burden on the health care system (Turtzo & McCullough, 2008). Women are also more likely than men to report and experience depression after stroke, further complicating recovery (Turtzo & McCullough, 2008).

Investigating sex differences in stroke must involve biological, social, and political strategies since they are significant variations in stroke mortality and post-

stroke outcomes in women based solely on socioeconomic status and race (Albright et al., 2016). Black women for example have the worse post-stroke outcomes than any other groups of women (Albright et al., 2016).

There are major race disparities in stroke for Black Americans. Stroke mortality is two times higher for the black population (Centers for Disease & Prevention, 2005; Gaines & Burke, 1995; Horn, Deutscher, Smout, DeJong, & Putman, 2010). This population faces increased stroke morbidity and increased post-stroke complications compared to whites (Kittner et al., 1993). Despite having a higher prevalence within the community, Blacks, as a whole, have less understanding of stroke and its complications (Sharrief, Johnson, Abada, & Urrutia, 2016). The cause of these disparities are multifaceted, however socioeconomics plays a significant role in perpetuating this inequality. Blacks tend to have lower educational attainment, lower incomes, less degrees of social support, less health care access, and less trust of health care practitioners (Gaines & Burke, 1995; Howard et al., 2016; Kind et al., 2010). All these factors combine to create a perfect storm for stroke health inequality.

1.3. The Need for More Acute Interventions in Acute Stroke

Tissue plasminogen (tPA) is the gold standard care for acute ischemic stroke (Almasi, Razmeh, Habibi, & Rezaee, 2016; Anaissie et al., 2016). For two decades, since June 1996, U.S. physicians have used tPA as the sole recommended therapy for early-presenting acute stroke patient (Ciccone et al., 2013; Elgendy, Mahmoud, Mansoor, Mojadidi, & Bavry, 2016). tPA works by dissolving the clot and improving reperfusion. If given within its optimal time window, tPA significantly reduces mortality

and morbidity. Unfortunately, 4.5 hours after stroke onset, tPA's detriments outweigh its benefits and use is not recommended (Elgendy et al., 2016).

Beside short therapeutic window (>4.5 hours), tPA has other disadvantages, including increased risk of hemorrhage and a low rate of recanalization, re-opening of the occluded vessel (Elgendy et al., 2016). Initially, only 3-4% of stroke patients receive tPA due mostly to the short therapeutic window (de Los Rios la Rosa et al., 2012). Though, from 2003 -2011, its use has double (Lewandowski et al., 2015). But despite increased use, many eligible patients are not treated. But even they are lucky enough to receive tPA, half of these treated patients do not completely recover or die (Ciccone et al., 2013).

Acute stroke is also treated with endovascular procedures, however these procedures are more invasive and have strict criteria. Overall, most patients receive only palliative care and rehabilitation after a stroke (Ciccone et al., 2013). Because of the limited options for acute interventions, there are a strong drive to uncover for more effective stroke therapies, especially in populations affected disproportionately, such as women.

1.4. Animal Models for Stroke

To discover new therapies, researchers have relied heavily on animal models to mimic stroke pathology in the laboratory (Kumar, Aakriti, & Gupta, 2016). The use of these designed animals models is necessary to predict the efficacy, relevance, and toxicity of new therapeutics before human trials (Bacigaluppi, Comi, & Hermann, 2010; Durukan & Tatlisumak, 2009). Most researchers used rats and mice, however rabbits,

gerbils, cats, dogs, pigs and monkeys are used to provide a more thorough understanding of the stroke pathology and therapeutic efficiency (Kumar et al., 2016). No model is prefect, and each animal model offers its own advantages and disadvantages. Rats have a particular advantage in stroke research, due to their close resemblance with humans in vascular anatomy and physiology and availability of scientific reagents (Kumar et al., 2016). Changes in socialized, psychological, and tactile behaviors, which are extremely important in humans, are difficult to model in the rats (Yin, Guven, & Dietis, 2016). But, importantly, some unmodifiable factors, particularly sex and age, reflect the human condition (Liu & McCullough, 2011).

Female rats have been useful in studying women's age-related increase in stroke mortality (Koebele & Bimonte-Nelson, 2016). Like in humans, at mid-age, female rats undergo a hormonal and reproductive shift midlife that results in a loss of fertility (Gorodeski, 2000). Middle-aged (10-12 month old) female rats also have worse post-stroke outcomes in measured behavior and larger infarcts compared to the young adult (6-7 month old) female rats, mirroring the age-dependent worsening of clinical outcomes seen in women (Selvamani & Sohrabji, 2010b).

Initially, laboratory of this dissertation replaced estrogen in the acyclic middle-aged female rats. However, estrogen replacement was seen to be neurotoxic (Selvamani & Sohrabji, 2010a). In searching for hormones to provide as treatment, our laboratory uncovered neuroprotection effects of insulin-like growth factor (IGF)-1 as powerful neuro-protectant for aging women (Bake, Selvamani, Cherry, & Sohrabji, 2014).

1.5. Insulin-like Growth Factor & Stroke

Insulin-like growth factor-1 discovered in 1957, as an important hormone in child development, however the precise action of IGF-I wasn't appreciated until the 1980s will genetic recombination became a prominent force in the scientific world, leading to the creation of recombinant human IGF-I (Laron, 2001; Piotrowska et al., 2013).

IGF-1 is a single-chain 70 amino acids polypeptide which has three intramolecular disulfide bridge and is approximately 7.5 kilo Daltons (Daughaday, 1997). Most of the available IGF-1 is produced in the liver(Laron, 2004). Systemically, IGF-1 is carried, like many hormones, on binding proteins (IGF-BP), specifically IGFBP-3 carries most of the IGF-1 in the blood at a 1:1 ratio (Ranke, 2015). IGF-1 has always been associated with growth. For example, in humans, IGF-1 levels reaches its peak during puberty, a period of high physical growth (Soliman, De Sanctis, Elalaily, & Bedair, 2014). The main symptom of IGF-1 deficiency, clinically known as Laron deficiency, is short statue (Laron, Lilos, & Klinger, 1993). The main treatment for Laron deficiency is IGF-1 replacement, thus highlighting the important of IGF-1 in growth (Puche & Castilla-Cortazar, 2012).

IGF-1 and its receptor, IGF-1R, are implicated in the regulation of protein turnover and exert potent mitogenic, differentiating effects in cells (Laviola, Natalicchio, & Giorgino, 2007). IGF-1 binds at high affinity to IGF-1R, which is a cell surface receptor and at low affinity of insulin reception, which has a high homology to IGF-1R (M. C. Lawrence, McKern, & Ward, 2007). However, most of the IGF-1's observed

effects, such as cell growth, differentiation, and survival, are mediated through the IGF-1 receptor signaling (Delafontaine, Song, & Li, 2004).

IGF-1R activates small G-protein Ras, which in turn activates Raf and extracellular-signal-regulated kinase (ERK) kinase (Mendoza, Er, & Blenis, 2011). This pathway is coupled to transcription and mitogenic factors (Kiessling & Rogler, 2015). Additionally, IGF-1R has been linked the MAP kinase cascade, Jnk-1 and -2 cascade, and p38 MAP kinase, which also has a role in survival (Latres et al., 2005). Insulin-like growth factor 1 and the insulin pathways closely related in terms of biological activity and primary sequence (M. C. Lawrence et al., 2007; Xu & Messina, 2009).

When Peter Gluckman published his findings in the early 1990s that exogenous IGF-1 is neuroprotective in hypoxia-ischemic conditions, it was also known the insulin offered some neuroprotection at high levels (Gluckman et al., 1992). IGF-1, however, exerts its functions of cell growth and development, cell survival, learning and memory on the IGF-1 receptor (IGF-1R) (Guan, Bennet, Gluckman, & Gunn, 2003; Zhang, Jiang, & Meng, 2015). The neuroprotection offered by insulin is now believed to be due to insulin's promiscuity on IGF-1R (Duarte, Santos, Oliveira, & Rego, 2005; Duarte, Santos, Oliveira, Santos, & Rego, 2008). IGFs were first known as "sulfation factors" because they were first defined by their involvement in cartilage sulfation; this name then changed to the somatomedins due to their ability to mediate growth hormone actions (Haddad, 1967).

In the brain, IGF-1 activates canonical PI3K-Akt and Ras-Raf-MAP pathways in several cell types and is produced in all major CNS cell types in the cortex,

hippocampus, cerebellum, and hypothalamus(Dyer, Vahdatpour, Sanfeliu, & Tropea, 2016). IGF-1 has consequential importance in neurogenesis, neuroplasticity, neurodevelopment, and neuro-degenerative disease (Guan & Gluckman, 2009). IGF-1 reduces cell loss and improves long-term neurological function and IGF-1 signaling dysfunction has been linked to several models of neurodegeneration, such as a diabetic peripheral neuropathy (DPN) (Rauskolb, Dombert, & Sendtner, 2017), Alzheimer's (AD) (Vidal et al., 2016), Parkinson's (PD) (Bernhard et al., 2016), and Huntington's diseases (HD) (Humbert et al., 2002).

IGF-1 availability decreases with age (D. K. Lewis, Bake, Thomas, Jezierski, & Sohrabji, 2010; Selvamani & Sohrabji, 2010a). Though the cause of the decline of IGF-1 secretion over an organism's lifespan is unknown (Arvat, Broglio, & Ghigo, 2000; Muller et al., 2012). Decreases in growth hormone pulses over an organism's lifespan may cause the decrease in IGF-1 secretion (A. L. Lewis et al., 2015; Owens, Johnson, Campbell, & Ballard, 1990). The age-related reduction in spontaneous and GHRH-induced GH secretion pulses reflect age-related changes in neurotransmitter control (Ghigo et al., 2000). Low IGF-1 levels have neuropathological consequences and have been correlated with frailty and decreases in cognitive abilities (Vidal et al., 2016).

Unfortunately, IGF-1 levels decrease with age, the incidence of stroke increases (Bake et al., 2014; Selvamani & Sohrabji, 2010a). Some studies report low IGF-1 availability as an independent risk factor for stroke. IGF-1's neuroprotective properties have been witnessed in a number of male animal models, showcasing that administration of IGF-1 post-stroke in male rats up to 6 hours after ischemia yielded a time dependent

reduction of infarct volume. The sooner after the MCAo that IGF-1 is given the greater the effect. However, gene transfer in gerbils also demonstrated increased survival and recovery when the transfer occurred 30 min after ischemia using the Sendai virus. Using the aging female model, the laboratory had shown that IGF-1 decreases the amount of Evans blue dye extravasation into the brain, as well as cause a global decrease of both pro- and anti-inflammatory cytokines and chemokines (Bake et al., 2014). After microRNA profiling, putative gene targets associated with extracellular matrix, survival pathways, and blood-brain barrier/endothelial function has been implicated in IGF-1 treatment post-stroke (Bake et al., 2014). Taken together, the downstream effects of IGF-1 signaling strongly suggests a strengthening of the blood brain barrier as its mechanism of action.

The research presented here will analyze the neuroprotective effect of IGF-1 on the blood brain barrier in a stroke model on aging females.

1.6. References

Adams, H. P., Jr., Brott, T. G., Furlan, A. J., Gomez, C. R., Grotta, J., Helgason, C. M., Thies, W. (1996). Guidelines for thrombolytic therapy for acute stroke: a supplement to the guidelines for the management of patients with acute ischemic stroke. A statement for healthcare professionals from a Special Writing Group of the Stroke Council, American Heart Association. *Circulation, 94*(5), 1167-1174.

Ahnstedt, H., McCullough, L. D., & Cipolla, M. J. (2016). The Importance of Considering Sex Differences in Translational Stroke Research. *Transl Stroke Res, 7*(4), 261-273. doi:10.1007/s12975-016-0450-1

Albright, K. C., Boehme, A. K., Tanner, R. M., Blackburn, J., Howard, G., Howard, V. J., Limdi, N. (2016). Addressing Stroke Risk Factors in Black and White Americans: Findings from the National Health and Nutrition Examination Survey, 2009-2010. *Ethn Dis, 26*(1), 9-16. doi:10.18865/ed.26.1.9

Almasi, M., Razmeh, S., Habibi, A. H., & Rezaee, A. H. (2016). Does Intravenous Administration of Recombinant Tissue Plasminogen Activator for Ischemic Stroke can Cause Inferior Myocardial Infarction? *Neurol Int, 8*(2), 6617. doi:10.4081/ni.2016.6617

Anaissie, J. E., Monlezun, D. J., Siegler, J. E., Waring, E. D., Dowell, L. N., Samai, A. A., Martin-Schild, S. (2016). Intravenous Tissue Plasminogen Activator for Wake-Up

Stroke: A Propensity Score-Matched Analysis. *J Stroke Cerebrovasc Dis*. doi:10.1016/j.jstrokecerebrovasdis.2016.06.044

Arvat, E., Broglio, F., & Ghigo, E. (2000). Insulin-Like growth factor I: implications in aging. *Drugs Aging, 16*(1), 29-40.

Bacigaluppi, M., Comi, G., & Hermann, D. M. (2010). Animal models of ischemic stroke. Part two: modeling cerebral ischemia. *Open Neurol J, 4*, 34-38. doi:10.2174/1874205X01004020034

Bake, S., Selvamani, A., Cherry, J., & Sohrabji, F. (2014). Blood brain barrier and neuroinflammation are critical targets of IGF-1-mediated neuroprotection in stroke for middle-aged female rats. *PLoS One, 9*(3), e91427. doi:10.1371/journal.pone.0091427

Bejot, Y., Troisgros, O., Gremeaux, V., Lucas, B., Jacquin, A., Khoumri, C., Giroud, M. (2012). Poststroke disposition and associated factors in a population-based study: the Dijon Stroke Registry. *Stroke, 43*(8), 2071-2077.

Bernhard, F. P., Heinzel, S., Binder, G., Weber, K., Apel, A., Roeben, B., Berg, D. (2016). Insulin-Like Growth Factor 1 (IGF-1) in Parkinson's Disease: Potential as Trait-, Progression- and Prediction Marker and Confounding Factors. *PLoS One, 11*(3), e0150552. doi:10.1371/journal.pone.0150552

Centers for Disease, C., & Prevention. (2005). Differences in disability among black and white stroke survivors--United States, 2000-2001. *MMWR Morb Mortal Wkly Rep, 54*(1), 3-6.

Ciccone, A., Valvassori, L., Nichelatti, M., Sgoifo, A., Ponzio, M., Sterzi, R., . . . Investigators, S. E. (2013). Endovascular treatment for acute ischemic stroke. *N Engl J Med, 368*(10), 904-913. doi:10.1056/NEJMoa1213701

Counsell, C., Dennis, M., McDowall, M., & Warlow, C. (2002). Predicting outcome after acute and subacute stroke: development and validation of new prognostic models. *Stroke, 33*(4), 1041-1047.

Daughaday, W. H. (1997). Sulfation factor revisited: the one-two punch of insulin-like growth factor-I action on cartilage. *J Lab Clin Med, 129*(4), 398-399.

de Los Rios la Rosa, F., Khoury, J., Kissela, B. M., Flaherty, M. L., Alwell, K., Moomaw, C. J., Kleindorfer, D. O. (2012). Eligibility for Intravenous Recombinant Tissue-Type Plasminogen Activator Within a Population: The Effect of the European Cooperative Acute Stroke Study (ECASS) III Trial. *Stroke, 43*(6), 1591-1595. doi:10.1161/STROKEAHA.111.645986

Delafontaine, P., Song, Y. H., & Li, Y. (2004). Expression, regulation, and function of IGF-1, IGF-1R, and IGF-1 binding proteins in blood vessels. *Arterioscler Thromb Vasc Biol*, *24*(3), 435-444. doi:10.1161/01.ATV.0000105902.89459.09

Dotson, A. L., & Offner, H. (2017). Sex differences in the immune response to experimental stroke: Implications for translational research. *J Neurosci Res*, *95*(1-2), 437-446. doi:10.1002/jnr.23784

Duarte, A. I., Santos, M. S., Oliveira, C. R., & Rego, A. C. (2005). Insulin neuroprotection against oxidative stress in cortical neurons--involvement of uric acid and glutathione antioxidant defenses. *Free Radic Biol Med*, *39*(7), 876-889. doi:10.1016/j.freeradbiomed.2005.05.002

Duarte, A. I., Santos, P., Oliveira, C. R., Santos, M. S., & Rego, A. C. (2008). Insulin neuroprotection against oxidative stress is mediated by Akt and GSK-3beta signaling pathways and changes in protein expression. *Biochim Biophys Acta*, *1783*(6), 994-1002. doi:10.1016/j.bbamcr.2008.02.016

Durukan, A., & Tatlisumak, T. (2009). Animal models of ischemic stroke. *Handb Clin Neurol*, *92*, 43-66. doi:10.1016/S0072-9752(08)01903-9

Dyer, A. H., Vahdatpour, C., Sanfeliu, A., & Tropea, D. (2016). The role of Insulin-Like Growth Factor 1 (IGF-1) in brain development, maturation and neuroplasticity. *Neuroscience, 325*, 89-99. doi:10.1016/j.neuroscience.2016.03.056

Elgendy, I. Y., Mahmoud, A. N., Mansoor, H., Mojadidi, M. K., & Bavry, A. A. (2016). Evolution of acute ischemic stroke therapy from lysis to thrombectomy: Similar or different to acute myocardial infarction? *Int J Cardiol, 222*, 441-447. doi:10.1016/j.ijcard.2016.07.251

Gaines, K., & Burke, G. (1995). Ethnic differences in stroke: black-white differences in the United States population. SECORDS Investigators. Southeastern Consortium on Racial Differences in Stroke. *Neuroepidemiology, 14*(5), 209-239.

George, M. G., Tong, X., Kuklina, E. V., & Labarthe, D. R. (2011). Trends in stroke hospitalizations and associated risk factors among children and young adults, 1995-2008. *Ann Neurol, 70*(5), 713-721. doi:10.1002/ana.22539

Ghigo, E., Arvat, E., Gianotti, L., Lanfranco, F., Broglio, F., Aimaretti, G., Camanni, F. (2000). Hypothalamic growth hormone-insulin-like growth factor-I axis across the human life span. *J Pediatr Endocrinol Metab, 13 Suppl 6*, 1493-1502.

Girijala, R. L., Sohrabji, F., & Bush, R. L. (2016). Sex differences in stroke: Review of current knowledge and evidence. *Vasc Med*. doi:10.1177/1358863X16668263

Gluckman, P., Klempt, N., Guan, J., Mallard, C., Sirimanne, E., Dragunow, M., Nikolics, K. (1992). A role for IGF-1 in the rescue of CNS neurons following hypoxic-ischemic injury. *Biochem Biophys Res Commun, 182*(2), 593-599.

Go, A. S., Mozaffarian, D., Roger, V. L., Benjamin, E. J., Berry, J. D., Blaha, M. J., Stroke Statistics, S. (2014). Heart disease and stroke statistics--2014 update: a report from the American Heart Association. *Circulation, 129*(3), e28-e292. doi:10.1161/01.cir.0000441139.02102.80

Goldstein, L. B., Bertels, C., & Davis, J. N. (1989). Interrater reliability of the NIH stroke scale. *Arch Neurol, 46*(6), 660-662.

Gorodeski, G. I. (2000). Nonprimate animal models of menopause: workshop report. *Menopause, 7*(1), 1-2.

Grotta, J. C. (1988). Post-stroke management concerns and outcomes. *Geriatrics, 43*(7), 40-48.

Guan, J., Bennet, L., Gluckman, P. D., & Gunn, A. J. (2003). Insulin-like growth factor-1 and post-ischemic brain injury. *Prog Neurobiol, 70*(6), 443-462.

Guan, J., & Gluckman, P. D. (2009). IGF-1 derived small neuropeptides and analogues: a novel strategy for the development of pharmaceuticals for neurological conditions. *Br J Pharmacol, 157*(6), 881-891. doi:10.1111/j.1476-5381.2009.00256.x

Haddad, H. M. (1967). Humoral factors in endocrine exophthalmos: the sulfation factors. *Surv Ophthalmol, 12*(1), 1-11.

Hinkle, J. L., & Guanci, M. M. (2007). Acute ischemic stroke review. *J Neurosci Nurs, 39*(5), 285-293, 310.

Horn, S. D., Deutscher, D., Smout, R. J., DeJong, G., & Putman, K. (2010). Black-white differences in patient characteristics, treatments, and outcomes in inpatient stroke rehabilitation. *Arch Phys Med Rehabil, 91*(11), 1712-1721. doi:10.1016/j.apmr.2010.04.013

Howard, G., Moy, C. S., Howard, V. J., McClure, L. A., Kleindorfer, D. O., Kissela, B. M., Investigators, R. (2016). Where to Focus Efforts to Reduce the Black-White Disparity in Stroke Mortality: Incidence Versus Case Fatality? *Stroke, 47*(7), 1893-1898. doi:10.1161/STROKEAHA.115.012631

Humbert, S., Bryson, E. A., Cordelieres, F. P., Connors, N. C., Datta, S. R., Finkbeiner, S., Saudou, F. (2002). The IGF-1/Akt pathway is neuroprotective in Huntington's disease and involves Huntingtin phosphorylation by Akt. *Dev Cell, 2*(6), 831-837.

Kiessling, M. K., & Rogler, G. (2015). Targeting the RAS pathway by mitogen-activated protein kinase inhibitors. *Swiss Med Wkly, 145*, w14207. doi:10.4414/smw.2015.14207

Kind, A. J., Smith, M. A., Liou, J. I., Pandhi, N., Frytak, J. R., & Finch, M. D. (2010). Discharge destination's effect on bounce-back risk in Black, White, and Hispanic acute ischemic stroke patients. *Arch Phys Med Rehabil, 91*(2), 189-195. doi:10.1016/j.apmr.2009.10.015

Kittner, S. J., McCarter, R. J., Sherwin, R. W., Sloan, M. A., Stern, B. J., Johnson, C. J., Price, T. R. (1993). Black-white differences in stroke risk among young adults. *Stroke, 24*(12 Suppl), I13-15; discussion I20-11.

Koebele, S. V., & Bimonte-Nelson, H. A. (2016). Modeling menopause: The utility of rodents in translational behavioral endocrinology research. *Maturitas, 87*, 5-17. doi:10.1016/j.maturitas.2016.01.015

Koennecke, H. C., Belz, W., Berfelde, D., Endres, M., Fitzek, S., Hamilton, F., Berlin Stroke Register, I. (2011). Factors influencing in-hospital mortality and morbidity in patients treated on a stroke unit. *Neurology, 77*(10), 965-972. doi:10.1212/WNL.0b013e31822dc795

Kumar, A., Aakriti, & Gupta, V. (2016). A review on animal models of stroke: An update. *Brain Res Bull, 122*, 35-44. doi:10.1016/j.brainresbull.2016.02.016

Laron, Z. (2001). Insulin-like growth factor 1 (IGF-1): a growth hormone. *Mol Pathol, 54*(5), 311-316.

Laron, Z. (2004). IGF-1 and insulin as growth hormones. *Novartis Found Symp, 262*, 56-77; discussion 77-83, 265-268.

Laron, Z., Lilos, P., & Klinger, B. (1993). Growth curves for Laron syndrome. *Arch Dis Child, 68*(6), 768-770.

Latres, E., Amini, A. R., Amini, A. A., Griffiths, J., Martin, F. J., Wei, Y., . . . Glass, D. J. (2005). Insulin-like growth factor-1 (IGF-1) inversely regulates atrophy-induced genes via the phosphatidylinositol 3-kinase/Akt/mammalian target of rapamycin (PI3K/Akt/mTOR) pathway. *J Biol Chem, 280*(4), 2737-2744. doi:10.1074/jbc.M407517200

Laviola, L., Natalicchio, A., & Giorgino, F. (2007). The IGF-I signaling pathway. *Curr Pharm Des, 13*(7), 663-669.

Lawrence, M., & Kinn, S. (2012). Determining the needs, priorities, and desired rehabilitation outcomes of young adults who have had a stroke. *Rehabil Res Pract, 2012*, 963978. doi:10.1155/2012/963978

Lawrence, M. C., McKern, N. M., & Ward, C. W. (2007). Insulin receptor structure and its implications for the IGF-1 receptor. *Curr Opin Struct Biol, 17*(6), 699-705. doi:10.1016/j.sbi.2007.07.007

Lewandowski, C., Mays-Wilson, K., Miller, J., Penstone, P., Miller, D. J., Bakoulas, K., & Mitsias, P. (2015). Safety and outcomes in stroke mimics after intravenous tissue plasminogen activator administration: a single-center experience. *J Stroke Cerebrovasc Dis, 24*(1), 48-52. doi:10.1016/j.jstrokecerebrovasdis.2014.07.048

Lewis, A. L., Jordan, F., Patel, T., Jeffery, K., King, G., Savage, M., Illum, L. (2015). Intranasal Human Growth Hormone (hGH) Induces IGF-1 Levels Comparable With Subcutaneous Injection With Lower Systemic Exposure to hGH in Healthy Volunteers. *J Clin Endocrinol Metab, 100*(11), 4364-4371. doi:10.1210/jc.2014-4146

Lewis, D. K., Bake, S., Thomas, K., Jezierski, M. K., & Sohrabji, F. (2010). A high cholesterol diet elevates hippocampal cytokine expression in an age and estrogen-dependent manner in female rats. *J Neuroimmunol, 223*(1-2), 31-38. doi:10.1016/j.jneuroim.2010.03.024

Liu, F., & McCullough, L. D. (2011). Middle cerebral artery occlusion model in rodents: methods and potential pitfalls. *J Biomed Biotechnol, 2011*, 464701. doi:10.1155/2011/464701

Lutfiyya, M. N., Ng, L., Asner, N., & Lipsky, M. S. (2009). Disparities in stroke symptomology knowledge among US midlife women: an analysis of population survey data. *J Stroke Cerebrovasc Dis, 18*(2), 150-157.

Maaijwee, N. A., Rutten-Jacobs, L. C., Arntz, R. M., Schaapsmeerders, P., Schoonderwaldt, H. C., van Dijk, E. J., & de Leeuw, F. E. (2014). Long-term increased risk of unemployment after young stroke: a long-term follow-up study. *Neurology, 83*(13), 1132-1138. doi:10.1212/WNL.0000000000000817

Mendoza, M. C., Er, E. E., & Blenis, J. (2011). The Ras-ERK and PI3K-mTOR pathways: cross-talk and compensation. *Trends Biochem Sci, 36*(6), 320-328. doi:10.1016/j.tibs.2011.03.006

Mozaffarian, D., Benjamin, E. J., Go, A. S., Arnett, D. K., Blaha, M. J., Cushman, M., . . . Stroke Statistics, S. (2015). Heart disease and stroke statistics--2015 update: a report from the American Heart Association. *Circulation, 131*(4), e29-322. doi:10.1161/CIR.0000000000000152

Muller, A. P., Fernandez, A. M., Haas, C., Zimmer, E., Portela, L. V., & Torres-Aleman, I. (2012). Reduced brain insulin-like growth factor I function during aging. *Mol Cell Neurosci, 49*(1), 9-12. doi:10.1016/j.mcn.2011.07.008

Nedeltchev, K., der Maur, T. A., Georgiadis, D., Arnold, M., Caso, V., Mattle, H. P., Baumgartner, R. W. (2005). Ischaemic stroke in young adults: predictors of outcome and recurrence. *J Neurol Neurosurg Psychiatry, 76*(2), 191-195. doi:10.1136/jnnp.2004.040543

Onorato, E., Melzi, G., Casilli, F., Pedon, L., Rigatelli, G., Carrozza, A., . . . Anzola, G. P. (2003). Patent foramen ovale with paradoxical embolism: mid-term results of transcatheter closure in 256 patients. *J Interv Cardiol, 16*(1), 43-50.

Ovbiagele, B., Goldstein, L. B., Higashida, R. T., Howard, V. J., Johnston, S. C., Khavjou, O. A., Stroke, C. (2013). Forecasting the future of stroke in the United States: a policy statement from the American Heart Association and American Stroke Association. *Stroke, 44*(8), 2361-2375. doi:10.1161/STR.0b013e31829734f2

Owens, P. C., Johnson, R. J., Campbell, R. G., & Ballard, F. J. (1990). Growth hormone increases insulin-like growth factor-I (IGF-I) and decreases IGF-II in plasma of growing pigs. *J Endocrinol, 124*(2), 269-275.

Piotrowska, K., Borkowska, S. J., Wiszniewska, B., Laszczynska, M., Sluczanowska-Glabowska, S., Havens, A. M., Ratajczak, M. Z. (2013). The effect of low and high plasma levels of insulin-like growth factor-1 (IGF-1) on the morphology of major organs: studies of Laron dwarf and bovine growth hormone transgenic (bGHTg) mice. *Histol Histopathol, 28*(10), 1325-1336. doi:10.14670/HH-28.1325

Puche, J. E., & Castilla-Cortazar, I. (2012). Human conditions of insulin-like growth factor-I (IGF-I) deficiency. *J Transl Med, 10*, 224. doi:10.1186/1479-5876-10-224

Ranke, M. B. (2015). Insulin-like growth factor binding-protein-3 (IGFBP-3). *Best Pract Res Clin Endocrinol Metab, 29*(5), 701-711. doi:10.1016/j.beem.2015.06.003

Rasmussen, P. A. (2015). Stroke management and the impact of mobile stroke treatment units. *Cleve Clin J Med, 82*(12 Suppl 2), S17-21. doi:10.3949/ccjm.82.s2.04

Rauskolb, S., Dombert, B., & Sendtner, M. (2017). Insulin-like growth factor 1 in diabetic neuropathy and amyotrophic lateral sclerosis. *Neurobiol Dis, 97*(Pt B), 103-113. doi:10.1016/j.nbd.2016.04.007

Sacco, R. L., Kasner, S. E., Broderick, J. P., Caplan, L. R., Connors, J. J., Culebras, A., Metabolism. (2013). An updated definition of stroke for the 21st century: a statement for healthcare professionals from the American Heart Association/American Stroke Association. *Stroke, 44*(7), 2064-2089. doi:10.1161/STR.0b013e318296aeca

Sachdeva, G., Saeed, A., Jani, V., & Razak, A. (2016). Radiological Portrait of Embolic Strokes. *Cardiol Clin, 34*(2), 269-278. doi:10.1016/j.ccl.2015.12.008

Selvamani, A., & Sohrabji, F. (2010a). The neurotoxic effects of estrogen on ischemic stroke in older female rats is associated with age-dependent loss of insulin-like growth factor-1. *J Neurosci, 30*(20), 6852-6861. doi:10.1523/JNEUROSCI.0761-10.2010

Selvamani, A., & Sohrabji, F. (2010b). Reproductive age modulates the impact of focal ischemia on the forebrain as well as the effects of estrogen treatment in female rats. *Neurobiol Aging, 31*(9), 1618-1628. doi:10.1016/j.neurobiolaging.2008.08.014

Sharrief, A. Z., Johnson, B., Abada, S., & Urrutia, V. C. (2016). Stroke Knowledge in African Americans: A Narrative Review. *Ethn Dis, 26*(2), 255-262. doi:10.18865/ed.26.2.255

Sohrabji, F., Park, M. J., & Mahnke, A. H. (2017). Sex differences in stroke therapies. *J Neurosci Res, 95*(1-2), 681-691. doi:10.1002/jnr.23855

Soliman, A., De Sanctis, V., Elalaily, R., & Bedair, S. (2014). Advances in pubertal growth and factors influencing it: Can we increase pubertal growth? *Indian J Endocrinol Metab, 18*(Suppl 1), S53-62. doi:10.4103/2230-8210.145075

Spychala, M. S., Honarpisheh, P., & McCullough, L. D. (2017). Sex differences in neuroinflammation and neuroprotection in ischemic stroke. *J Neurosci Res, 95*(1-2), 462-471. doi:10.1002/jnr.23962

Swerdel, J. N., Rhoads, G. G., Cheng, J. Q., Cosgrove, N. M., Moreyra, A. E., Kostis, J. B., Myocardial Infarction Data Acquisition System Study, G. (2016). Ischemic Stroke Rate Increases in Young Adults: Evidence for a Generational Effect? *J Am Heart Assoc, 5*(12). doi:10.1161/JAHA.116.004245

Towfighi, A., Saver, J. L., Engelhardt, R., & Ovbiagele, B. (2007). A midlife stroke surge among women in the United States. *Neurology, 69*(20), 1898-1904. doi:10.1212/01.wnl.0000268491.89956.c2

Turtzo, L. C., & McCullough, L. D. (2008). Sex differences in stroke. *Cerebrovasc Dis, 26*(5), 462-474. doi:10.1159/000155983

van der Worp, H. B., & van Gijn, J. (2007). Clinical practice. Acute ischemic stroke. *N Engl J Med, 357*(6), 572-579. doi:10.1056/NEJMcp072057

Vidal, J. S., Hanon, O., Funalot, B., Brunel, N., Viollet, C., Rigaud, A. S., . . . Duron, E. (2016). Low Serum Insulin-Like Growth Factor-I Predicts Cognitive Decline in Alzheimer's Disease. *J Alzheimers Dis, 52*(2), 641-649. doi:10.3233/JAD-151162

Weimar, C., Konig, I. R., Kraywinkel, K., Ziegler, A., Diener, H. C., & German Stroke Study, C. (2004). Age and National Institutes of Health Stroke Scale Score within 6 hours after onset are accurate predictors of outcome after cerebral ischemia: development and external validation of prognostic models. *Stroke, 35*(1), 158-162. doi:10.1161/01.STR.0000106761.94985.8B

Xu, J., & Messina, J. L. (2009). Crosstalk between growth hormone and insulin signaling. *Vitam Horm, 80*, 125-153. doi:10.1016/S0083-6729(08)00606-7

Yin, X., Guven, N., & Dietis, N. (2016). Stress-based animal models of depression: Do we actually know what we are doing? *Brain Res, 1652*, 30-42. doi:10.1016/j.brainres.2016.09.027

2. FIRST STUDY: INSULIN-LIKE GROWTH FACTOR (IGF)-1 MODULATES ENDOTHELIAL BLOOD BRAIN BARRIER FUNCTION IN ISCHEMIC MIDDLE-AGED FEMALE RATS[1]

2.1. Overview of The First Study

In comparison with young females, middle-aged female rats sustain greater cerebral infarction and worse functional recovery after stroke. These poorer stroke outcomes in middle-aged females are associated with an age-related reduction in IGF-I levels. Poststroke IGF-I treatment decreases infarct volume in older females and lowers the expression of cytokines in the ischemic hemisphere. IGF-I also reduces transfer of Evans blue dye to the brain, suggesting that this peptide may also promote blood-brain barrier function. To test the hypothesis that IGF-I may act at the blood-brain barrier in ischemic stroke, 2 approaches were used. In the first approach, middle-aged female rats were subjected to middle cerebral artery occlusion and treated with IGF-I after reperfusion. Mononuclear cells from the ischemic hemisphere were stained for CD4 or triple-labeled for CD4/CD25/FoxP3 and subjected to flow analyses. Both cohorts of cells were significantly reduced in IGF-I–treated animals compared with those in vehicle controls. Reduced trafficking of immune cells to the ischemic site suggests that blood-brain barrier integrity is better maintained in IGF-I–treated animals. The second

[1] Reprinted with permission from Bake S, Okoreeh AK, Alaniz RC, Sohrabji F. Insulin-Like Growth Factor (IGF)-I Modulates Endothelial Blood-Brain Barrier Function in Ischemic Middle-Aged Female Rats. Endocrinology. 2016 Jan;157(1):61-9.

approach directly tested the effect of IGF-I on barrier function of aging endothelial cells. Accordingly, brain microvascular endothelial cells from middle-aged female rats were cultured ex vivo and subjected to ischemic conditions (oxygen-glucose deprivation). IGF-I treatment significantly reduced the transfer of fluorescently labeled BSA across the endothelial monolayer as well as cellular internalization of fluorescein isothiocyanate–BSA compared with those in vehicle-treated cultures, Collectively, these data support the hypothesis that IGF-I improves blood-brain barrier function in middle-aged females.

2.2. Introduction

Middle-aged females experience more severe stroke and poor functional recovery (Andersen et al., 2010; Towfighi et al., 2007), and this may be associated with the reduction in ovarian hormones and a concomitant decrease in other endocrine factors such as IGF-I (Selvamani et al., 2010). In rodent studies, greater infarct volume in acyclic middle-aged female rats (Selvamani and Sohrahji, 2010) is correlated with low levels of circulating and brain IGF-I expression compared with that in young females (Selvamani et al., 2010; Muller et al.; 2012).

The neuroprotective actions of IGF-I have been shown in several injury models, although the precise mechanisms underlying its actions are not well understood. IGF-I receptors are found on numerous brain cell types including neurons (Andersson, et al. 1988; Shemer, et al. 1987), astrocytes (Liu et al., 1994), endothelial cells (Torres-Aleman, et al., 1990; Chisalita, et al., 2004; Ungvari, et al., 2012), and microglia (Chesik, et al, 13). Furthermore, the IGF-I receptor, which is a ligand-activated receptor

tyrosine kinase, recruits the phosphatidylinositol 3-kinase/AKT/mammalian target of rapamycin survival pathway, and mediates inhibitory phosphorylation of the glycogen synthase kinase 3β, which promotes neuronal apoptosis (Hetman et al., 2000; Rangone et al., 2004). Hence IGF-I may promote survival of diverse cell types in the ischemic brain, including neurons and endothelial cells.

The effective maintenance of blood-brain barrier properties requires the coordinate action of endothelial cells, astrocytes, and pericytes (Abbott, et al., 1992; Ballabh, et al., 2004). Several lines of evidence from our previous work indicate that IGF-I may act on the blood-brain barrier to promote neuroprotection in ischemic stroke. Ischemic tissue from IGF-I and control animals subject to microRNA profiling and KEGG (Kyoto Encyclopedia of Genes and Genomes) analysis identified putative gene targets associated with extracellular matrix, survival pathways, and blood-brain barrier/endothelial function in middle-aged ischemic brain (Bake, et al., 2014). In addition, an IGF-I–mediated reduction in infarct volume was preceded by improved blood-brain barrier function as assessed by transfer of Evans dye. Finally, IGF-I also reduced the levels of proinflammatory and anti-inflammatory cytokines in the ischemic brain (Bake, et al., 2014). Postischemic inflammation plays a crucial role in stroke pathology (Nilupul Perera, et al., 2006; Amantea, et al., 2009), and signals from the ischemic brain can mobilize lymphocytes and macrophages, which are readily trafficked into the ischemic site (del Zoppo, et al., 2001; Wang, et. al., 2007; Gelderblom, et al. 2009; Jin, et al., 2010). IGF-I–mediated reductions in cytokines indirectly support the

hypothesis that this peptide may preserve barrier function by preventing extravasation of immune cells.

Therefore, in the present study we used 2 approaches to test the hypothesis that IGF-I promotes barrier function. In the first approach, an in vivo ischemic stroke model was used to determine whether IGF-I would affect the extent of peripheral immune cells recruited to the ischemic brain. In the second approach, an ex vivo system was used to determine the effect of IGF-I on primary brain endothelial cells from middle-aged female rats. Both approaches support the hypothesis that the neuroprotective effects of IGF may be mediated via direct action on endothelial cells to preserve blood-brain barrier function and reduce the trafficking of peripheral immune cells after stroke.

2.3. Materials and Methods

A total of 60 female Sprague-Dawley rats were used in these studies. Rats were purchased as middle-aged reproductive senescent females (retired breeders, 9–11 months; weight range, 325–350 g) from Harlan Laboratories. The middle-aged females met our previously established criteria for reproductive senescence (Bake, et al. 2004; Jezierski, et al., 2001). Daily vaginal smears were performed to determine that all senescent females were acyclic and in constant diestrus for at least 2 weeks before the experiment. All animals were housed in an American Association for Laboratory Animal Care–approved facility, maintained on a constant photoperiod (12-hour light/dark cycles), and fed ad libitum with laboratory chow (Harlan Teklad 8604) and water. All animal procedures were performed in accordance with the National Institutes of Health

guidelines for the humane care of laboratory animals and were approved by the Institutional Animal Care Committee.

2.3.1. Analysis of immune cell transfer to the brain post stroke

2.3.1.1. Surgical procedures

Middle-aged Sprague-Dawley females were anesthetized (with xylazine and ketamine) and placed in a stereotaxic instrument (David Kopf Instruments). A 28-gauge cannula was implanted into the right lateral ventricle using the following coordinates: −1.0 mm posterior to bregma, −1.4 mm lateral, and −3.5 mm from dural surface, as described previously (Selvamani and Sohrahji, 2010; Bake, et al., 2014). The cannula was anchored in place with Loctite 454 (Braintree Scientific). Animals were allowed to recover for 1 week after cannula implantation to ensure that any local inflammation caused by its placement was abated by the time the stroke surgery was performed.

2.3.2. Middle cerebral artery occlusion (MCAo)

Rats were anesthetized and subjected to MCAo via intraluminal suture, using the procedures described previously (Bake, et al., 2014). The intraluminal suture was maintained for 90 minutes and then withdrawn. The tissue perfusion rate was monitored using laser Doppler flowmetry (Moor Instruments), and the perfusion index was calculated for both ischemic and reperfusion time points. MCAo resulted in an 80% reduction of blood flow compared with the preocclusion rate, and reperfusion restored the perfusion index back to preocclusion levels. An osmotic minipump (flow rate, 1 μL/h, ALZET 1003D; Alzet Corp) filled with human recombinant IGF-I (100 μg/mL; R&D Laboratories) primed overnight was placed into a subcutaneous pocket between

the scapula and spine after 45 minutes of ischemia. Control animals were infused with artificial cerebrospinal fluid.

2.3.3. Isolation of central nervous system infiltrates and staining

Forty-eight hours after MCAo, animals were deeply anesthetized and perfused with saline. The brain was then removed and the ischemic and nonischemic cortices were dissected. Cortices were dissociated using a Neural Tissue Dissociation Kit (Miltenyi Biotech) and resuspended in X-VIVO-15 (Lonza). The homogenate was then layered on a Percoll gradient and centrifuged for 30 minutes at 500 × *g* at 4°C. Cells at the 70%–30% interphase were collected and resuspended in cell-staining buffer. The single-cell suspension was pipetted into 96-well plates, and the cells were counted on an automated cell counting apparatus (Countess; Life Technologies). Cells were washed with Flow Staining Buffer (eBioscience) and then incubated with anti-rat CD4-fluorescein isothiocyanate (FITC) (1:200) or triple labeled with anti-rat CD4-FITC (1:200)/anti-rat CD25 (1:100)/anti-mouse FoxP3 (1:100) (Table 2-1). After staining for surface markers, cells were fixed and made permeable according to the manufacturer's instructions (BD Biosciences) before staining for the intracellular marker. For each animal, 3 technical replicates were prepared and phenotyped via a FACSAria flow cytometer (BD Biosciences) and analyzed with FlowJo software (Tree Star).

The following gating strategy was used to identify $CD4^+$ cells and regulatory T cells. Dead cells and debris were removed from analysis via forward scatter and side scatter. Only singlets were considered during analysis. To control the cellular autofluorescence, unstained samples (without dye-conjugated antibodies) were prepared.

For $CD4^+$ cells, an initial gate was scaled where 99% of the unstained cells were excluded. For stained samples (samples that included dye-conjugated antibodies), any cells determined to be within the initial gate were considered positive. For T regulatory (Treg) cells, the quadrant system was created so that 99% of the unstained cells were in the third quadrant (quadrant 1, $FoxP3^+CD25^-$; quadrant 2, $FoxP3^+CD25^+$; quadrant 3, $FoxP3^-CD25^-$; and quadrant 4, $FoxP3^-CD25^+$). Only $CD4^+$ cells from stained samples that were determined to be in quadrant 2 ($FoxP3^+CD25^+$) were considered Treg cells. The number of $CD4^+$ or CD4/CD25/$FoxP3^+$ cells in the ischemic hemisphere was normalized to the number in the nonischemic hemisphere.

Table 2-1: Table of antibodies used in the first study

Peptide/Protein Target	**Antigen Sequence (if Known)**	**Name of Antibody**	**Manufacturer, Catalog No. and/or Name of Individual Providing the Antibody**	**Species Raised in; Monoclonal or Polyclonal**	**Dilution Used**
vWF		vWF	Labvision, MS-722	Mouse monoclonal	1:200
GFAP		GFAP	Millipore, MAB340	Mouse monoclonal	1:200

Peptide/Protein Target	**Antigen Sequence (if Known)**	**Name of Antibody**	**Manufacturer, Catalog No. and/or Name of Individual Providing the Antibody**	**Species Raised in; Monoclonal or Polyclonal**	**Dilution Used**
Iba-1		Iba-1	Abcam, AB156960	Mouse monoclonal	1:100
α-sma		Smooth muscle actin	Abcam, AB5694	Rabbit polyclonal	1:200
FoxP3		Anti-mouse/rat FoxP3 PE	eBioscience, E01764-1635	Mouse monoclonal	1:50
CD4		Anti-rat CD4	eBioscience, E00076-1632	Mouse monoclonal	1:500
CD25		Anti-rat CD25	eBioscience, E07136-1632	Mouse monoclonal	1:500

Table 4-1 **Continued**

2.3.3.1. Brain microvascular endothelial cell (BMEC) culture

To harvest primary BMECs, the brain was removed from deeply anesthetized (xylazine [13 mg/kg] and ketamine [87 mg/kg]) animals. Meninges and macroscopic vessels were discarded, and cortical tissue was collected in ice-cold 1× PBS (dPBS; Invitrogen). Tissues were washed in sterile PBS (3×) and homogenized with 10 gentle strokes of a loose-fitting pestle of a Dounce homogenizer. The homogenate was spun at 720 × *g* for 5 minutes at 4°C, and the pellet was suspended in PBS and layered over an equal volume of 18% dextran (Sigma-Aldrich). This mixture was spun at 3300 rpm for 1 hour at 4°C in a swinging bucket rotor centrifuge. The resulting pellet was suspended again in PBS and was filtered sequentially through a 150-μm filter followed by a 70-μm filter. The microvessels were recovered and digested in collagenase-dispase (1 mg/mL) at 37°C for 15 minutes. The digested vessel/cell mixture was recovered in Hanks' balanced salt solution (Invitrogen) and centrifuged at 125 × *g* for 5 minutes, and the resulting pellet was suspended in endothelial growth media, containing phenol red–free Iscove's modified Dulbecco's medium (Invitrogen) supplemented with 10% heat-inactivated fetal bovine serum (FBS) (Invitrogen), endothelial cell growth factor (25 μg/mL: BD Biosciences), heparin (100 μg/mL; Sigma-Aldrich), and penicillin-streptomycin (100 U/mL; Invitrogen, CA) and plated onto collagen IV (Sigma-Aldrich)–coated dishes. Cultures were maintained at 37°C in a humidified atmosphere of 5% CO_2-95% O_2 for 7 days and then were trypsinized and replated onto 60-mm culture dishes coated with collagen.

For subsequent assays, cells were plated in either 6- or 96-well dishes. For every assay, a single run consisted of cortical tissue pooled from 4 middle-aged (reproductive senescent) animals. Three such runs were performed for each assay. The cultures were passaged once before the experiment and were discarded after the experiment.

2.3.4. Characterization of endothelial cell cultures

Cells (harvested as described above) were grown on collagen-coated coverslips, fixed in 4% paraformaldehyde and processed for immunohistochemical analysis using primary antibodies for von Willebrand factor (vWF) (factor VIII), an endothelial cell marker (Labvision), and Alexa Fluor 594 secondary antibodies (Invitrogen). Cell cultures were also exposed to DiI-labeled acetylated low-density lipoprotein (Ac-LDL) (Sigma-Aldrich) in medium to detect Ac-LDL uptake. Cultures were also immunolabeled for glial fibrillary acidic protein (GFAP), an astrocytic marker (Millipore), ionized calcium-binding adaptor molecule 1 (Iba-1), a microglial marker (Abcam) and α-smooth muscle actin (Abcam), a marker for pericytes to determine the purity of endothelial cultures. Cells were counterstained with Hoechst dye for nuclear labeling.

2.3.5. Oxygen-glucose deprivation (OGD) procedure

Confluent cultures grown on 6-well culture plates were subject to hypoxia (1% O_2, 95% N_2, and 5% CO_2) in glucose- and FBS-free media with or without IGF-I (10 ng/mL). After 6 hours, the cultures were re-oxygenated in endothelial growth medium under normal conditions (5% CO_2 and 95% O_2). Medium was collected, and cells were photographed to record changes in cell morphology.

2.3.6. Lactate dehydrogenase (LDH) assay

Cell death was estimated by LDH in medium immediately after collection (Roche Applied Science). In brief, 50 μL of culture medium was added to each well of a 96-well plate and mixed with the catalyst and dye substrate mixture. After incubation for 30 minutes, 50 μL of stop solution was added to each well, and the plate was read at 490 nm absorbance on a plate reader (Tecan).

2.3.7. In vitro permeability assay: FITC-BSA transfer assay

Cells were plated at a density of 3 × 10 (4) onto collagen-coated inserts (0.4-μm pore size polycarbonate membrane; BD Biosciences) in FBS-free medium containing IGF-I or vehicle. After OGD and reoxygenation, FITC-BSA (250 μg/mL, 66 kDa; Sigma-Aldrich) was added to the medium in the top chamber. After 30 minutes, medium collected from the bottom chamber was loaded on a 96-well plate, and the plate was read at 492 nm (excitation)/520 nm (emission). Cells were stained with Hoechst dye and read at 350 nm (excitation)/420 nm (emission) and 492 nm (excitation)/520 nm (emission).

2.3.8. Statistical analysis

Group differences were analyzed by one-way ANOVA or paired *t* test using SPSS Statistic 20 software (IBM), and differences were considered significant at $P < .05$. For ex vivo cultures, 3 to 5 biological replicates were prepared, with 3 technical replicates per run. In each run, the normoxic group or the vehicle-treated group was set at 100, and the remaining groups were normalized accordingly.

2.4. Results

2.4.1. Effect of IGF-I on immune cell extravasation into the ischemic brain

To determine the effect of IGF-I on brain extravasation of immune cells in middle-aged females, mononuclear cells, harvested from ischemic and nonischemic cortex, were stained for CD4, a surface marker for a broad range of immune cells including T helper cells, macrophages, monocytes, and dendritic cells. The ratio of $CD4^+$ cells (ischemic/nonischemic hemisphere) was significantly reduced in IGF-I–treated animals compared with those in controls (Figure 2-1, A and B). In addition, cells were stained for CD4/CD25/FoxP3 to evaluate Treg cells. The ratio of this specific cohort of T cells was also significantly lower in IGF-I–treated groups than in vehicle-treated controls (Figure 2-1, C and D), suggesting that IGF-I reduces immune cell trafficking into the ischemic hemisphere.

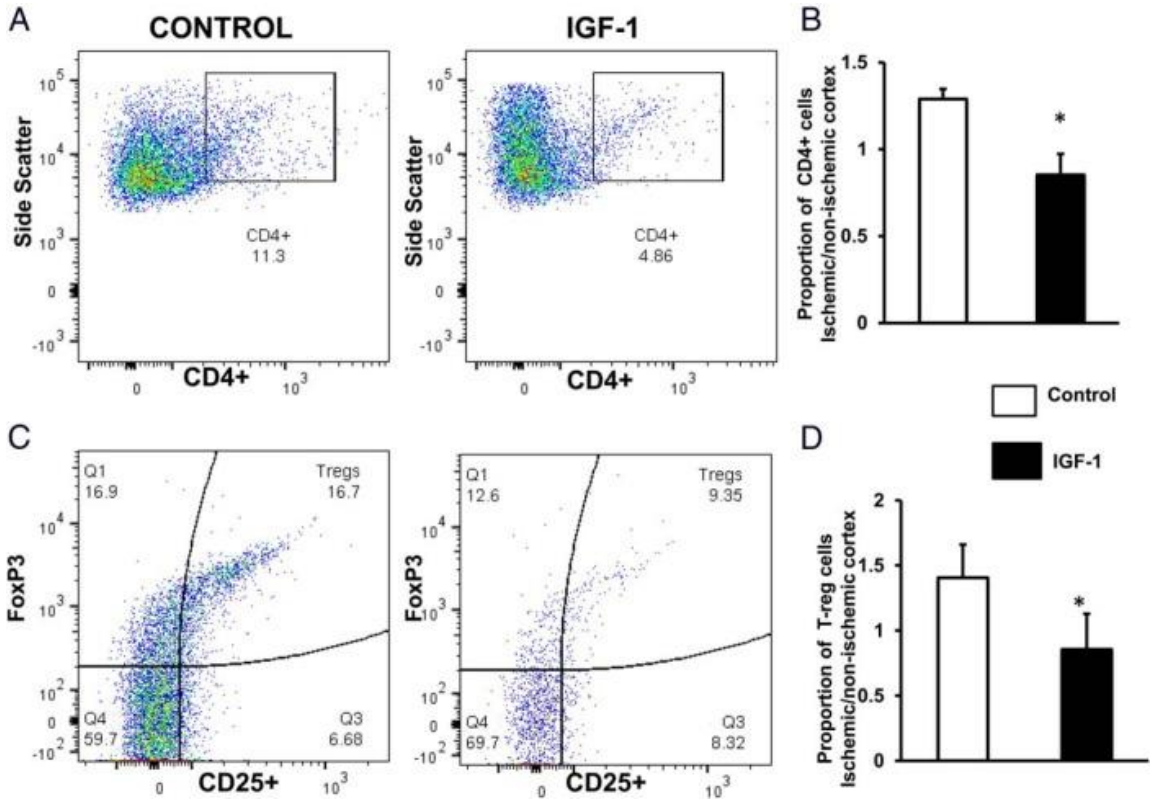

Figure 2-1: IGF-I regulates immune cell infiltration into ischemic cortex
A, Transient ischemia (90 minutes)/reperfusion (48 hours) resulted in an increased proportion of $CD4^+$ cells in the ischemic cortex of vehicle-treated middle-aged females (top left plot) compared with those of IGF-I–treated females (top right plot). B, IGF-I significantly reduced the ratio of $CD4^+$ cells in the ischemic vs nonischemic hemisphere compared with those in vehicle-treated animals. C and D, the ratio of Treg cells (cells stained positive for CD4/CD25/FoxP3) was also significantly decreased in the IGF-I–treated group compared with that in controls, suggesting IGF-I–mediated reduction in blood-brain barrier permeability in the ischemic cortex. n = 5 to 6; *, $P < .05$.

2.4.2. Characterization of primary BMECs cultures

Primary BMECs derived from female rat microvessels (described above) were plated on collagen-coated coverslips and immunostained for vWF (factor VIII, which is found exclusively in endothelial cells. As shown in Figure 2ai, virtually all cells were immunopositive for vWF. No staining was visible in cultures that were processed in the absence of the primary antibody (Figure 2-2aii). In cultures exposed to DiI-labeled Ac-LDL (which specifically identifies endothelial cells and macrophages), Ac-LDL uptake was seen in all cells (Figure 2-2aiii). Virtually no GFAP-positive (0%; Figure 2-2ci), Iba-1–positive (0%; Figure 2-2cii), or α-smooth muscle actin–positive (0.002%; Figure 2ciii) cells were seen in these cultures, indicating that these cultures were largely free of astrocytes, microglia, and pericytes.

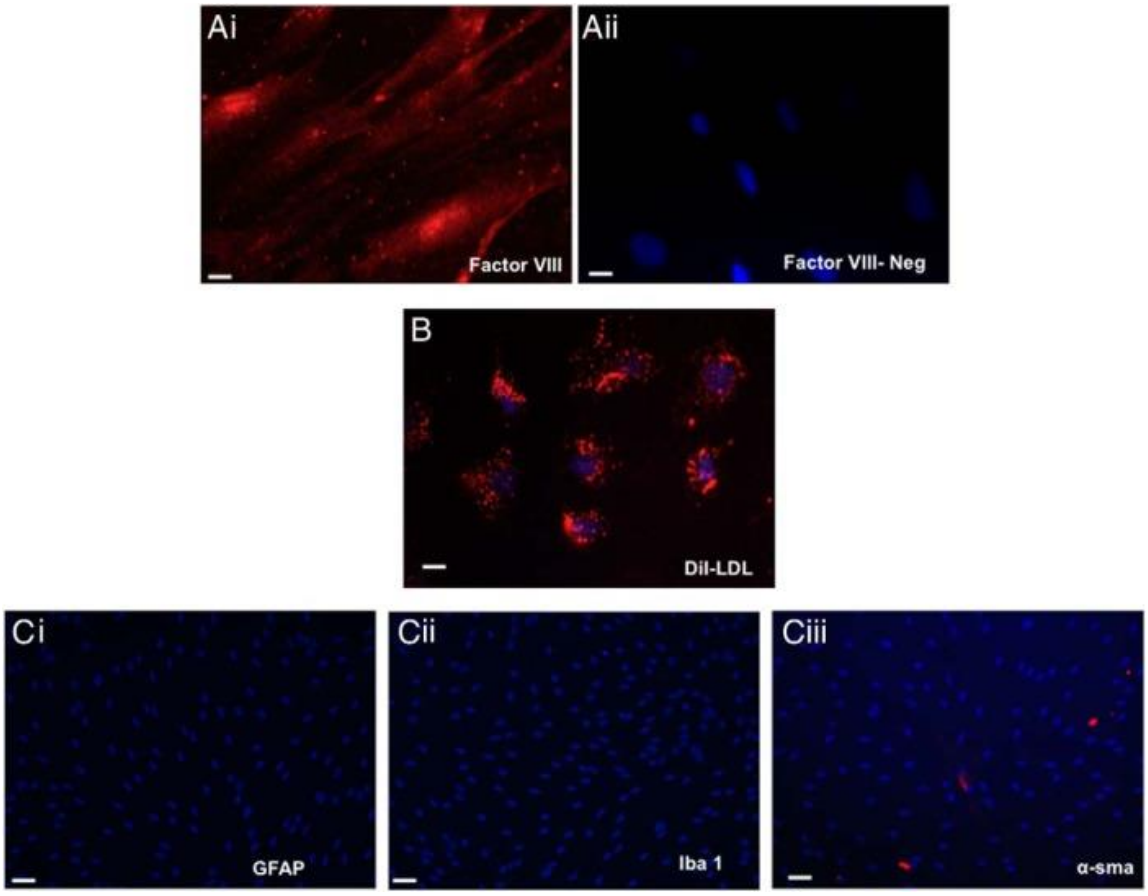

Figure 2-2: Characterization of BMECs from adult rat brain cortex
A, BMECs were immuno-labeled for the endothelial marker factor VIII (vWF). Virtually all cells were immunopositive for factor VII (red; ai), whereas no label was seen in cultures in which the primary antibody was omitted (aii). BMECs were counterstained with the nuclear dye, Hoechst dye, seen in blue. B, Cultures were exposed to fluorescence-labeled Ac-LDL in medium, which was internalized by all cells, and is visible here as red punctate labeling. C, BMECs were not immunopositive for the astrocytic marker GFAP (ci) or the microglial marker Iba-1 (cii), although <0.002% cells were positively labeled for α-smooth muscle actin, a pericyte marker (ciii). Cells were counterstained with a nuclear dye shown in blue. Bar, 20 μm (A and B); 50 μm (C).

2.4.3. OGD and reoxygenation cause cellular damage in middle-aged BMECs

To determine the impact of stroke-like conditions on aging endothelial cells, confluent monolayers of middle-aged derived BMECs were exposed to several combinations of oxygen deprivation and aglycemia. The most consistent results were obtained using 6 hours of OGD (1% O_2 and aglycemic medium) followed by 3 hours of reoxygenation in defined medium without FBS, and these conditions were used in all subsequent experiments. As shown in Figure 2-3, compared with normoxic controls (Figure 2-3ai), OGD caused visible changes to the morphology of BMECs (Figure 2-3aii). These included elongation and shrinkage of the cell body, resulting in fewer cell-cell contacts. In contrast, IGF-I–treated cultures showed reduced cell density, but cell bodies were not as elongated and cell-cell contacts were clearly visible (Figure 2-3aiii). After reoxygenation, BMECs still exhibited shrunken cytoplasmic profiles with reduced cell-cell contact (Figure 2-3av) compared with normoxic cells (Figure 2-3aiv), whereas IGF-I–treated cultures continued to show better cell-cell contacts (Figure 2-3avi).

Medium LDH levels were used to estimate OGD-induced cytotoxicity. LDH levels were increased more than 2-fold in cultures exposed to OGD as compared to normoxic controls, and IGF-I treatment did not affect LDH levels (Figure 2-3B). The medium replaced after OGD and collected 3 hours later had similar levels of LDH with all treatment conditions.

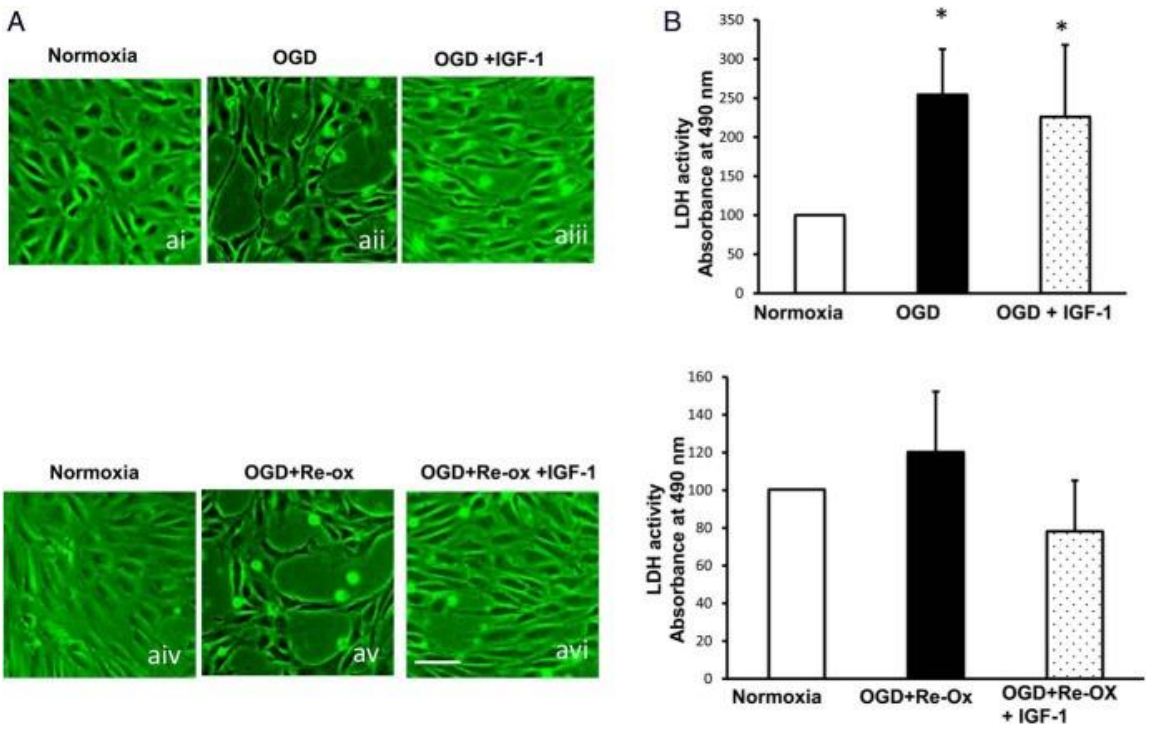

Figure 2-3: Effect of OGD, OGD and reoxygenation, and IGF-I on BMECs from middle-aged females

A, Compared with normoxic controls (ai), OGD resulted in morphological changes in endothelial cells including cell elongation, shrunken cell profiles, and reduced intercellular contact (aii). IGF-I–treated cultures showed less cellular elongation and fewer intercellular spaces indicating, greater cell-cell communication after OGD (aiii). Reoxygenation did not improve cell morphology and cell contacts in either untreated (av) or IGF-I–treated cultures (avi). B, LDH was measured in BMEC cultures exposed to IGF-I or vehicle after OGD and OGD and reoxygenation (Re-OX). OGD significantly increased medium LDH levels. However, IGF-I did not attenuate OGD-induced increase in LDH levels. LDH levels after reoxygenation were no different in vehicle and IGF-I–

treated cultures. The data shown represent 3 separate runs, with each run consisting of cells derived from 4 animals. *, P < .05 (compared to normoxia). Bar, 50 μm.

2.4.4. Effect of IGF-I on permeability of BMEC monolayers exposed to OGD reoxygenation

Our previous in vivo data showed that IGF-I reduced extravasation of Evans blue dye (18), a compound that binds serum albumin. Thus, to facilitate comparisons with the in vivo data, FITC-labeled albumin (FITC-BSA; 66 kDa) was used in these studies. BMEC cultures, treated with IGF-I or vehicle, were exposed to OGD reoxygenation. FITC-BSA was then added to the medium in the top chamber. IGF-I–treated cultures showed significantly lower levels of FITC-BSA in medium collected from the bottom chamber. In comparison to control-treated cultures, FITC-BSA transfer was reduced by 30% in IGF-I–treated cultures ($P < .05$) (Figure 2-4A).

Because BSA is also transferred by receptor-mediated transcytosis (27–29), FITC-BSA accumulation was also estimated in the BMEC monolayer. IGF-I–treated cultures had significant reductions in FITC-BSA (normalized to Hoechst dye measurement), indicating that IGF-I reduced the cellular uptake of FITC-BSA compared with that of controls (Figure 2-4B).

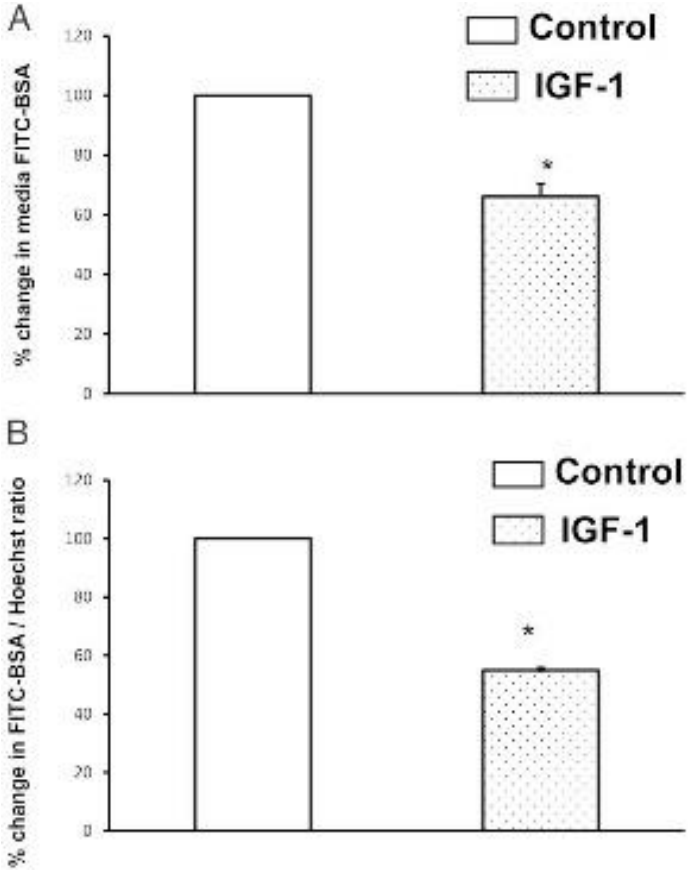

Figure 2-4: OGD and reoxygenation induced changes in barrier properties of endothelial cells

A, OGD induced changes in FITC-BSA transfer: FITC-BSA transport was measured across the monolayer of cells after OGD and reoxygenation. FITC-BSA transfer was significantly lower in cultures treated with IGF-I compared with vehicle treatment. B, FITC-BSA in the endothelial monolayer was normalized to nuclear dye (Hoechst) to determine the extent of BSA that was internalized by endothelial cells. There was a 50% decrease in the FITC-BSA/Hoechst ratio in IGF-I–treated cultures, suggesting reduced cellular uptake compared with that for vehicle treatment. The data represent the average from 3 independent runs, each run consisting of cells derived from 4 middle-aged females. *, $P < .05$.

2.5. Discussion

The present data show that poststroke IGF-I treatment reduces extravasation of immune cells into the ischemic cortex of middle-aged female rats. IGF-I also acts directly on aging endothelial cells to reduce protein transfer in an ex vivo model. In conjunction with our previous studies showing that IGF-I reduces transfer of Evans dye to the ischemic hemisphere (Bake, et al., 2014), the present study supports the hypothesis that immune cell extravasation is also greatly reduced by IGF-I treatment and provides direct evidence that IGF-I improves the barrier properties of the aging endothelial cell.

Poststroke inflammation plays a central role in stroke pathology (Samson, et al., 2005), and infiltration of immune cells into the ischemic central nervous system has been documented in a variety of experimental models (Jin, et al., 2010; Huang, et al., 2006; Banerjee, et al., 2013). T and B cells, macrophages, and natural killer cells are shown to invade the ischemic brain in the acute phase of stroke. T-cell infiltration is detrimental during the early phase of ischemic brain injury (Ren, et al., 2011; Gu, et al., 2015), and depletion of T and B cells is shown to reduce the cortical infarct volume at 22 hours poststroke (Hurn, et al., 2007). Blocking of T-cell function with recombinant T-cell receptor ligand RTL1000 attenuates inflammation and improves infarct size in middle-aged mice (Subramanian, et al., 2009, Zhu, et al. 2015). The role of Treg cells in stroke is controversial. Liesz et al. (2009) have shown that Treg cell depletion increases infarct volume, whereas another study using an alternative approach to deplete Treg cells showed no effect on infarct volume (Ren, et al., 2011). Furthermore, selective depletion

of Treg cells significantly reduced infarct volume and improved neurological function (Kleinschnitz, et al., 2013), whereas adoptive transfer of Treg cells protected against ischemia. In the present study, decreased Treg cell proportions in IGF-I–treated animals may suggest that decreased Treg cell function is associated with better stroke recovery. The fact that IGF-I decreased generic $CD4^+$ cells, which represent a wide range of immune cells, supports the alternate explanation that IGF-I blocks their passage across the blood-brain barrier. This is further supported by the ex vivo data showing that IGF-I treatment reduced transfer of FITC-BSA across the endothelial monolayer.

Most studies in the literature show that IGF-I is a proangiogenic growth factor. Age-related change in cerebral microvessel density is correlated with changes in GH and IGF-I, and GH treatment, which up-regulates IGF-I, increases cortical vascular density in older animals (Sonntag, et al., 1997). In adult animals, systemic IGF-I infusion promotes brain vessel formation (Lopez-Lopez, et al., 2004). IGF-I is also implicated in retinal vascularization in humans (Hellström, et al., 2002) and mice (Smith, et al., 1999). In the present study, IGF-I did not reduce cell death (as measured by LDH) in aging endothelial cells, although IGF-I may increase proliferation in these cells over the long term.

Although the effect of IGF-I on cerebral microvasculature is well known, the effect of IGF-I on blood-brain barrier permeability is less studied and more controversial. In the spinal cord, topical applications of IGF-I at high doses reduced the breakdown of the blood-spinal cord barrier, reduced spinal edema, and improved axonal repair in a traumatic injury to the T10–T11 segments (Sharma, et al., 2005). Low-dose

IGF-I was ineffective for all these measures. In an acute demyelinating experimental autoimmune encephalomyelitis (EAE) model of multiple sclerosis, intravenous IGF-I given over 8 days reduced permeability of the blood-spinal cord barrier and improved motor outcomes. Here also, high doses of IGF-I were more effective than low doses (Liu, et al., 1995). However, other evidence indicates that IGF-I treatment in an acute inflammatory condition may actually increase blood-brain barrier permeability. Intraventricular injections of lipopolysaccharide in a neonatal rat, which is an experimental model of periventricular leukomalacia, cause rapid dysregulation of the blood-brain barrier, activation of microglia and astrocytes, and recruitment of leukocytes to the brain. Low-dose IGF-I treatment in this model prevented cell death associated with this injury. However, IGF-I also increased the permeability of the blood-brain barrier and recruitment of leukocytes and caused intracerebral hemorrhage (Pang, et al., 2010). High doses of IGF-I in conjunction with LPS increased mortality, indicating that the peptide hormone may have anomalous effects in acute inflammation. Cerebral edema due to cirrhotic liver disease and portal vein occlusion was not improved by IGF-I treatment (Odena, et al., 2012). In fact, in peripheral tissues, IGF-I treatment is known to cause mild generalized and reversible edema. In a small study with 8 healthy participants, IGF-I treatment resulted in greater vascular permeability in skin and retina than in controls (Hussain, et al., 1995). In contrast, IGF-I preserved barrier properties in aging endothelial cell cultures in this study, suggesting a unique role for IGF-I in aging cerebral microvessels.

Neuroprotective strategies have been largely neuron-centric, and clinical trials and experimental stroke studies in which the primary therapeutic focus is the rescue of neurons are only partly successful (Berezowski, et al., 2012; Lo, et al., 2004). Experimental and clinical studies have repeatedly shown that microvascular dysfunction is a critical factor for neuronal death during the early phase of ischemia-reperfusion injury (del Zoppo, et al., 1994; Gursoy-Ozdemir, et al., 2012; Kaur, et al., 2011), and accumulating evidence suggests that brain microvessels play an important role in the clinical outcome of stroke patients. The present studies implicate the microvasculature as a target for stroke therapies in middle-aged females.

2.6. Abbreviations

The following abbreviations were used in the First Study:

ac-LPL: acetylated low-density lipoprotein

BMEC: brain microvascular endothelial cell

FBS: fetal bovine serum

FITC: fluorescein isothiocyanate

GFAP: glial fibrillary acidic protein

Iba-1: ionized calcium-binding adaptor molecule 1

LDH: lactate dehydrogenase

MCAo: middle cerebral artery occlusion

OGD: oxygen-glucose deficiency

Treg: T regulatory

vWF: Von Willebrand factor.

2.7. References

Andersen K, Andersen Z, Olsen T. Age- and gender-specific prevalence of cardiovascular risk factors in 40,102 patients with first-ever ischemic stroke: a Nationwide Danish Study. *Stroke.* 2010;41:2768–2774.

Towfighi A, Saver JL, Engelhardt R, Ovbiagele B. A midlife stroke surge among women in the United States. *Neurology*. 2007;69:1898–1904.

Selvamani A, Sohrabji F. The neurotoxic effects of estrogen on ischemic stroke in older female rats is associated with age-dependent loss of insulin-like growth factor-1. *J Neurosci.* 2010;30:6852–6861.

Selvamani A, Sohrabji F. Reproductive age modulates the impact of focal ischemia on the forebrain as well as the effects of estrogen treatment in female rats. *Neurobiol Aging*. 2010;31:1618–1628

Muller AP, Fernandez AM, Haas C, Zimmer E, Portela LV, Torres-Aleman I. Reduced brain insulin-like growth factor I function during aging. *Mol Cell Neurosci.* 2012;49:9–12.

Andersson IK, Edwall D, Norstedt G, Rozell B, Skottner A, Hansson HA. Differing expression of insulin-like growth factor I in the developing and in the adult rat cerebellum. *Acta Physiol Scand.* 1988;132:167–173.

Shemer J, Raizada MK, Masters BA, Ota A, LeRoith D. Insulin-like growth factor I receptors in neuronal and glial cells. Characterization and biological effects in primary culture. *J Biol Chem.* 1987;262:7693–7699.

Liu X, Yao DL, Bondy CA, et al. Astrocytes express insulin-like growth factor-I (IGF-I) and its binding protein, IGFBP-2, during demyelination induced by experimental autoimmune encephalomyelitis. *Mol Cell Neurosci.* 1994;5:418–430.

Torres-Aleman I, Naftolin F, Robbins RJ. Trophic effects of insulin-like growth factor-I on fetal rat hypothalamic cells in culture. *Neuroscience.* 1990;35:601–608.

Chisalita SI, Arnqvist HJ. Insulin-like growth factor I receptors are more abundant than insulin receptors in human micro- and macrovascular endothelial cells. *Am J Physiol Endocrinol Metab.* 2004;286:E896–E901.

Ungvari Z, Csiszar A. The emerging role of IGF-1 deficiency in cardiovascular aging: recent advances. *J Gerontol Ser A Biol Sci Med Sci.* 2012;67:599–610.

Chesik D, Glazenburg K, Wilczak N, Geeraedts F, De Keyser J. Insulin-like growth factor binding protein-1-6 expression in activated microglia. *Neuroreport.* 2004;15:1033–1037.

Smith AM, Gibbons HM, Oldfield RL, et al. M-CSF increases proliferation and phagocytosis while modulating receptor and transcription factor expression in adult human microglia. *J Neuroinflammation*. 2013;10:85.

Hetman M, Cavanaugh JE, Kimelman D, Xia Z. Role of glycogen synthase kinase-3β in neuronal apoptosis induced by trophic withdrawal. *J Neurosci*. 2000;20:2567–2574.

Rangone H, Poizat G, Troncoso J, et al. The serum- and glucocorticoid-induced kinase SGK inhibits mutant huntingtin-induced toxicity by phosphorylating serine 421 of huntingtin. *Eur J Neurosci.* 2004;19:273–279.

Abbott NJ, Hughes CC, Revest PA, Greenwood J. Development and characterization of a rat brain capillary endothelial culture: towards an in vitro blood-brain barrier. *J Cell Sci.* 1992;103(Pt 1):23–37.

Ballabh P, Braun A, Nedergaard M. The blood-brain barrier: an overview: structure, regulation, and clinical implications. *Neurobiol Dis.* 2004;16:1–13.

Bake S, Selvamani A, Cherry J, Sohrabji F. Blood brain barrier and neuroinflammation are critical targets of IGF-1-mediated neuroprotection in stroke for middle-aged female rats. *PLoS One*. 2014;9:e91427.

Nilupul Perera M, Ma HK, Arakawa S, et al. Inflammation following stroke. *J Clin Neurosci.* 2006;13:1–8.

Amantea D, Nappi G, Bernardi G, Bagetta G, Corasaniti MT. Post-ischemic brain damage: pathophysiology and role of inflammatory mediators. *FEBS J.* 2009;276:13–26.

del Zoppo GJ, Becker KJ, Hallenbeck JM. Inflammation after stroke: is it harmful? *Arch Neurol.* 2001;58:669–672.

Wang Q, Tang XN, Yenari MA. The inflammatory response in stroke. *J Neuroimmunol.* 2007;184:53–68.

Gelderblom M, Leypoldt F, Steinbach K, et al. Temporal and spatial dynamics of cerebral immune cell accumulation in stroke. *Stroke.* 2009;40:1849–1857.

Jin R, Yang G, Li G. Inflammatory mechanisms in ischemic stroke: role of inflammatory cells. *J Leukoc Biol.* 2010;87:779–789.

Bake S, Sohrabji F. 17β-Estradiol differentially regulates blood-brain barrier permeability in young and aging female rats. *Endocrinology.* 2004;145:5471–5475.

Jezierski MK, Sohrabji F. Neurotrophin expression in the reproductively senescent forebrain is refractory to estrogen stimulation. *Neurobiol Aging.* 2001;22:309–319.

Esposito C, Gerlach H, Brett J, Stern D, Vlassara H. Endothelial receptor-mediated binding of glucose-modified albumin is associated with increased monolayer permeability and modulation of cell surface coagulant properties. *J Exp Med.* 1989;170:1387–1407.

Schnitzer JE. gp60 is an albumin-binding glycoprotein expressed by continuous endothelium involved in albumin transcytosis. *Am J Physiol.* 1992;262:H246–H254.

John TA, Vogel SM, Tiruppathi C, Malik AB, Minshall RD. Quantitative analysis of albumin uptake and transport in the rat microvessel endothelial monolayer. *Am J Physiol Lung Cell Mol Physiol.* 2003;284:L187–L196.

Samson Y, Lapergue B, Hosseini H. Inflammation and ischaemic stroke: current status and future perspectives [in French]. *Revue Neurol* (Paris). 2005;161:1177–1182.

Huang J, Upadhyay UM, Tamargo RJ. Inflammation in stroke and focal cerebral ischemia. *Surg Neurol.* 2006;66:232–245.

Banerjee A, Wang J, Bodhankar S, Vandenbark AA, Murphy SJ, Offner H. Phenotypic changes in immune cell subsets reflect increased infarct volume in male vs. female mice. *Transl Stroke Res.* 2013;4:554–563.

Ren X, Akiyoshi K, Vandenbark AA, Hurn PD, Offner H. $CD4^{+}FoxP3^{+}$ regulatory T-cells in cerebral ischemic stroke. *Metab Brain Dis.* 2011;26:87–90.

Gu L, Jian Z, Stary C, Xiong X. T cells and cerebral ischemic stroke. *Neurochem Res.* 2015;40:1786–1791.

Hurn PD, Subramanian S, Parker SM, et al. T- and B-cell-deficient mice with experimental stroke have reduced lesion size and inflammation. *J Cereb Blood Flow Metab.* 2007;27:1798–1805.

Subramanian S, Zhang B, Kosaka Y, et al. Recombinant T cell receptor ligand treats experimental stroke. *Stroke.* 2009;40:2539–2545.

Zhu W, Dotson AL, Libal NL, et al. Recombinant T-cell receptor ligand RTL1000 limits inflammation and decreases infarct size after experimental ischemic stroke in middle-aged mice. *Neuroscience*. 2015;288:112–119.

Liesz A, Suri-Payer E, Veltkamp C, et al. Regulatory T cells are key cerebroprotective immunomodulators in acute experimental stroke. *Nat Med.* 2009;15:192–199.

Kleinschnitz C, Wiendl H. Con: Regulatory T cells are protective in ischemic stroke. *Stroke*. 2013;44:e87–e88.

Sonntag WE, Lynch CD, Cooney PT, Hutchins PM. Decreases in cerebral microvasculature with age are associated with the decline in growth hormone and insulin-like growth factor 1. *Endocrinology*. 1997;138:3515–3520.

Lopez-Lopez C, LeRoith D, Torres-Aleman I. Insulin-like growth factor I is required for vessel remodeling in the adult brain. *Proc Natl Acad Sci USA*. 2004;101:9833–9838.

Hellström A, Carlsson B, Niklasson A, et al. IGF-I is critical for normal vascularization of the human retina. *J Clin Endocrinol Metab.* 2002;87:3413–3416.

Smith LE, Shen W, Perruzzi C, et al. Regulation of vascular endothelial growth factor-dependent retinal neovascularization by insulin-like growth factor-1 receptor. *Nat Med.* 1999;5:1390–1395.

Sharma HS. Neuroprotective effects of neurotrophins and melanocortins in spinal cord injury: an experimental study in the rat using pharmacological and morphological approaches. *Ann NY Acad Sci*. 2005;1053:407–421.

Liu X, Yao DL, Webster H. Insulin-like growth factor I treatment reduces clinical deficits and lesion severity in acute demyelinating experimental autoimmune encephalomyelitis. *Mult Scler*. 1995;1:2–9.

Pang Y, Zheng B, Campbell LR, Fan LW, Cai Z, Rhodes PG. IGF-1 can either protect against or increase LPS-induced damage in the developing rat brain. *Pediatr Res*. 2010;67:579–584.

Odena G, Miquel M, Serafín A, et al. Rifaximin, but not growth factor 1, reduces brain edema in cirrhotic rats. *World J Gastroenterol*. 2012;18:2084–2091.

Hussain MA, Studer K, Messmer EP, Froesch ER. Treatment with insulin-like growth factor I alters capillary permeability in skin and retina. *Diabetes*. 1995;44:1209–1212.

Berezowski V, Fukuda AM, Cecchelli R, Badaut J. Endothelial cells and astrocytes: a concerto en duo in ischemic pathophysiology. *Int J Cell Biol*. 2012;2012:176287.

Lo EH, Broderick JP, Moskowitz MA. tPA and proteolysis in the neurovascular unit. *Stroke*. 2004;35:354–356.

del Zoppo GJ. Microvascular changes during cerebral ischemia and reperfusion. *Cerebrovasc Brain Metab Rev.* 1994;6:47–96.

Gursoy-Ozdemir Y, Yemisci M, Dalkara T. Microvascular protection is essential for successful neuroprotection in stroke. *J Neurochem.* 2012;123(suppl 2):2–11.

Kaur J, Tuor UI, Zhao Z, Barber PA. Quantitative MRI reveals the elderly ischemic brain is susceptible to increased early blood-brain barrier permeability following tissue plasminogen activator related to claudin 5 and occludin disassembly. *J Cereb Blood Flow Metab.* 2011;31:1874–1885.

3. SECOND STUDY: INSULIN-LIKE GROWTH FACTOR (IGF)-1 TREATMENT STABILIZES THE MICROVASCULAR CYTOSKELETON UNDER ISCHEMIC CONDITIONS[2]

3.1. Overview of the Second Study

Our previous studies showed that Insulin-like Growth Factor (IGF)-1 reduced blood brain barrier permeability and decreased infarct volume caused by middle cerebral artery occlusion (MCAo) in middle aged female rats. Similarly, cultures of primary brain microvessel endothelial cells from middle-aged female rats and exposed to stroke-like conditions (oxygen glucose deprivation; OGD) confirmed that IGF-1 reduced dye transfer across this cell monolayer. Surprisingly, IGF-1 did not attenuate endothelial cell death caused by OGD. To reconcile these findings, the present study tested the hypothesis that, at the earliest phase of ischemia, IGF-1 promotes barrier function by increasing anchorage and stabilizing cell geometry of surviving endothelial cells. Cultures of human brain microvessel endothelial cells were subject to oxygen-glucose deprivation (OGD) in the presence of IGF-1, IGF-1+JB-1 (IGFR inhibitor) or vehicle. OGD disrupted the cell monolayer and reduced cell-cell interactions, which was preserved in IGF-1-treated cultures and reversed by concurrent treatment with JB-1. IGF-1-mediated preservation of the endothelial monolayer was reversed with LY294002

---

[2] Reprinted with permission from Bake S, Okoreeh A, Khosravian H, Sohrabji F. Insulin-like Growth Factor (IGF)-1 treatment stabilizes the microvascular cytoskeleton under ischemic conditions. Exp Neurol. 2019 Jan.;311:162-172.

treatment, but not by Rapamycin, indicating that IGF-1s actions on cell-cell contacts are likely mediated via the PI3K pathway. In vivo, microvessel morphology was evaluated in middle-aged female rats that were subjected to ischemia by MCAo, and treated ICV with IGF-I, IGF-1+JB-1, or artificial CSF (aCSF; vehicle) after reperfusion. Compared to vehicle controls, IGF-1 treated animals displayed larger microvessel diameters in the peri-infarct area and increased staining density for vinculin, an anchorage protein. Both these measures were reversed by concurrent IGF-1+JB-1 treatment. Moreover these effects were restricted to 24h after ischemia-reperfusion and no treatment effects were seen at 5d post stroke. Collectively, these data suggest that in the earliest hours during ischemia, IGF-1 promotes receptor-mediated anchorage of endothelial cells, and its actions may be accurately characterized as vasculoprotective.

3.2. Introduction

Ischemic stroke causes loss of nutrients to brain tissue and initiates a sequence of harmful events within neurons including rapid failure of ATP-dependent processes, increased release of glutamate and calcium, and rapid cell death (Pulsinelli, 1992; Moskowitz et al., 2010; Khatri et al., 2012). The earliest impact of ischemia includes changes in the blood brain barrier, followed by vasogenic edema in the brain (Yang et al., 2007). These deleterious changes to the barrier are accompanied by disruption of intercellular tight junction assembly causing microvessel hyperpermeability (Kreuger and Phillipson, 2016), heightened inflammatory responses (Gidday et al., 2005; Kleinschnitz and Wiendl, 2013) and loss of anchorage of endothelial cells (Baldo et al., 2015). Cell surface alterations on the endothelium such as the upregulation of adhesion

molecules ICAM-1 and CCL2 facilitates infiltration of neutrophils and macrophages into the brain during the early phase of injury (Dimitrijevic et al., 2007; Wu et al., 2015; Shi et al., 2016; Zhu et al., 2016). Blood brain barrier hyperpermeability and edema is associated with poor prognosis (Khatri et al., 2012), and consistent with this observation, stroke-induced brain damage and disability and blood-brain barrier permeability is significantly higher in older animals as compared to young animals (Dinapoli et al., 2008; Liu et al., 2009; Montagne et al., 2015). Hence, the blood brain barrier and its component cells are critical for stroke pathophysiology and are considered important targets for stroke therapy (Borlongan et al., 2012; Merali et al., 2016)

Our previous studies show that middle-aged female rats sustain larger infarcts and worse stroke outcomes as compared to younger females (Selvamani and Sohrabji, 2010a, Selvamani and Sohrabji, 2010b), and this is associated with decreased levels of circulating and parenchymal IGF-1. Accordingly, intracerebroventricular (ICV) delivery of IGF-1 2 h after ischemia to middle-aged female rats reduces infarct volume when measured 24 h after stroke. In silico analysis of epigenetic modulators indicated that IGF-1 regulated microRNAs that improve extracellular matrix interactions and endothelial cells. We focused on blood brain barrier changes and reported that as early as 4 h after MCAo, IGF-1 treatment decreased blood brain barrier permeability to small molecules (Bake et al., 2014) although the peptide did not reduce infarct volume at this time point. At 48 h after MCAo, when brain trafficking of T-regulatory cells was seen, IGF-1 reduced passage of these larger elements as well (Bake et al., 2014; Bake et al., 2016). Ex vivo cultures of primary brain microvascular endothelial cells (BMECs) from

middle-aged rats subject to OGD showed that IGF-1 reduced transfer of FITC-BSA transfer across the monolayer (Bake et al., 2016), but did not prevent cell death. These data suggest that IGF-1 actions during the earliest phase of ischemia are not dependent on cell survival, but may act via a different mechanism. The present study employed complementary in vivo and in vitro approaches to test whether IGF-1 prevents ischemia-induced cytoskeletal rearrangement and cell detachment from the extracellular matrix.

3.3. Materials and Methods

3.3.1. In vitro studies

3.3.1.1. Cell culture and oxygen glucose deprivation (OGD)

Human brain microvascular endothelial cells (hBMEC) were purchased from Millipore Corp. MA (hCMEC/D3,) and grown with EndoGro medium (Millipore Corp. MA) on type I collagen-coated T-75 flasks. For experiments, cells (5 × 104) were plated either on collagen-coated coverslips or in 96-well plates and maintained until confluent. Cultures were grown in normoxic conditions (5% CO2 and 21% O2; 37 °C) until confluent. Cells were then subject to OGD (1% O2, 95% N2 and 5% CO2 in glucose free DMEM) for 6 h with IGF-1 (10 ng/ml), IGF-1 + JB-1 (IGF-1 receptor antagonist; 2 ng/ml), IGF1+ LY294002 (reversible PI3-kinase inhibitor, 1 μg/ml) and rapamycin (mTOR inhibitor, 1μg/ml) or vehicle (PBS or DMSO). Culture media was collected for assays and cells were fixed for histological analysis. All assays were conducted with 3–5 replicate runs and each run consisted of 5–6 technical replicates.

3.3.1.2. Quantitative (q)RT-PCR

Human IGF1R mRNA expression in hBMEC was assessed using real-time qRT-PCR. Total RNA was extracted using QIAzol reagent and RNA Mini extraction kit (Qiagen, CA) using our previous procedures (Okoreeh et al., 2017). RNA yield and purity were evaluated with a NanoDrop ND-1000 spectrophotometer (NanoDrop Technologies/Thermo Scientific). 100 ng of purified total RNA was used to generate cDNA, using a cDNA Synthesis Kit (Quantbio, MA) following manufacturer's protocol. cDNA was diluted 80 fold and real time PCR reaction were run on Applied Biosystems 7900HT real-time PCR instrument (Applied Biosystems, CA) using a SYBR green-based real-time PCR reaction kit (Quantabio, MA). 18 s mRNA was used as a normalization control. Human IGF-1R (Forward:5′- TTA AGA ACC AGT GGC GAA AG -3′, Reverse: 5′- GGA GCA CTC ACT TCT CCA AA -3′ Realtime primers, PA) and 18S primers (Forward:%'-ATGGCCGTTCTTAGTTGGTG -3′; Reverse: 5′-CGCTGAGCCAGTCAGTGTAG-3′, Life Technologies, CA).

3.3.1.3. Cell death/survival assays

3.3.1.3.1. LDH assay

Cell death was estimated by lactate dehydrogenase (LDH) in media immediately after collection, using a colorimetric assay (Thermofisher, MA) and our previous procedures (Bake et al., 2016). Briefly, 50 µl of culture media was added to each well of a 96-well plate and mixed with catalyst and dye substrate mixture. After incubation for 30 min, 50 µl of stop solution was added to each well and the plate was read at 490 nm absorbance on a colorometric plate reader (Tecan, Switzerland). Calcein assay: Cell

viability was determined using the Calcein-AM dye (Life Technologies,CA). After OGD, cells were incubated with calcein-AM (2.5 μm) in PBS for 20 min at 37 °C and the fluorescence was measured on a plate reader (Tecan, Switzerland) with excitation/ emission set at 480 and 530 nm respectively.

3.3.1.3.2. Phalloidin staining

Endothelial cells grown on coverslips were washed and fixed with 4% paraformaldehyde, and then permeabilized in 0.1% triton-X and washed three times with PBS. Cells were then incubated with 3% BSA for 20 min followed by two washes and stained with Alexa Fluor 488 phalloidin (Life technologies, CA) for 30 min, washed with PBS and mounted with Prolong antifade mounting media (Life technologies, CA). Images were captured on the FSX100 Olympus microscope.

3.3.1.3.3. Vinculin immunohistochemistry

Endothelial cells grown on coverslips were processed for immunohistochemistry using our previously published procedures (Bake et al., 2016). Briefly, cells were incubated in a blocking solution (2% normal goat serum and 2% triton X-100 in dPBS) for 1 h at room temperature, followed by incubation with the antibody for vinculin (eBioscience, San Diego, CA, 1:100) overnight. Following 3 PBS washes, cells were then incubated for 1 h with fluorescent-labeled secondary antibody (Alexa Fluor 594 goat anti-mouse, 1:500 dilution) and were counterstained with nuclear dye (Hoechst, 1:500) and coverslipped with Prolong antifade mounting media (Life technologies, CA). Images were captured using an Olympus confocal microscope.

3.3.1.3.4. Lectin staining

In vitro analysis: Endothelial cells grown on coverslips were washed and fixed with 4% paraformaldehyde, and then permeabilized in 0.1% triton-X and washed three times with PBS. Cells were then incubated with 3% BSA for 20 min followed by two washes and stained with lectin (1:1000, Vector Laboratories, CA) for 30 min, washed with PBS and mounted with Prolong antifade mounting media. Images were captured on the FSX100 Olympus microscope. Determination of intercellular spaces: Lectin-stained cell cultures (3 experimental replicates) were photographed, coded and analyzed for continuity of the monolayer using a novel algorithm to determine intercellular 'spaces'. Briefly, all images were first converted into grayscale images. A threshold was calibrated for each image to convert the grayscale image into a black and white one, such that cells are in white and everything else remains black. Thus, the total number of gaps between cells in each image was estimated by the total number of black pixels. Once the cells were identified, the two images were overlaid to find all the cells and the near empty areas in the image. The spaces near cells were calculated using the Canny edge detection algorithm. The above algorithm was coded in Python and OpenCV.

3.3.2. In vivo studies

3.3.2.1. Animals

Female Sprague Dawley (SD) rats were purchased as retired breeders (10–12 months; weight range 325–350 g) from Envigo Laboratories (previously Harlan Labs, IN). This group met our previously established criteria for reproductive senescence, namely, at least five successful pregnancies and current acyclicity determined by daily

vaginal smears. All animals were housed in an AAALAC–approved facility, maintained on a constant photoperiod (12-h light/dark cycles), and fed ad libitum with laboratory chow (Harlan Teklad 8604) and water. All animal procedures were performed in accordance with the National Institutes of Health guidelines for the humane care of laboratory animals and were approved by the Institutional Animal Care Committee and the Institutional Biosafety Committee. A total of 55 animals were used in this study, with 7–9 animals per group for behavioral analysis and 5–6 animals per group for histological analysis.

3.3.2.2. Surgical procedures

3.3.2.2.1. Cannula implantation

Animals were placed in a stereotaxic instrument (David Kopf instruments, CA), a 28 gauge cannula was implanted into the right lateral ventricle using the co-ordinates –1.0 mm posterior to bregma, −1.4 mm medial lateral, −3.5 mm from dural surface, and anchored in place with loctite 454 (Braintree Scientific, MA). Animals were allowed to recover for 1 week following cannula implantation and prior to stroke surgery. Alzet osmotic minipumps (1003D & 1007D, Alzet corp., CA, flow rate 0.5 and 1 μl/h) filled with human recombinant (rh)IGF-1 (R&D Laboratories, 100 μg/ml) or rhIGF-1 and JB-1 (20 μg/ml) were primed overnight and placed into a subcutaneous pocket between the scapula and spine, after 45 min of ischemia. IGF-1 delivery to the brain initiated 2 h after the onset of ischemia. Previous studies have shown that IGF-1 is stable in Alzet minipumps for up to 7 days. Control animals were infused with artificial CSF. All animals were terminated either 1 day or 5 days post-reperfusion.

3.3.2.2.2. Middle cerebral artery occlusion (MCAo)

Animals were subjected to middle cerebral artery occlusion (MCAo) via intraluminal suture 1 week after cannula implantation, using our previous procedures (Bake et al., 2014; Bake et al., 2016). Briefly, rats were anesthetized with isoflurane and maintained at 37 °C on heating pads in dorsal recumbency. The neck region was shaved and disinfected and a ventral midline incision was made on the skin. Superficial fascia on the right side of the neck was dissected and the underlying muscles were blunt dissected to expose the right common carotid (CCA), external (ECA), and internal carotid (ICA) arteries. The ECA was separated from the vagus nerve and tied off distally with silk sutures after cauterizing the small branches. Microsurgical clamps were placed on CCA and ICA. A loose tie was placed on the ECA, and the free stump of ECA was aligned with the ICA. 22 mm of suture of the appropriate size (37–41) with a silicon-coated round tip (Doccol Corp., CA) was inserted into ICA lumen through a small nick on the ECA between the two ties. The suture was advanced along the ICA until it reached the origin of the MCA (~20 mm of suture) and secured in position with nylon ties. The intraluminal suture was maintained for 90 min and then withdrawn. Tissue perfusion rate was monitored using Laser-Doppler Flowmetry (Moor Instruments, UK) and the perfusion index was calculated for both ischemic and reperfusion time points. MCAo resulted in an 80% reduction of blood flow compared to the pre-occlusion rate and re-perfusion restored the perfusion index back to pre-occlusion levels. All animals were carefully monitored after surgery and terminated 1 day or 5 days after ischemia.

3.3.2.3. Behavioral analysis

3.3.2.3.1. Neurological score

Functional tests were performed 1 day after MCAo. Each animal underwent five tests in succession to assess motility, grasping, righting reflex, forepaw disability, and circling, as described in (Bake et al., 2016; Okoreeh et al., 2017). For each test, a higher score indicates a more severe deficit.

3.3.2.3.2. Histological analyses

Animals were deeply anesthetized with ketamine/xylazine (ketamine: 87 mg/kg; xylazine: 13 mg/kg) and then perfused transcardially with saline followed by a perfusion fix solution (4% paraformaldehyde, 4% sucrose in dPBS) and decapitated. Heads were placed in a container filled with perfusion fix solution overnight at room temperature. Subsequently, the brains were removed from the cranial vault and stored in Dulbecco's phosphate saline with 0.01% sodium azide until shipped to Neuroscience Associates (NSA, Nashville, TN) for processing. Briefly, brains were block embedded in MultiBrain® blocks and freeze-sectioned at 40 μm with a sliding microtome, yielding free-floating sections collected in antigen preservation solution.

3.3.2.3.3. Vinculin immunohistochemistry

Brain sections (40 μm) containing cortex and striatum were mounted and adhered to gelatin-coated glass slides and processed for vinculin immunohistochemistry as described above and analyzed as follows. Three images were captured from the peri-infarct zone of the cortex and striatum of the immunostained section for each animal, using a Q-color camera attached to the FSX100 Olympus microscope. The section was

at the interaural level 8.7 mm, bregma −0.30 mm (Paxinos and Watson, 1986). Photomicrographs were coded and then analyzed for vinculin staining density using ImageJ software (NIH, MD). In each image, three regions were demarcated and the area occupied by vinculin particles were measured in each region. The area occupied by vinculin particles was then normalized to the area of the box to obtain the density of vinculin label. For each animal, density measurements were obtained separately for the cortex and striatum and then combined to obtain a single value for each animal. Both the ischemic and non-ischemic hemispheres were analyzed. Data was decoded and analyzed by 2 way ANOVA coded for hemisphere (repeated measure) and treatment condition. Separate analyses were performed for day 1 and day 5 post stroke (SPSS, IBM).

3.3.2.3.4. Lectin

Brain sections (40 μm) were mounted and adhered to gelatin-coated glass slides and stained for lectin as described above. Lectin-stained vessels were analyzed in the following way. Three images were captured each from the cortex and striatum of the immunostained section for each animal, using a Q-color camera attached to the FSX100 Olympus microscope. The section was at the interaural level 8.7 mm, bregma −0.30 mm (Paxinos and Watson, 1986). Images were coded and processed in Autoquant X3 (Mediacybernetics,US) and were analyzed for diameter and length of microvessels with Imaris (Bitplane, US). For each animal, values were obtained separately for the cortex and striatum and then combined and binned into 3 groups, 1-5 um, 6–10 um, 11+ um. Data was decoded and analyzed by 2 way ANOVA coded for treatment condition and bin (repeated measure). Due to the volume of data and the possibility of spurious errors,

separate analyses were performed for each hemisphere and for day 1 and day 5 post stroke (SPSS, IBM).

3.3.3. Statistical analysis

Group differences were analyzed using SPSS Statistic 23 software (IBM) and differences were considered significant at $p < 0.05$. For in vitro studies, 3 to 4 biological replicates were prepared with 6 technical replicates per run. Each run was normalized to its normoxic control group and one way ANOVA was used to evaluate group differences, with planned comparisons. For in vivo studies, neurological scores were analyzed by one way ANOVA. Vinculin and lectin histology was analyzed as described above. Data are expressed as mean ± SEM.

3.4. Results

3.4.1. IGF-1 does not reduce OGD-induced cell death

Media LDH from normoxic cultures and cultures exposed to OGD, with various treatments, was used as a surrogate marker for cytotoxicity (Figure 3-1A). Groups were compared using a one-way ANOVA with planned post hoc comparisons ($F(5,18)$: 2.56, $p = 0.084$). Compared to normoxia, LDH levels were significantly elevated by 6 h of OGD ($p = 0.045$). Neither IGF-1 ($p = 0.46$) nor concurrent IGF-1 + JB-1 ($p = 0.37$) reduced LDH release under OGD conditions. Similarly, LY294002 ($p = 0.94$) or Rapamycin ($p = 0.55$) also did not reduce OGD induced levels of LDH. In addition, cell survival was also determined by the calcein-AM assay (Figure 3-1B), using a one way ANOVA and planned post hoc comparisons ($F(5,17)$:2.73; $p = 0.077$). OGD significantly decreased cell survival as measured by calcein ($p = 0.017$). Here also IGF-1

treatment (p = 0.67), with and without Rapamycin (p = 0.83), or LY294002 (p = 0.56) did not improve cell survival. Collectively, these studies confirm that IGF-1 does not reduce cell death in the ongoing ischemic environment. Expression of IGF1R in hBMECs were confirmed with qRT-PCR and did not show any difference between normoxia and OGD.

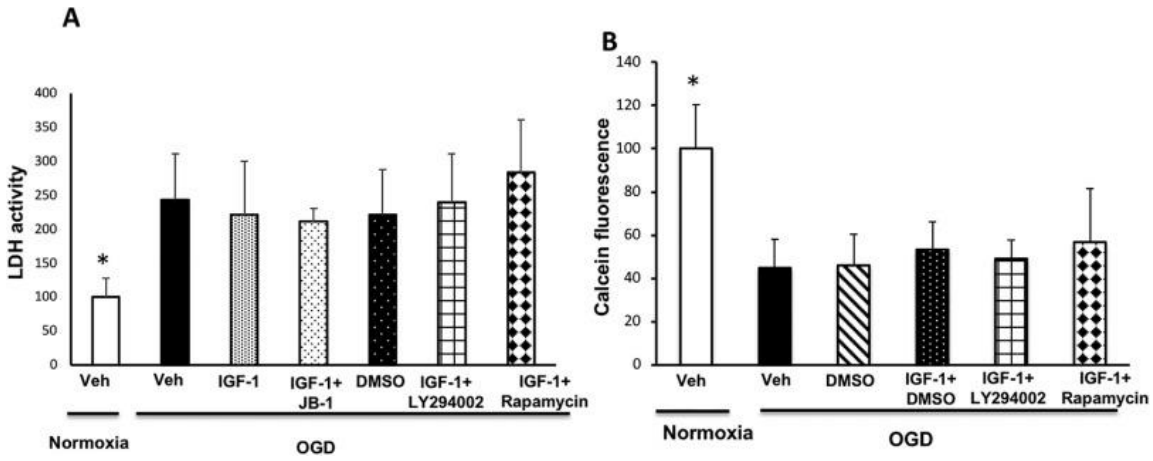

Figure 3-1: Graphical Representation of the Effect of IGF-1 on hBMECs cell adhesion and cytoskeletal organization.
Compared to normoxic conditions (A and B), cultures exposed to OGD show retracted cells with low vinculin labeling (C) and bright stress fibers (green phalloidin, D). IGF-1-treated cells displayed flattened cell morphology, similar to normoxic conditions, with brighter vinculin staining both in the cytoplasm and at the cell perimeter (E), with fewer stress fibers compared to OGD (F), while this pattern was reversed in cells treated concurrently with IGF-1 + JB-1 (G&H). Bar: 50 um.

3.4.2. IGF-1 preserved the actin cytoskeleton of human brain microvascular endothelial cells after OGD

To determine whether IGF-1 improved endothelial cytoskeletal organization and cell adherence under OGD, cells were probed for phalloidin (actin) and vinculin, a membrane-cytoskeletal protein associated with cell-cell and cell-matrix junctions. Normoxic cells displayed either round or flattened profiles, with actin staining (in green, Figure 3-2B) localized to the edges of the cell (circular actin). While flattened cells displayed pale phalloidin staining, vinculin labeling (shown in red; Figure 3-2A) was seen in the cytoplasm as well as at the cell perimeter. Oxygen-glucose deprivation (OGD) visibly decreased cell density and caused cytoskeletal reorganization of surviving cells. Thick, brightly stained stress fibers (in green) can be seen in cells that are elongated (Figure 3-2C,) and with decreased vinculin staining. Under the same conditions, cells treated with IGF-1 showed flattened cell morphology with bright vinculin labeling in the cytoplasm and at the edges (Figure 3-2E) with reduced density of polymerized actin across the cells (Figure 3-2F). This pattern was reversed by concurrent treatment with JB-1. Cells treated concurrently with IGF-1 + JB-1 closely resembled the OGD treated cultures in the pattern of brightly stained stress fibers with more retraction of actin and diffuse vinculin labeling (Figure 3-2 G and H) indicating a receptor-mediated effect of IGF-1 on cytoskeletal reorganization.

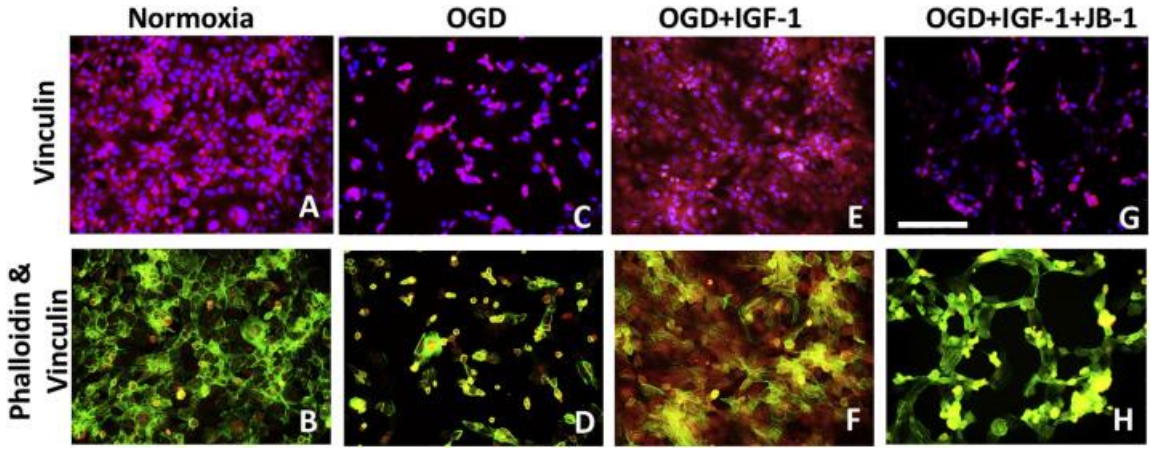

Figure 3-2: Cytology of the Effect of IGF-1 on hBMECs cell adhesion and cytoskeletal organization.
Compared to normoxic conditions (A and B), cultures exposed to OGD show retracted cells with low vinculin labeling (C) and bright stress fibers (green phalloidin, D). IGF-1-treated cells displayed flattened cell morphology, similar to normoxic conditions, with brighter vinculin staining both in the cytoplasm and at the cell perimeter (E), with fewer stress fibers compared to OGD (F), while this pattern was reversed in cells treated concurrently with IGF-1 + JB-1 (G&H). Bar: 50 um.

To quantify the extent of OGD-dependent retraction of the endothelial cell monolayer, cultures were stained with lectin (Figure 3-3Ai). Lectin staining further confirmed that oxygen glucose deprivation caused significant retraction of cells resulting in discontinuous aggregates of small groups of cells. This pattern was quantified using a novel algorithm that calculates intercellular (IC) spaces (Figure 3-3Aii). This analysis showed an overall affect of OGD and IGF-1 on interceullar spaces ($F(3,12)$: 5.864, $p = 0.020$). Specifically, OGD increased intercellular spaces as compared to normoxia ($p = 0.017$), while IGF-1 treatment reduced cell shrinkage due to OGD, and was no different from normoxia ($p = 0.226$). IGF-1 effects were reversed in cultures

concurrently exposed to IGF-1 + JB1 ($p = 0.004$, compared to normoxia). Quantitation of the intercellular gaps (Figure 3-3Bii) also confirmed that IGF-1 signaling inhibitors had distinct effects on IC spaces ($F(5,12)$: 4.99, $p = 0.01$). Thus while OGD and OGD (vehicle control or DMSO) caused a > 5 fold increase in intercellular spaces as compared to normoxic cultures ($p = 0.001$), this was reversed by. IGF1 ($p > 0.05$). The effect of IGF-1 on IC spaces was abrogated by concurrent treatment with LY294002 ($p = 0.020$ compared to normoxia), but not Rapamycin ($p = 0.277$) compared to normoxia), indicating that IGF-1 actions on the endothelial monolayer are mediated by PI3K but not the mTOR pathway.

3.4.3. Impact of IGF-1 on microvessel architecture in vivo

To determine if IGF-1 acts on microvessel anchorage and morphology in vivo, middle-aged female rats were subject to MCAo for 90 mins and treated with IGF-1 or IGF-1 + JB-1 or aCSF (vehicle) 2 h after the onset of ischemia. Neurological score, an assessment of motor function, was performed 24 h after reperfusion by an investigator (AO) blind to the treatment conditions. Vehicle-treated controls had a high mean score (4.28) indicative of greater disability, as compared to IGF-1-treated animals (2.5) ($p = 0.0477$) (Figure 3-4). In contrast, animals that received concurrent IGF-1 + JB-1 performed as poorly (3.9), as the vehicle-treated controls ($p = 0.612$) and were significantly higher than animals which received IGF-1 only ($p = 0.016$), indicating that IGF-1 treatment protects motor function and mobility post-stroke in a receptor-mediated process.

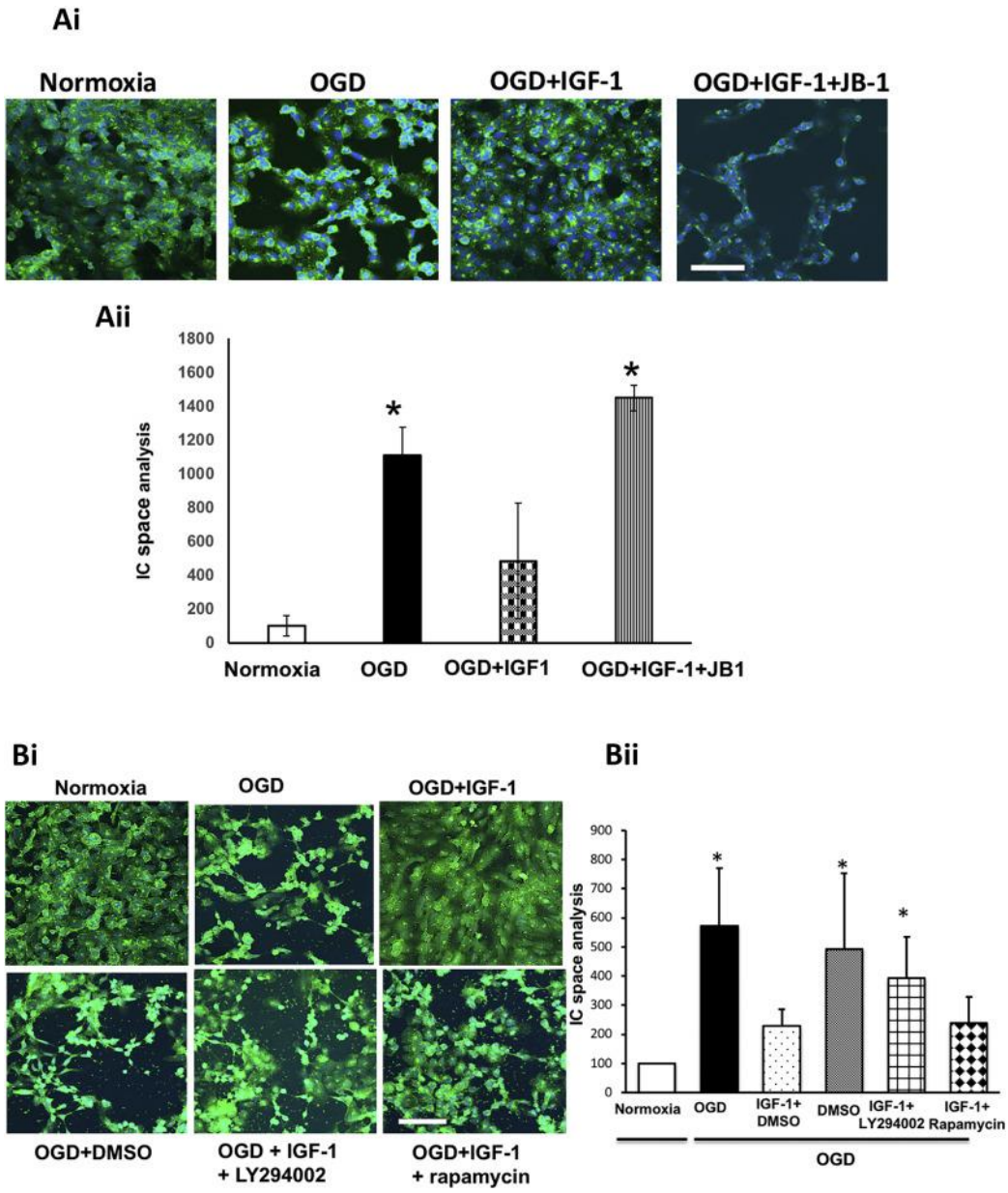

Figure 3-3: Lectin staining of human brain microvessel endothelial cells (hBMEC) under normoxic and OGD conditions

Ai. Effect of IGF-1 and its receptor antagonist on intercellular spaces: Photomicrographs of lectin-stained cultures show that the even, confluent monolayer seen in normoxia is changed under OGD to smaller, densely-stained cells with large intercellular spaces.

Intercellular spaces were completely abrogated in IGF-1 treated cultures and this was reversed with concurrent exposure to JB-1. Aii Histogram shows average intercellular space estimates using the Canny Edge algorithm. B ii. Effect of IGF-1 and signaling pathway inhibitors on intercellular spaces: Photomicrographs of lectin-stained cultures confirm that IGF-1 abrogates intercellular spaces caused by OGD. All experimental groups are compared to the normoxia group. Concurrent treatment with IGF-1 + LY294002 treated cultures shows greater gaps between cells compared to IGF-1 group, while concurrent treatment with Rapamycin is no different from IGF-1 alone. Each data point is the average of 3 technical replicates, and shown here is the average from 3 separate experiments. *$p < 0.05$. Bar: 100 um.

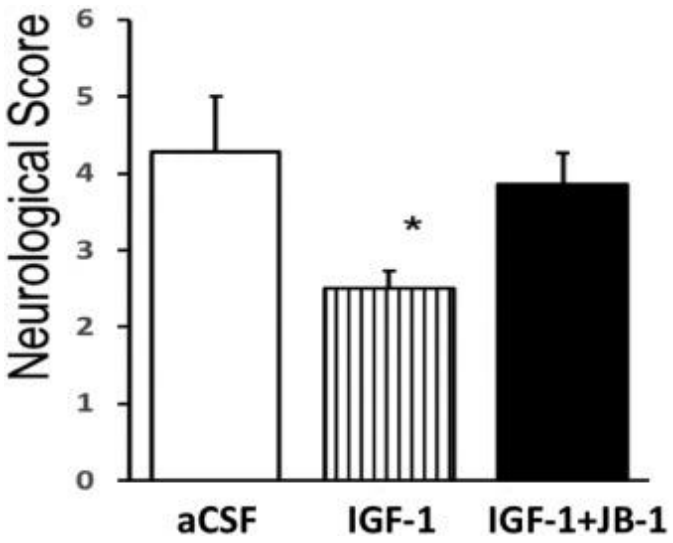

Figure 3-4: Effect of post-stroke IGF-1 treatment on neurological function 1 day after MCAo

Histogram depicts mean neurological score of vehicle (artificial CSF; aCSF), IGF-1 and IGF-1 + JB-1 treated groups. Neurological function was significantly better in IGF-1-treated animals as compared to vehicle control and IGF-1 + JB-1 treated groups. All graphs represent mean ± S.E.M., n = 5–7 in each group, * $p < 0.05$.

3.4.4. Effect of post-stroke IGF-1 treatment on vinculin staining

Brain sections from animals subject to MCAo were probed for vinculin immunohistochemistry. Striatal and overlying cortical regions were analyzed for density of vinculin labeling. Representative sections of each group at 1 day post stroke are shown in Figure 3-5A. Punctate vinculin label was seen in the cortex and striatum of all experimental groups 24 h after ischemia-reperfusion (Figure 3-5A), however, vinculin staining density was significantly higher in the IGF-1-treated group as compared to the vehicle-treated controls or to groups that received concurrent IGF-1 + JB-1 ($F(2,13)$:

5.021; p = 0.028) (interaction effect). At 5-day post-stroke, there was no statistical difference in vinculin staining density between treatment groups (Figure 3-5B).

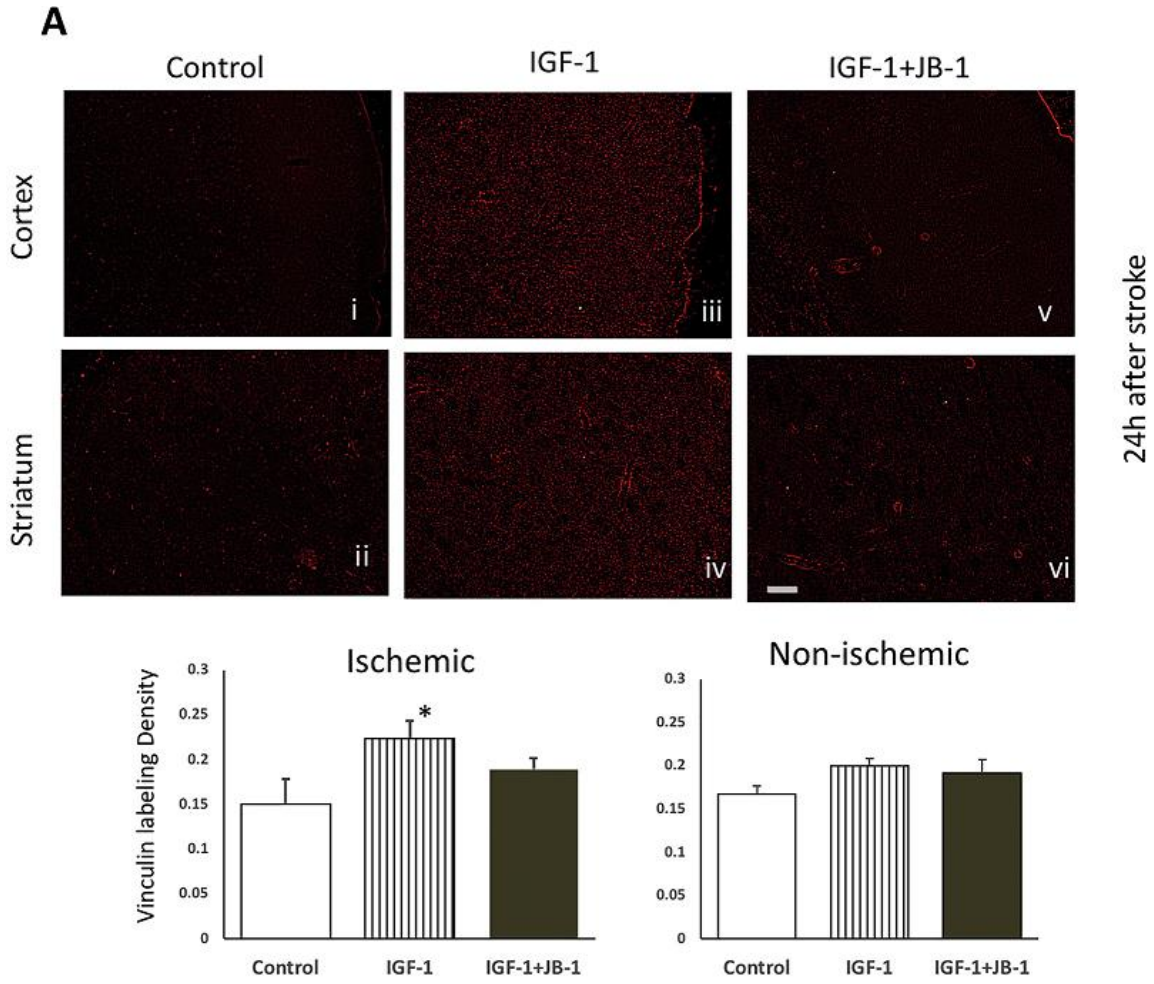

Figure 3-5: Effect of post-stroke IGF-1 treatment on vinculin expression (A) 1d post stroke

Effect of post-stroke IGF-1 treatment on vinculin expression (A) 1d post stroke: Photomicrographs of vinculin immunostained representative sections from the ischemic cortex and striatum of control (i,ii), IGF-1 treated (iii,iv) and IGF-1 + JB-1 treated (v,vi) animals. Histograms depict mean and SEM of the density of vinculin staining in each

group in the ischemic and non-ischemic hemisphere. (B) 5d after stroke: Photomicrographs of vinculin immunostained representative sections from the ischemic cortex and striatum of control (i,ii), IGF-1 treated (iii,iv) and IGF-1 + JB-1 treated (v,vi) animals. Histograms depict mean and SEM of the density of vinculin staining in each group in the ischemic and non-ischemic hemisphere. N = 4–6 in each group. *: $p < 0.05$. Bar: 100 um.

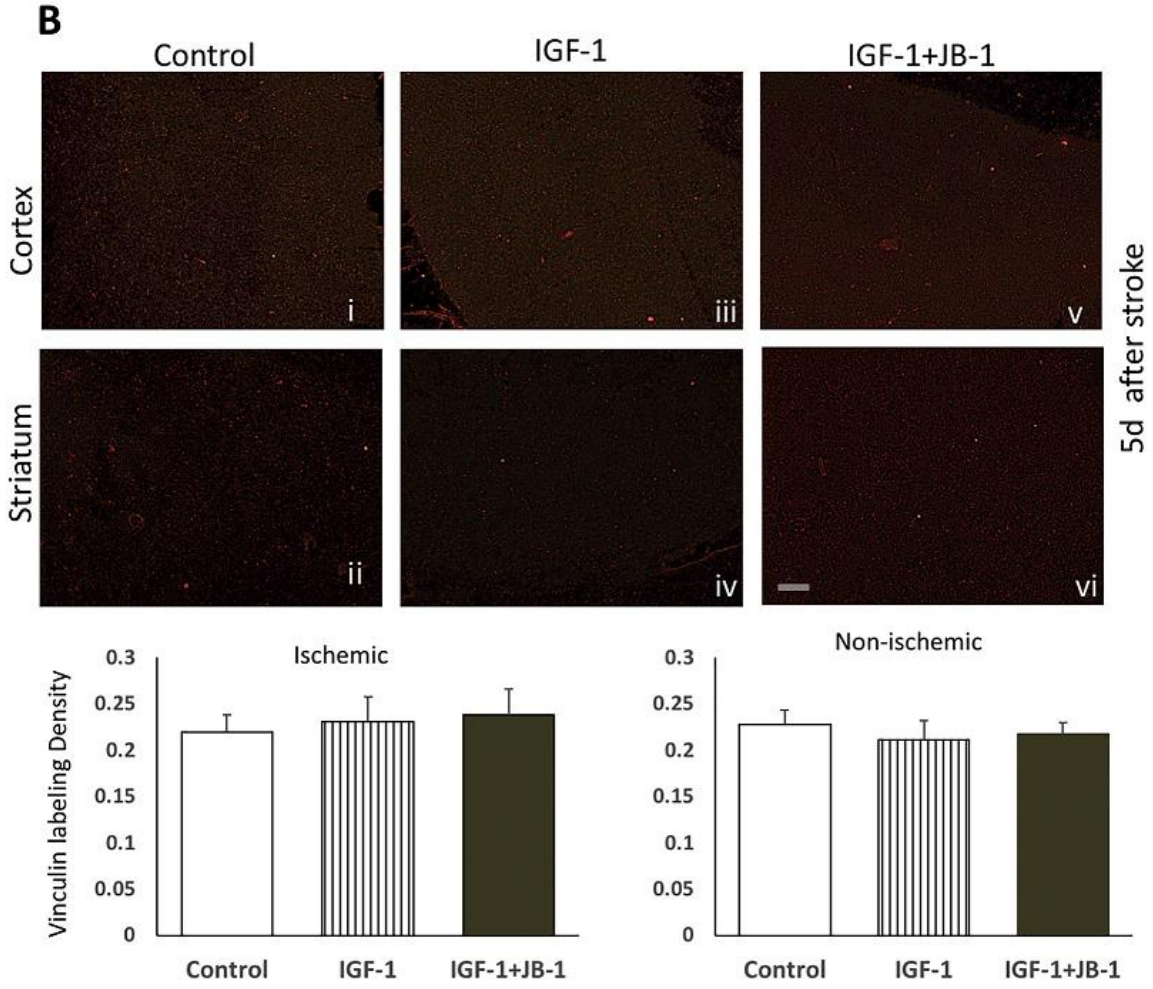

Figure 3-5 Continued

3.4.5. Effect of post-stroke IGF-1 treatment on microvessel morphology

Sections from control, IGF-1 and IGF-1 + JB-1 treated groups subject to MCAo were stained for lectin histochemistry. Representative sections of each group at 1 day post-stroke is shown in Figure 3-6A. A minimum of 50 vessels were analyzed per animal and grouped as small (1–5 μm) medium (6–10 μm) or large (11+ μm) diameter vessels. In the ischemic hemisphere, IGF-1-treated animals had a significantly greater proportion of large diameter vessels as compared to vehicle-treated controls or JB-1 treated animals ($F(2,11) = 21.707$; $p < 0.001$) and the lowest proportion of small diameter vessels ($F(2,11) = 9.696$; $p = 0.004$), indicating that IGF-1 treatment skews the distribution towards larger-diameter microvessels. A similar pattern was also seen in the non-ischemic hemisphere, where IGF-1 treated animals displayed the highest proportion of large diameter vessels ($F(2,12) = 6.639$; $p < 0.011$), and the lowest proportion of small diameter vessels ($1F(2,12) = 8.752$; $p = 0.005$) as compared to vehicle treated controls and JB-1 treated animals.

At 1 day post stroke, microvessel length was partly influenced by IGF-1 treatment. There was a significant decrease in the proportion of short length vessels ($F(2,11) = 4.169$; $p < 0.042$), and a trend towards longer length vessels ($F(2,12) = 3.01$; $p < 0.087$) in IGF-1 treated animals as compared to vehicle treated controls or JB-1 treated animals (Figure 3-6A). On the non-ischemic hemisphere, there were no differences in vessel length between IGF-1 and vehicle treated controls.

At 5 days post stroke (Figure 3-6B), all groups had a similar proportion (19%–20%) of large diameter vessels, while IGF-1 treated animals had more small diameter

vessels and fewer medium diameter vessels as compared to vehicle treated controls or JB-1 treated animals. No treatment effects were noted for the non-ischemic hemisphere at 5d post stroke, although most microvessels fell in the medium and large diameter category unlike the ischemic side where most vessels fell in the medium and small diameter category, indicating an overall shift in vessel diameter due to ischemia.

There were no treatment effects on microvessel length at 5d after stroke, in either the ischemic or non-ischemic hemisphere (Figure 3-6B). Moreover, both sides showed similar distributions in small, medium and large length vessels. Overall, IGF-1 exerted an early effect on vessel diameter.

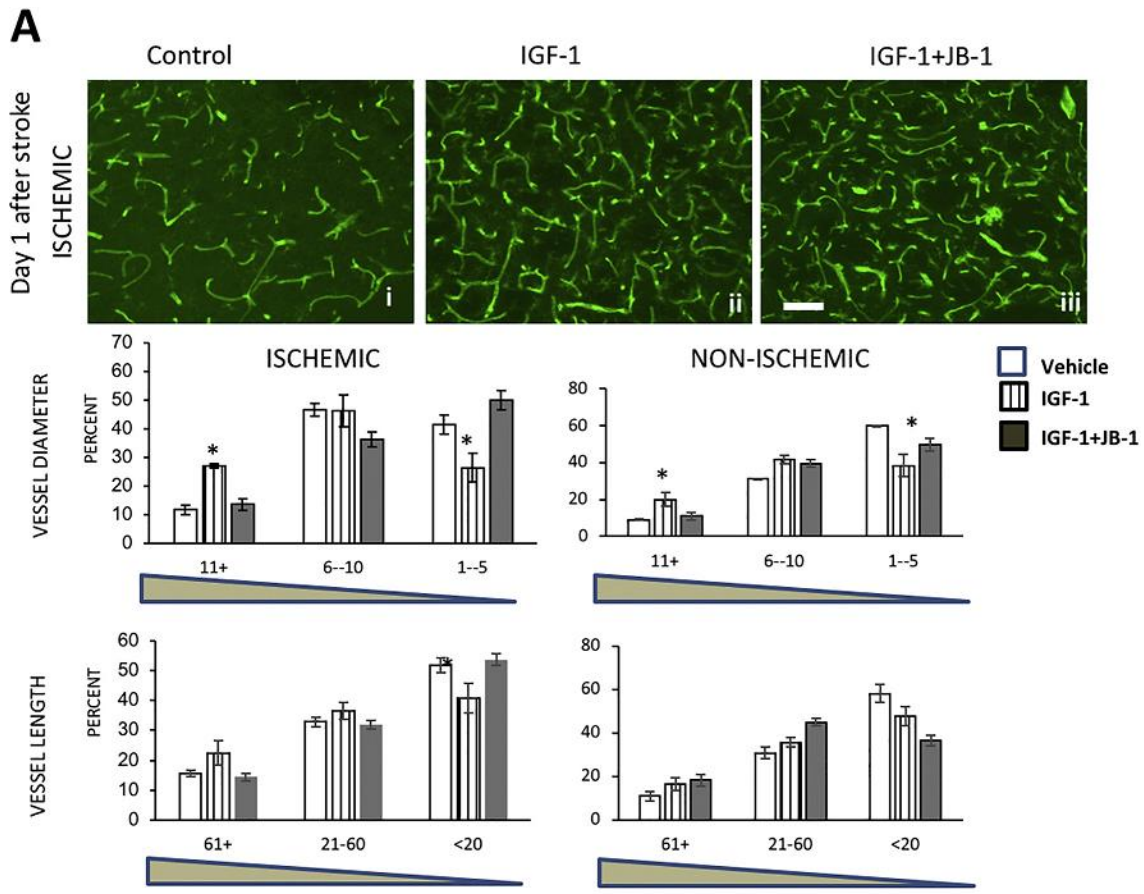

Figure 3-6: Effect of post-stroke IGF-1 treatment on microvessel morphology.
(A) 1d post stroke: Photomicrographs of lectin-sectioned microvessels from the ischemic hemisphere of control (i), IGF-1 treated (ii) and IGF-1 + JB-1 treated (iii) animals. Histograms depict the mean distribution of microvessel diameter (top) and microvessel length (bottom) from the ischemic and non-ischemic hemisphere. IGF-1 treated animals showed greater number of vessels in the largest bin (11+) compared to vehicle control or IGF + JB-1 treated groups in both ischemic and non-ischemic sides, and fewer short length vessels on the ischemic hemisphere. * $p < 0.05$, main effect of IGF1 treatment. (B) 5d post stroke: Photomicrographs of lectin-stained microvessels from the ischemic

hemisphere of control (i), IGF-1 treated (ii) and IGF-1 + JB-1 treated (iii) animals. Histograms depict the mean distribution of microvessel diameter (top) and microvessel length (bottom) from the ischemic and non-ischemic hemisphere. IGF-1-treated animals showed greater number of small diameter vessels as compared to other two groups in the ischemic hemisphere. N = 4–6 in each group. * $p < 0.05$, Bar: 100 um.

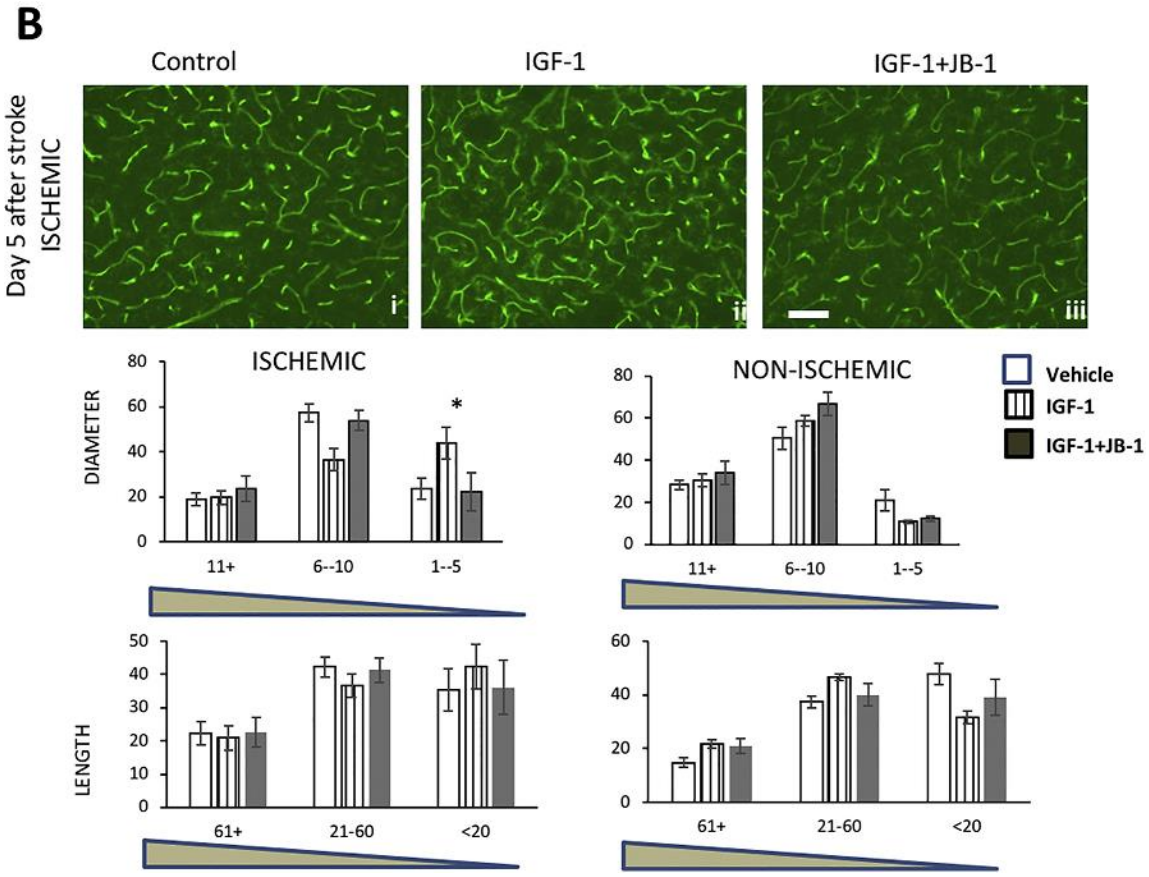

Figure 3-6 Continued

3.5. Discussion

Our previous work showed that IGF-1 treatment to endothelial cell cultures protects the barrier properties of these cells under OGD conditions. We also reported that IGF-1 does not prevent cell death during OGD conditions, which seems paradoxical

in light of IGF-1's effects on barrier function. The current studies provide an answer to this paradox, by showing that while OGD conditions cause endothelial cells shrinkage (and therefore prominent intercellular spaces), IGF-1 treatment preserves the flattened morphology and anchorage of surviving cells (fewer intercellular spaces), thus potentially maintaining a more effective barrier. In view of the short duration of OGD (6 h), it is unlikely that the reduced intercellular space is due to cell proliferation, and likely represents IGF-1 action on the actin cytoskeleton of surviving cells. In vivo, microvessel diameter, a surrogate measure of cell contraction (Shen et al., 2009) showed that IGF-1 treated animals had larger microvessel diameter in the ischemic region at 24 h after stroke and greater density of vinculin staining, further supporting the idea that IGF-1 stabilizes the endothelium. Together with our previous in vivo studies showing that IGF-1 treatment to middle-aged female rats decreases BBB permeability (Bake et al., 2014) and infiltration of CD4+ cells into the ischemic brain (Bake et al., 2016), the current studies show that IGF-1 is a vasculoprotective factor in stroke.

IGF-1 is considered neuroprotective because it reduces ischemic injury in many species (Gluckman et al., 1992; Lee et al., 1992; Johnston et al., 1996; Guan et al., 2001) and promotes neuronal survival, neuronal myelination and angiogenesis (Wang et al., 2000; Smith, 2003). However, vascular pathology is among the earliest events in ischemic stroke. During the acute phase after reperfusion, accumulation of toxic oxygen radicals impair endothelial function leading to a leaky blood brain barrier. In the hours following stroke (sub-acute phase), barrier permeability is increased due to the generation of inflammatory cytokines, endothelial adhesion molecules and proteinases

such as MMPs that cause pathologic remodeling of the endothelium and the basement membrane. The chronic phase of stroke (days/weeks) involves regulation of apoptotic genes which leads to cell death as well as angiogenic factors that lead to repair. A recent study (Shi et al., 2016) showed that blood brain barrier leakiness seen in the earliest phase of ischemia (30 min) is independent of matrix cleavage and MMP production. During this time, BBB undergoes subtle changes including the rapid reorganization of the actin cytoskeleton in endothelial cells, which alters their morphology and permits fluid and small molecules to enter the brain, and these events precede neuronal damage. Accordingly, MMP-9 gene deletion failed to ameliorate the early leakiness of the BBB to small-sized dextrans, while overexpression of the actin depolymerization factor reduced leakiness to the small sized dextrans (Shi et al., 2016). This early 'hyper-permeability' of the BBB facilitates diapedesis of peripheral immune cells and extravasation of plasma proteins that are toxic to neurons. Our studies suggest that IGF-1 may rescue infarct volume using a similar vasculoprotective strategy. Thus, IGF-1 treatment after MCAo reduces infarct volume when measured at 24 h, which is preceded by reduced BBB hyper-permeability in the early hours after stroke (4 h) (Bake et al., 2014). The current studies build on this foundation to show that IGF-1 treatment acts directly on endothelial cells to preserve the actin cytoskeleton and its anchorage.

The in vitro model used in these studies show that the effect of IGF-1 on endothelial cell geometry is mediated by the PI3K pathway. Oxygen glucose deprivation (OGD) is commonly used to model cerebral ischemia in vitro (Doukas et al., 1994; Stanimirovic et al., 1997; Guo et al., 2012; Bake et al., 2016), and produces many of the

same events seen in in vivo ischemic models, including activation of cell death pathways (Liao et al., 2016), generation of reactive oxygen species, reduced ATP production (Imai et al., 2017), and dysregulates tight junction protein expression and barrier function (Shi et al., 2016). IGF-1 is known to regulate the PI3K/Akt signaling pathway in several cell types. In mouse fibroblasts, for example, IGF-1 reduces OGD-induced cell death which is reversed by the PI3K inhibitor LY294002 (Liu et al., 2017). However, inhibition of mTOR via rapamycin did not abrogate the effect of IGF-1 on intercellular spaces. This finding is surprising since recent studies show that, in addition to its role in cell survival, autophagy, nutrient/energy sensing, mTOR is also implicated in cell adhesion (Chen et al., 2015). Alternately, this process may be mediated by mTOR2, which is rapamycin insensitive (Jacinto et al., 2004).

Changes in endothelial cell geometry is commonly seen after ischemia and ischemia-induced generation of free radicals and inflammatory cytokines (Gulino-Debrac, 2013; Stamatovic et al., 2016). Formation of thick stress fibers results in cell contractions, loss of anchorage to the matrix, and loss of tight junctions. OGD increases stress fiber formation thus changing cell geometry to a narrow, elongated form and reduces anchorage to the matrix (van der Heijden et al., 2008; Gao et al., 2012; Alluri et al., 2014). Disorganized actin cytoskeleton, such as in the dystrophin KO mouse, leads to increased vascular permeability (Nico et al., 2003), indicating the importance of actin assembly in the maintenance of the endothelial barrier. IGF-1 may alter cytoskeletal dynamics through regulation of cell adhesion via extracellular matrix proteins such as collagen and integrins(Valastyan and Weinberg, 2011). This process may occur through

IGF-1 regulation of small non-coding RNA (miRNA) that act as translational repressors. Mir29 has been shown to increase collagen deposition and to improve outcomes in a renal injury model (Liu et al., 2010), and reduce fibrotic scars in a rat model of myocardial infarction (van Rooij et al., 2008). In silico analysis of vinculin shows consensus sites for mir29 and mir33, both of which are regulated by IGF-1 in vivo (Bake et al., 2016). However, further studies are warranted to examine the cytoskelelal regulatory role of these miRNAs in coordinating endothelial actin re-organization and cell-matrix adhesion under ischemia.

The present study also indicates that IGF-1 may exert different effects in the early and late acute stages of ischemia. IGF-1 has been shown to affect more immediate processes such as glucose metabolism in astrocytes (Hernandez-Garzon et al., 2016) and activation of PI-3 K/Akt signaling in microglia (Streit, 2002) and cerebellar neurons (Dudek et al., 1997), as well as long-term changes such as proliferation (Torres-Aleman et al., 1998) and neurogenesis in the hypothalamus, olfactory bulb and hippocampus (Pixley et al., 1998; Perez-Martin et al., 2010; Pardo et al., 2016). Some of these processes may be linked such that early effects on actin cytoskeleton and substrate adhesion may have durable effects on other aspects of stroke recovery such as cell survival, while others may be independent processes. This may be specifically relevant in the case of microvessel morphology. Microvessel density and diameter are reduced during occlusion of the parent vessel, and then recover gradually at reperfusion and in the days following the stroke (Dziennis et al., 2015). Thus, in the control group, the proportion of microvessels in the large bin increases from day 1 after stroke to day 5. In

the IGF-1 group, the proportion of microvessels in the same large bin stays relatively stable between day 1 and day 5. Thus, it appears that IGF-1 prevents microvessel shrinkage during the crucial early period of ischemia, possibly improving microcirculation in the ischemic hemisphere, and subsequently decreasing blood brain barrier permeability and inflammation (shown in our previous studies (Bake et. al., 2014; Bake et. al., 2016).

In conclusion, the data from the present study underscores the importance of the microvasculature as an important early target for stroke therapies in older females, and IGF-1 as a good candidate for stroke therapy. However, defining the effective dose and timing of IGF-1 will be critical for translational applications, since the majority of stroke patients may not arrive at a medical facility prior to 2 h. While IGF-1 improves stroke recovery, its effectiveness diminishes when the treatment is delayed. In a study comparing normotensive and hypertensive male rats, subcutaneous IGF-1 significantly decreased infarct volume when given 30 mins after ischemia, but not at 2 h or 4 h later (De Geyter et al., 2013). Similarly, intranasal IGF-1 was more effective in reducing infarct volumes when given at 2 h post-stroke (54%), as compared to 4 h after stroke (39%), however behavioral improvement was only seen with early (2 h) treatment (Liu et al., 2004), similar to data from our studies. The evidence presented here shows that IGF-1's later neuroprotective actions are likely preceded by its early vasculoprotective effects.

3.6. References

Alluri, H., Stagg, H.W., Wilson, R.L., Clayton, R.P., Sawant, D.A., Koneru, M., Beeram, M.R., Davis, M.L., Tharakan, B., 2014. Reactive oxygen species-caspase-3 relationship in mediating blood-brain barrier endothelial cell hyperpermeability following oxygen-glucose deprivation and reoxygenation. *Microcirculation* 21, 187–195.

Bake, S., Selvamani, A., Cherry, J., Sohrabji, F., 2014. Blood brain barrier and neuroinflammation are critical targets of IGF-1-mediated neuroprotection in stroke for middle-aged female rats. *PLoS One* 9, e91427.

Bake, S., Okoreeh, A.K., Alaniz, R.C., Sohrabji, F., 2016. Insulin-like growth factor (IGF)-I modulates endothelial blood-brain barrier function in ischemic middle-aged female rats. *Endocrinology* 157, 61–69.

Baldo, C., Lopes, D.S., Faquim-Mauro, E.L., Jacysyn, J.F., Niland, S., Eble, J.A., Clissa, P.B., Moura-Da-Silva, A.M., 2015. Jararhagin disruption of endothelial cell anchorage is enhanced in collagen enriched matrices. *Toxicon* 108, 240–248.

Borlongan, C.V., Glover, L.E., Sanberg, P.R., Hess, D.C., 2012. Permeating the blood brain barrier and abrogating the inflammation in stroke: implications for stroke therapy. *Curr. Pharm. Des.* 18, 3670–3676.

Chen, L., Xu, B., Liu, L., Liu, C., Luo, Y., Chen, X., Barzegar, M., Chung, J., Huang, S., 2015. Both mTORC1 and mTORC2 are involved in the regulation of cell adhesion. *Oncotarget* 6, 7136–7150.

De Geyter, D., Stoop, W., Sarre, S., De Keyser, J., Kooijman, R., 2013. Neuroprotective efficacy of subcutaneous insulin-like growth factor-I administration in normotensive and hypertensive rats with an ischemic stroke. *Neuroscience* 250, 253–262.

Dimitrijevic, O.B., Stamatovic, S.M., Keep, R.F., Andjelkovic, A.V., 2007. Absence of the chemokine receptor CCR2 protects against cerebral ischemia/reperfusion injury in mice. *Stroke* 38, 1345–1353.

Dinapoli, V.A., Huber, J.D., Houser, K., Li, X., Rosen, C.L., 2008. Early disruptions of the blood-brain barrier may contribute to exacerbated neuronal damage and prolonged functional recovery following stroke in aged rats. *Neurobiol. Aging* 29, 753–764.

Doukas, J., Cutler, A.H., Boswell, C.A., Joris, I., Maino, G., 1994. Reversible endothelial cell relaxation induced by oxygen and glucose deprivation. A model of ischemia in vitro. *Am. J. Pathol*. 145, 211–219.

Dudek, H., Datta, S.R., Franke, T.F., Birnbaum, M.J., Yao, R., Cooper, G.M., Segal, R.A., Kaplan, D.R., Greenberg, M.E., 1997. Regulation of neuronal survival by the serinethreonine protein kinase Akt. *Science* 275, 661–665.

Dziennis, S., Qin, J., Shi, L., Wang, R.K., 2015. Macro-to-micro cortical vascular imaging underlies regional differences in ischemic brain. *Sci. Rep.* 5, 10051.

Gao, C., Li, R., Liu, Y., Ma, L., Wang, S., 2012. Rho-kinase-dependent F-actin rearrangement is involved in the release of endothelial microparticles during IFNalpha-induced endothelial cell apoptosis. *J. Trauma Acute Care Surg*. 73, 1152–1160.

Gidday, J.M., Gasche, Y.G., Copin, J.C., Shah, A.R., Perez, R.S., Shapiro, S.D., Chan, P.H., Park, T.S., 2005. Leukocyte-derived matrix metalloproteinase-9 mediates blood-brain barrier breakdown and is proinflammatory after transient focal cerebral ischemia. Am. J. Physiol. Heart Circ. *Physiol.* 289, H558–H568.

Gluckman, P., Klempt, N., Guan, J., Mallard, C., Sirimanne, E., Dragunow, M., Klempt, M., Singh, K., Williams, C., Nikolics, K., 1992. A role for IGF-1 in the rescue of CNS neurons following hypoxic-ischemic injury. *Biochem. Biophys. Res. Commun*. 182, 593–599.

Guan, J., Miller, O.T., Waugh, K.M., McCarthy, D.C., Gluckman, P.D., 2001. Insulin-like growth factor-1 improves somatosensory function and reduces the extent of cortical infarction and ongoing neuronal loss after hypoxia-ischemia in rats. *Neuroscience* 105, 299–306.

Gulino-Debrac, D., 2013. Mechanotransduction at the basis of endothelial barrier function. *Tissue Barriers* 1, e24180.

Guo, J., Duckles, S.P., Weiss, J.H., Li, X., Krause, D.N., 2012. 17beta-Estradiol prevents cell death and mitochondrial dysfunction by an estrogen receptor-dependent mechanism in astrocytes after oxygen-glucose deprivation/reperfusion. *Free Radic. Biol. Med.* 52, 2151–2160.

Hernandez-Garzon, E., Fernandez, A.M., Perez-Alvarez, A., Genis, L., Bascunana, P., Fernandez De La Rosa, R., Delgado, M., Angel Pozo, M., Moreno, E., McCormick, P.J., Santi, A., Trueba-Saiz, A., Garcia-Caceres, C., Tschop, M.H., Araque, A., Martin, E.D., Torres Aleman, I., 2016. The insulin-like growth factor I receptor regulates glucose transport by astrocytes. *Glia.* 64, 1962–1971.

Imai, T., Mishiro, K., Takagi, T., Isono, A., Nagasawa, H., Tsuruma, K., Shimazawa, M., Hara, H., 2017. Protective effect of bendavia (SS-31) against oxygen/glucose-

deprivation stress-induced mitochondrial damage in human brain microvascular endothelial cells. *Curr. Neurovasc. Res.* 14, 53–59.

Jacinto, E., Loewith, R., Schmidt, A., Lin, S., Ruegg, M.A., Hall, A., Hall, M.N., 2004. Mammalian TOR complex 2 controls the actin cytoskeleton and is rapamycin insensitive. *Nat. Cell Biol*. 6, 1122–1128.

Johnston, B.M., Mallard, E.C., Williams, C.E., Gluckman, P.D., 1996. Insulin-like growth factor-1 is a potent neuronal rescue agent after hypoxic-ischemic injury in fetal lambs. *J. Clin. Invest*. 97, 300–308.

Khatri, R., McKinney, A.M., Swenson, B., Janardhan, V., 2012. Blood-brain barrier, reperfusion injury, and hemorrhagic transformation in acute ischemic stroke. *Neurology* 79, S52–S57.

Kleinschnitz, C., Wiendl, H., 2013. Con: Regulatory T cells are protective in ischemic stroke. *Stroke* 44, e87–e88.

Kreuger, J., Phillipson, M., 2016. Targeting vascular and leukocyte communication in angiogenesis, inflammation and fibrosis. *Nat. Rev. Drug Discov.* 15, 125–142.

Lee, W.H., Clemens, J.A., Bondy, C.A., 1992. Insulin-like growth factors in the response to cerebral ischemia. *Mol. Cell. Neurosci*. 3, 36–43.

Liao, L.X., Zhao, M.B., Dong, X., Jiang, Y., Zeng, K.W., Tu, P.F., 2016. TDB protects vascular endothelial cells against oxygen-glucose deprivation/reperfusion-induced injury by targeting miR-34a to increase Bcl-2 expression. *Sci. Rep*. 6, 37959.

Liu, X.F., Fawcett, J.R., Hanson, L.R., Frey 2nd, W.H., 2004. The window of opportunity for treatment of focal cerebral ischemic damage with noninvasive intranasal insulin like growth factor-I in rats. *J. Stroke Cerebrovasc. Dis.* 13, 16–23.

Liu, F., Yuan, R., Benashski, S.E., McCullough, L.D., 2009. Changes in experimental stroke outcome across the life span. *J. Cereb. Blood Flow Metab*. 29, 792–802.

Liu, Y., Taylor, N.E., Lu, L., Usa, K., Cowley Jr., A.W., Ferreri, N.R., Yeo, N.C., Liang, M., 2010. Renal medullary microRNAs in Dahl salt-sensitive rats: miR-29b regulates several collagens and related genes. *Hypertension* 55, 974–982.

Liu, Q., Guan, J.Z., Sun, Y., Le, Z., Zhang, P., Yu, D., Liu, Y., 2017. Insulin-like growth factor 1 receptor-mediated cell survival in hypoxia depends on the promotion of autophagy via suppression of the PI3K/Akt/mTOR signaling pathway. *Mol. Med. Rep*. 15, 2136–2142.

Merali, S., Cameron, J.I., Barclay, R., Salbach, N.M., 2016. Characterising community exercise programmes delivered by fitness instructors for people with neurological conditions: a scoping review. *Health Soc. Care Community* 24, e101–e116.

Montagne, A., Barnes, S.R., Sweeney, M.D., Halliday, M.R., Sagare, A.P., Zhao, Z., Toga, A.W., Jacobs, R.E., Liu, C.Y., Amezcua, L., Harrington, M.G., Chui, H.C., Law, M.,Zlokovic, B.V., 2015. Blood-brain barrier breakdown in the aging human hippocampus. *Neuron* 85, 296–302.

Moskowitz, M.A., Lo, E.H., Iadecola, C., 2010. The science of stroke: mechanisms in search of treatments. *Neuron* 67, 181–198.

Nico, B., Frigeri, A., Nicchia, G.P., Corsi, P., Ribatti, D., Quondamatteo, F., Herken, R., Girolamo, F., Marzullo, A., Svelto, M., Roncali, L., 2003. Severe alterations of endothelial and glial cells in the blood-brain barrier of dystrophic mdx mice. *Glia* 42, 235–251.

Okoreeh, A.K., Bake, S., Sohrabji, F., 2017. Astrocyte-specific insulin-like growth factor-1 gene transfer in aging female rats improves stroke outcomes. *Glia* 65, 1043–1058.

Pardo, J., Uriarte, M., Console, G.M., Reggiani, P.C., Outeiro, T.F., Morel, G.R., Goya, R.G., 2016. Insulin-like growth factor-I gene therapy increases hippocampal neurogenesis, astrocyte branching and improves spatial memory in female aging rats. *Eur. J. Neurosci.* 44, 2120–2128.

Paxinos, G., Watson, C., 1986. The Rat Brain in Stereotaxic Coordinates. *Academic Press Inc*, New York.

Perez-Martin, M., Cifuentes, M., Grondona, J.M., Lopez-Avalos, M.D., Gomez-Pinedo, U., Garcia-Verdugo, J.M., Fernandez-Llebrez, P., 2010. IGF-I stimulates neurogenesis in the hypothalamus of adult rats. *Eur. J. Neurosci.* 31, 1533–1548.

Pixley, S.K., Dangoria, N.S., Odoms, K.K., Hastings, L., 1998. Effects of insulin-like growth factor 1 on olfactory neurogenesis in vivo and in vitro. *Ann. N. Y. Acad. Sci.* 855, 244–247.

Pulsinelli, W., 1992. Pathophysiology of acute ischaemic stroke. Lancet 339, 533–536.

Selvamani, A., Sohrabji, F., 2010a. The neurotoxic effects of estrogen on ischemic stroke in older female rats is associated with age-dependent loss of insulin-like growth factor-1. *J. Neurosci*. 30, 6852–6861.

Selvamani, A., Sohrabji, F., 2010b. Reproductive age modulates the impact of focal ischemia on the forebrain as well as the effects of estrogen treatment in female rats. *Neurobiol. Aging* 31, 1618–1628.

Shen, Q., Wu, M.H., Yuan, S.Y., 2009. Endothelial contractile cytoskeleton and microvascular permeability. *Cell Health Cytoskeleton* 2009, 43–50.

Shi, Y., Zhang, L., Pu, H., Mao, L., Hu, X., Jiang, X., Xu, N., Stetler, R.A., Zhang, F., Liu, X., Leak, R.K., Keep, R.F., Ji, X., Chen, J., 2016. Rapid endothelial cytoskeletal reorganization enables early blood-brain barrier disruption and long-term ischaemic reperfusion brain injury. *Nat. Commun*. 7, 10523.

Smith, P.F., 2003. Neuroprotection against hypoxia-ischemia by insulin-like growth factor-I (IGF-I). *IDrugs* 6, 1173‑1177.

Stamatovic, S.M., Johnson, A.M., Keep, R.F., Andjelkovic, A.V., 2016. Junctional proteins of the blood-brain barrier: New insights into function and dysfunction. *Tissue Barriers* 4, e1154641.

Stanimirovic, D.B., Ball, R., Durkin, J.P., 1997. Stimulation of glutamate uptake and Na,KATPase activity in rat astrocytes exposed to ischemia-like insults. *Glia* 19, 123‑134.

Streit, W.J., 2002. Microglia as neuroprotective, immunocompetent cells of the CNS. *Glia* 40, 133‑139.

Torres-Aleman, I., Villalba, M., Nieto-Bona, M.P., 1998. Insulin-like growth factor-I modulation of cerebellar cell populations is developmentally stage-dependent and mediated by specific intracellular pathways. *Neuroscience* 83, 321‑334.

Valastyan, S., Weinberg, R.A., 2011. Roles for microRNAs in the regulation of cell adhesion molecules. *J. Cell Sci.* 124, 999‑1006.

van der Heijden, M., Versteilen, A.M., Sipkema, P., van Nieuw Amerongen, G.P., Musters, R.J., Groeneveld, A.B., 2008. Rho-kinase-dependent F-actin rearrangement is involved in the inhibition of PI3-kinase/Akt during ischemia-reperfusion-induced endothelial cell apoptosis. *Apoptosis* 13, 404‑412.

van Rooij, E., Sutherland, L.B., Thatcher, J.E., Dimaio, J.M., Naseem, R.H., Marshall, W.S., Hill, J.A., Olson, E.N., 2008. Dysregulation of microRNAs after myocardial infarction reveals a role of miR-29 in cardiac fibrosis. *Proc. Natl. Acad. Sci. U. S. A.*105, 13027‑13032.

Wang, J.M., Hayashi, T., Zhang, W.R., Sakai, K., Shiro, Y., Abe, K., 2000. Reduction of ischemic brain injury by topical application of insulin-like growth factor-I after transient middle cerebral artery occlusion in rats. *Brain Res.* 859, 381‑385.

Wu, L., Walas, S., Leung, W., Sykes, D.B., Wu, J., Lo, E.H., Lok, J., 2015. Neuregulin1-beta decreases IL-1beta-induced neutrophil adhesion to human brain microvascular endothelial cells. *Transl Stroke Res* 6, 116‑124.

Yang, Y., Estrada, E.Y., Thompson, J.F., Liu, W., Rosenberg, G.A., 2007. Matrix metalloproteinase- mediated disruption of tight junction proteins in cerebral vessels is reversed by synthetic matrix metalloproteinase inhibitor in focal ischemia in rat. *J. Cereb. Blood Flow Metab.* 27, 697‑709.

Zhu, L., Han, B., Wang, L., Chang, Y., Ren, W., Gu, Y., Yan, M., Wu, C., Zhang, X.Y., He, J., 2016. The association between serum ferritin levels and post-stroke depression. *J. Affect. Disord.* 190, 98‑102.

4. THIRD STUDY: ASTROCYTE-SPECIFIC INSULIN-LIKE GROWTH FACTOR-1 (IGF-1) GENE TRANSFER IN AGING FEMALE RATS IMPROVES STROKE OUTCOMES[3]

4.1. Overview of the Third Study

Middle aged female rats sustain larger stroke infarction and disability than younger female rats. This older group also shows age-related reduction of insulin like growth factor (IGF)-1 in serum and in astrocytes, a cell type necessary for post stroke recovery. To determine the impact of astrocytic IGF-1 for ischemic stroke, these studies tested the hypothesis that gene transfer of IGF-1 to astrocytes will improve stroke outcomes in middle aged female rats. Middle aged (10–12 month old), acyclic female rats were injected with recombinant adeno-associated virus serotype 5 (AAV5) packaged with the coding sequence of the human (h)IGF-1 gene downstream of an astrocyte-specific promoter GFAP (AAV5-GFP-hIGF-1) into the striatum and cortex. The AAV5-control consisted of an identical shuttle vector construct without the hIGF-1 gene (AAV5-GFAP-control). Six to eight weeks later, animals underwent transient (90 mins) middle cerebral artery occlusion via intraluminal suture. While infarct volume was not altered, AAV5-GFAP-hIGF-1 treatment significantly improved blood pressure and neurological score in the early acute phase of stroke (2 days) and sensory-motor

[3] Reprinted with permission from Okoreeh AK, Bake S, Sohrabji F. Astrocyte-specific insulin-like growth factor-1 gene transfer in aging female rats improves stroke outcomes. Glia. 2017 Jul;65(7):1043-1058.

performance at both the early and late (5 days) acute phase of stroke. AAV5-GFAP-hIGF-1 treatment also reduced circulating serum levels of GFAP, a biomarker for blood brain barrier permeability. Flow cytometry analysis of immune cells in the brain at 24h post stroke showed that AAV5-GFAP-hIGF-1 altered the type of immune cells trafficked to the ischemic hemisphere, promoting an anti-inflammatory profile. Collectively, these studies show that targeted enhancement of IGF-1 in astrocytes of middle-aged females improves stroke-induced behavioral impairment and neuroinflammation.

4.2. Introduction

Ischemic stroke is the 5th leading cause of mortality, and the major cause of long term disability, especially among the elderly (Mozaffarian et al. 2015). Loss of nutrients, due to occlusion of a cerebral vessel, initiates a sequence of damaging events within neurons including rapid failure of ATP-dependent processes (Rossi et al. 2007), increased release of glutamate and calcium (Bano et al. 2005), and a loss of cellular integrity (Lo et al. 2003). Transient ischemia, followed by reperfusion, also increases permeability of the blood brain barrier and increases brain trafficking of cytotoxic cells and proteins. Non-neuronal cells such as astrocytes and endothelial cells, that are critical constituents of the blood brain barrier, also play a critical role in ischemic injury and repair (Panickar and Norenberg 2005; Posada-Duque et al. 2014).

Astrocytes are well positioned for neuroprotection during ischemia. They provide growth factors (Karki et al. 2014), clear glutamate (Olsen and Sontheimer 2008), preserve blood brain barrier function (Abbott et al. 2006) (Cekanaviciute and

Buckwalter 2016), interact with the immune system (Xie and Yang 2015), combat oxidative stress (Xu et al. 2010) and produce functional extracellular mitochondria to support neuronal viability (Hayakawa et al. 2016). Astrocytes are less vulnerable to ischemic injury than neurons (Dienel and Hertz 2005)and have a greater capacity for self-preservation (Allaman et al. 2011), indicating that these cells may play a crucial role in post-stroke recovery.

The ability of astrocyte's to promote neuroprotection deteriorates with age, when the CNS is more prone to disease pathology particularly stroke (reviewed in Chisholm et al., 2015). Proliferation of reactive astrocytes after injury is greater (Topp et al. 1989) and persists longer in the aged brain (Manwani et al. 2011) and results in accelerated glial scar formation in this group (Badan et al. 2003). Aged reactive astrocytes exhibited an upregulation of genes associated with inflammation and scar formation as compared to adult astrocytes (Buga et al. 2008). Moreover, aging also affects astrocytic functions critical for stroke recovery such reduced glutamate uptake capacity in aging male rats (Latour et al. 2013) and in middle aged female rats (Lewis et al. 2012). Similarly, while astrocytes normally release a variety of trophic factors that promote neuronal survival and curb CNS degeneration (Ridet et al. 1997) including IGF-1 and VEGF (Chisholm and Sohrabji 2016), these secretions decrease with age (Bhat et al. 2012; Lewis et al. 2012). The loss of IGF-1 observed in aging astrocytes may result in more severe stroke outcomes observed in middle aged female rats.

IGF-1 plays an important role in development, cell differentiation, neuronal plasticity, and cell survival of the nervous system (Bondy and Cheng 2004). IGF-1 also

reduces cell death in a variety of experimental neurologic disease models, such Parkinson's (Ayadi et al. 2016) traumatic brain injury (Madathil et al. 2013), and spinal cord injury (Utada et al. 2015). With age, plasma levels of IGF-1 decrease in many species and in female rats, this decrease is seen as early as middle age, when stroke induced infarction is more severe as compared to young females (Selvamani and Sohrabji, 2010). Intracerebroventricular (ICV) treatment with IGF-1 post-stroke has been reported to decrease infarct volumes in this group (Bake et al., 2014), suggesting that the loss of IGF-1 with age may underlie the more severe stroke outcomes seen in middle-aged females.

In view of the crucial role that astrocytes play in brain injury along with the age-related loss of IGF-1 in middle-aged females, we hypothesize that worse stroke outcomes in this age group is due to reduced availability of astrocytic IGF-1, and that increasing IGF-1 expression in aging astrocytes will improve post-stroke outcomes in this group. To test this hypothesis, middle-aged females were injected with recombinant human (h)IGF-1 placed downstream of the GFAP promoter and packaged in recombinant adeno-associated virus serotype 5 (AAV5) or with control construct. Following stroke, animals were tested for behavioral impairments, extent of infarction, and neuroinflammation. Our studies show that gene transfer of IGF-1 to astrocytes significantly improves stroke-induced behavioral impairment, without reducing infarct volume, and further reduces neuroinflammation in a model of ischemia reperfusion.

4.3. Materials and Methods

4.3.1. Animals

Female Sprague Dawley (SD) rats were purchased as retired breeders (10 – 12 months; weight range 325 – 350 g) from Envigo Laboratories. This group met our previously established criteria for reproductive senescence: briefly, at least five successful pregnancies and current acyclicity as defined by vaginal cytology assessed via daily vaginal smears (Jezierski and Sohrabji 2001). All animals were housed in an AAALAC–approved facility, maintained on a constant photoperiod (12-hour light/dark cycles), and fed ad libitum with laboratory chow (Harlan Teklad 8604) and water. All animal procedures were performed in accordance with the National Institutes of Health guidelines for the humane care of laboratory animals and were approved by the Institutional Animal Care Committee and the Institutional Biosafety Committee. A total of 112 animals were used in this study.

4.3.2. Adenovirus constructs

Recombinant adeno associated virus serotype 5 (AAV5) was packaged (Signagen, MD) with the ORF of the human (h)IGF-1 gene downstream of the astrocyte-specific promotor, GFAP (AAV5-GFAP-hIGF-1; see Figure 4-1). The construct also contained the mCherry reporter gene under the CMV minimal promoter to visually detect transfected cells. The control construct consisted of an identical shuttle vector without the hIGF-1 gene (AAV5-GFAP-control).

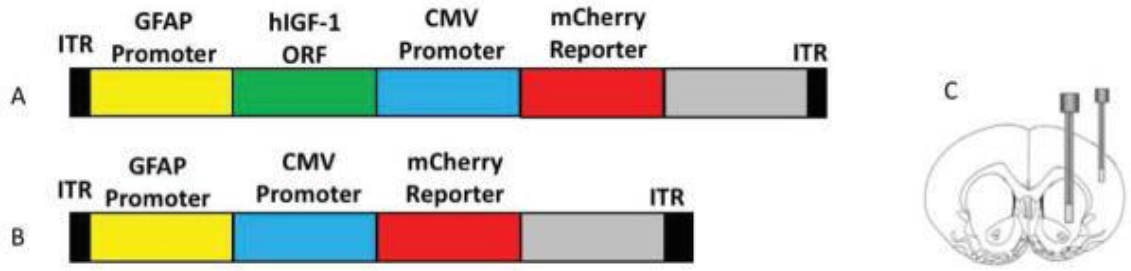

Figure 4-1: AAV5 constructs.
Schematic representations of the AAV serotype 5 viral constructs for AAV5-GFAP-hIGF-1 (1A) and AAV5-GFAP-control (1B). (C.) AAV5 virus was injected into the cortex and the striatum on the same hemisphere.

4.3.3. Surgical Procedures

4.3.3.1. AAV5 Injections

Animals were anesthetized (ketamine: 87 mg/kg; xylazine: 13 mg/kg) and placed in a stereotaxic instrument (David Kopf Instruments). Two small holes were drilled into the skull at the following coordinates relative to bregma. For striatum: +0.9 mm anterior posterior, +3.6 mm medial lateral, and a depth of 6.5 mm relative to the dura. For cortex: +0.9 mm anterior posterior, +5.5 mm medial lateral, and a depth of 6.0 mm relative to the dura. In each case, a needle, attached to a Hamilton syringe was lowered to the required depth and AAV5 was delivered slowly to the parenchyma at the rate of 0.02 μL/30 seconds for a total of 3.5 μL. All animals received one injection each into both the right striatum and right cortex of either the AAV5-GFAP-hIGF-1 construct or the AAV5-GFAP-control construct (Figure 1C). Two concentrations of AAV5 were used: 2.5×10^{11} viral particles (VP)/mL (low dose) and 2.5 × 1012 (VP)/mL (high dose).

Animals were allowed to recover for 6–8 weeks after injections to allow full integration of the viral particles.

4.3.3.2. Middle cerebral artery occlusion (MCAo)

Animals were subjected to middle cerebral artery occlusion (MCAo) via intraluminal suture using our previous procedures (Bake et al. 2016; Bake et al. 2014). Briefly, rats were anesthetized with isoflurane and maintained at 37°C on heating pads in dorsal recumbency. The neck region was shaved and disinfected and a ventral midline incision was made on the skin. Superficial fascia on the right side of the neck was dissected and the underlying muscles were blunt dissected to expose the right common carotid (CCA), external (ECA), and internal carotid (ICA) arteries. The ECA was separated from the vagus nerve and tied off distally with silk sutures after cauterizing the small branches. Microsurgical clamps were placed on the CCA and ICA. A loose tie was placed on the ECA, and the free stump of ECA was aligned with the ICA. Twenty-two mm of suture of the appropriate size with a silicon-coated round tip (Doccol Corp., CA) was inserted into ICA lumen through a small nick on the ECA between the two ties. The suture was advanced along the ICA until it reached the origin of the MCA (~20 mm of suture) and secured in position with nylon ties. The intraluminal suture was maintained for 90 min and then withdrawn. Tissue perfusion rate was monitored using Laser-Doppler Flowmetry (Moor Instruments, UK) and the perfusion index was calculated for both ischemic and reperfusion time points. MCAo resulted in an 80% reduction of blood flow compared to the pre-occlusion rate and re-perfusion restored the perfusion index back to pre-occlusion levels. In a subset of animals, a permanent (p)MCAo was

performed, where the suture was maintained in place for the duration of the experiment. All animals were carefully monitored after surgery and terminated 2 days (early acute phase) or 5 days (late acute phase) after ischemia.

4.3.4. Confirmation of AAV5 localization

A subset of AAV5-GFAP-control and AAV5-GFAP-hIGF-1 injected animals were terminated 2 days after MCAo and processed for histological analyses to determine uptake of the AAV5 construct. Animals were perfused transcardially with dPBS (Thermo Fisher, MA) followed by 4% paraformaldehyde. The brains were removed from the cranial vault and post fixed in 4% paraformaldehyde overnight at 4°C. Brains were transferred to 15% sucrose overnight at 4°C and subsequently embedded in Richard-Allan Scientific Neg 50™ (ThermoFisher, MA) and then sectioned (30 microns) using a cryostat (Microm HM 550, ThermoFisher, MA).

Sections were collected on superfrost slides (Thermo Scientific, MA), air dried, and fixed with 4% paraformaldehyde for 30 mins and blocked in blocking buffer (2% normal goat serum or rabbit serum and 0.2% triton X-100 in dPBS) for 1 hour at room temperature. Sections were then incubated with primary antibodies for hIGF-1 (Sigma, 1:80 dilution) or GFAP (Sigma, CA, 1:80 dilution), (overnight ~16 hours) followed by a 1 hour incubation with fluorescent-labeled secondary antibodies (Oregon green 488 donkey anti-goat, 1:500 dilution and Oregon green 488 goat anti-rabbit, 1:500 dilution, respectively). Fluorescent labeling was visualized on the Olympus FSX100 Bio Imaging Navigator and captured digitally by FSX-BSW software (Waltham, MA).

4.3.5. Infarct Analysis

Infarct volume was measured using our previous published procedures (Selvamani and Sohrabji 2010). Two or 5 days after MCAo rats were deeply anesthetized and decapitated, and the brain was rapidly removed. Coronal slices (2 mm thick) between −2.00 mm and +4.00 mm from bregma were sectioned in an adult rat brain slicer matrix (Roboz Surgicals, Gaithersburg, MD) and incubated in a 2% Triphenyl tetrazolium chloride (TTC) solution at 37°C for 20 mins. Stained slices were photographed using an Olympus E950 digital camera attached to a dissecting microscope Infarct volume was determined from digitized images using the Quantity One software package (Bio-Rad, CA). Typically, 3 such slices were used for analysis. The area of the cortical and striatal infarct was measured separately in all slices, and the area of the entire contralateral hemisphere was also measured. The volume of the infarct was normalized to the volume of the contralateral (non-occluded) hemisphere. To ensure reliable and consistent detection of the infarct zone, images were digitally converted to black and white and magnified. Images were coded and the sections were analyzed by an investigator blind to the code (AO).

4.3.6. Behavioral analysis

Animals were evaluated for sensorimotor performance pre- and post- stroke using the vibrissae evoked forelimb placing task (Woodlee et al. 2005) as described in (Selvamani and Sohrabji 2010). Animals were subject to same-side placing trials and cross-midline placing trials elicited by stimulating the ipsi- and contra-lesional vibrissae. Same-side placing test: The animal was gently held such that all four limbs were free to

move. The animal's ipsi-lesional vibrissae were brushed against the edge of a table to elicit a forelimb placing response, which typically consisted of the forelimb ipsi-lateral to the stimulated vibrissae. Ten trials were performed before the same was repeated for the contra-lesional vibrissae.

4.3.7. Cross-midline placing test

The animal was held gently by the upper body such that the ipsi-lesional vibrissae lie perpendicularly to the tabletop and the forelimb on that side is gently restrained as the vibrissae was brushed on the top of the table to evoke a response from the contralateral limb and vice versa. Between each trial, the animal was allowed to rest all four limbs briefly on the tabletop to help relax its muscles. Trials in which the animal seemed to struggle or make premature forelimb movements were not counted.
The vibrissae-elicited forelimb placing test was carried out after AAV5 injection, but before and after MCAo surgeries. An unscored pretest was performed 3 days before MCAo to help acclimatize the animal to the testing procedure. The scored testing schedule was as follows: 2 days prior to the MCAo, 48h (2d after MCAo) and 5d after MCAo. Each testing and pretesting session consisted of 40 trials per animal, 10 trials each for the same-side placing (left and right) and 10 trials each for left and right cross-midline placing. Each trial is rapid and the entire procedure on a single day is approximately 5 min/animal.

Scoring was based on a 4-point scale. A vibrissae-elicited response of the forelimb that included a brisk forward and upward movement that ended in the paw pads making a flat, full contact with the tabletop was scored as 3. If there was a slow or

sluggish movement of the limb forward and upward, resulting in just the toes or claws contacting the tabletop, the trial was given a score of 2. When there was a limb movement forward but not upward and the paw made no contact with the tabletop, the trial was scored 1. If the limb did not move in response to stimulation, the trial was given a score 0. Trials scored as a 2 or 3 were counted as a successful placement and the once scored 1 or 0 were considered unsuccessful.

4.3.8. Neurological Score

A neurological score was obtained based on the following functional tests that were performed 2 days after MCAo. Described below are five tests performed in succession for each animal. For each test, a higher score indicates a more severe deficit.

4.3.8.1. Motility Test

Animals were placed on an open surface and their movement was monitored. Animals that walked normally received a score of 0. Animal with any difficulties were given a 1. Deficits includes immobility, inability to walk straight, circling and falling down (Normal = 0, maximum = 1).

4.3.8.2. Grasping

Animals were suspended by its forelimbs on a small beam. Grasping ability and forelimb strength were assessed. Animals that grasped the beam with both paws were given a 0. Animals that grasped only with the ipsi-lesional paw were given a 1. Animals that could not grasp the beam were given a 2. (Normal = 0, maximum = 2).

4.3.8.3. Righting Reflex

To test the righting reflex, rats were placed on their backs. If the animal took less than 3 seconds to right itself, the animal received a score of 0. An animal that took longer than 3 seconds or was not able to perform the task was given a score of 1. (Normal = 0, maximum = 1)

4.3.8.4. Forepaw Disability

Animals were placed a cylinder and observed. Animals that were able to rear and make contact with the wall of the cylinder with both paws were scored as 0. Animals that were only able to consistently place the ipsi-lesional paw were scored 1. Animals didn't place either paw in 2 mins, were scored as 2. (Normal = 0, maximum = 2)

4.3.8.5. Circling

Animals with no circling behavior were given a 0. Animals with an inability to walk straight and a flexion of the forelimb towards the paretic side after suspension by the tail were given a score of 1. Animals with constant circling to the paretic side were given a score of 2. Animals with constant circling to the paretic side which a slight tendency to fall were given a score of 3. Animals that were barreling were given a score of 4. Animals that were comatose were given a score of 5. (Normal = 0, maximum = 5)

4.3.9. Physiological measurements

4.3.9.1. Body weight

Animals were weighed before and after MCAo (2 days) and body weight changes were recorded.

4.3.9.2. Systolic Blood Pressure

Blood pressure was determined by Tail Cuff Blood Pressure Systems (IITC Life Science Inc, CA). Three days prior to baseline testing rats were placed in the apparatus to help acclimatize the animal to the testing environment. A pre-recording was performed 2 days prior to MCAo and a post-surgery recording was performed 2 days after surgery. Each testing and pretesting session consisted of 8 readings per animal, which were averaged.

4.3.10. Quantitative RT-PCR

4.3.10.1. mRNA isolation

Total RNA was extracted using the Qiagen miReasy kit (Qiagen, CA) from the ischemic and non-ischemic hemispheres as well as astrocytes obtained by magnetic purification from a different set of ischemic and non-ischemic hemispheres. For each sample, 15 μL was transferred to a new tube, and 700 μL QIAzol lysis reagent was added. Following a 5-min incubation at RT, 140 μL chloroform was added to each sample. Following a 2 min incubation at RT, samples were centrifuged at 12,000 × g for 15 min at 4°C. The aqueous phase was then transferred to a fresh tube and mixed with ethanol (1.5 vol). The sample was then loaded on to an RNeasy Mini Spin Column and centrifuged for 30 seconds at RT, 13,000 × g. After sequential washes in RWT and RPE buffers, the columns were transferred to a fresh tube and RNA eluted with 50 μL of DNase/RNase-free water. Sample purity was assessed by Nanodrop technology and a ratio of 1.8 was considered acceptable. Samples were stored at −80°C until use.

4.3.10.2. Real-time RT-PCR

mRNA expression for specific genes in AAV5-GFAP-control and AAV5-GFAP-hIGF-1 -treated animals was assessed using real-time qRT-PCR. 200 ng of purified total RNA was used to generate cDNA, using a Universal cDNA Synthesis Kit (Exiqon, Denmark) according to the manufacturer's protocol. 1 μL of cDNA samples were used as a PCR reaction template in a 10 μl PCR reaction. PCR reactions were run in triplicate on an Applied Biosystems 7900HT real-time PCR instrument (Applied Biosystems, CA) using a SYBR green-based real-time PCR reaction kit (Exiqon, Denmark). 18s mRNA was used as a normalization control. Specificity of the amplification was evaluated by thermal stability analysis of the amplicon. Individual and reference gene primer sets (Integrated DNA Technologies, Coralville, IA) are listed in the Table 4-1.

Gene Name	**Forward Primer**	**Reverse Primer**
Human IGF-1	AGATGCACACCATGTCCTCC	CATCCACGATGCCTGTCTGA
Rat IGF-1	GCTGGTGGACGCTCTTCAGT	TTCAGCGGAGCACAGTACAT

Table 4-1: Gene Sequence

Gene Name	Forward Primer	Reverse Primer
GLAST	AATGAAGCCATCATGAGATTGGT	CCCTGCGATCAAGAAGAGGAT
GFAP	GGTGGAGAGGGACAATCTCA	CCAGCTGCTCCTGGAGTTCT
Iba1	CCATGAAGCCTGAGGAAATTTCA	TTATATCCACCTCCAATTAGGGCA
PECAM	TTGTGACCAGTCTCCGAAGC	TGGCTGTTGGTTTCCACACT
18S	ATGGCCGTTCTTAGTTGGTG	CGCTGAGCCAGTCAGTGTAG

Table 4-1 **Continued**

4.3.11. Cell preparation

Animals were anesthetized (xylazine and ketamine i.p.) and perfused intracardially with 100 mL of cold 1X PBS. Ischemic and non-ischemic hemispheres were collected and minced using a blade. Following a wash with X-VIVO 15 (Lonza, TX), a chemically-defined, serum free hematopoetic medium, tissues were first enzymatically dissociated using the Neural Dissociation Kit P (Miltenyi Biotech, CA)

and then transferred to a glass Dounce homogenizer and mechanically dissociated. The suspension was then filtered through a 30 μm strainer, and washed twice in X-VIVO 15.

4.3.12. For astrocyte separation

Cells were incubated with anti-GLAST antibody (1:5) for 10 min. GLAST was selected as a marker because it is an astrocyte-specific, membrane-associated protein and results in a virtually pure astrocyte population (Chisholm et al. 2015). Cells were then washed and spun at 300 × g for 10 min followed by incubation with biotin microbeads for 15 min. Cells were subsequently washed, spun (300 × g; 10 min), and resuspended in 2 mL of buffer and passed through LS columns. The columns were washed with buffer (3× 3 mL), and the flow-through discarded. The LS column was then removed from the magnetic stand. Astrocytes were then eluted from the column and washed in cold dPBS.

4.3.13. For flow cytometry of immune cells

The cell pellet retrieved was resuspended in 6 ml of X-VIVO 15, and applied to an Opti-Prep gradient (Axis Shield, Olso, Norway). The gradient was composed of four 1-mL layers of Opti-prep diluted in X-VIVO 15, arranged in the following order (from bottom to top): 35%, 25%, 20%, and 15%. The 10 mL tube containing the cell suspension and gradient was centrifuged at 1900 RPM for 15 min at 20°C with low acceleration and no brake. Following centrifugation, the top 7 mL of solution containing myelin and debris, was aspirated and discarded. The remaining 3 mL, containing inflammatory cells and glia, was washed twice in X-VIVO 15 and counted (Countess, Life Technologies). The single-cell suspension was then pipetted into three 96-well

plates and incubated with conjugated antibodies for the following markers: CD11b, Iba1, CD45, CD86, CD68, CD206, CD163, CD4, CD25, and FoxP3.

For each animal, 2 technical replicates were prepared and phenotyped using a FACSAria flow cytometer (BD Biosciences, CA) and analyzed with FlowJo software (Tree Star Inc., OR). The following gating strategy was used to identify microglia/macrophages. First, dead cells and debris was removed from the analysis by gating on forward and side scatter. To control for cellular auto-fluorescence, unstained samples were prepared. Any cells determined to be positive were selected in a gate with >1% unstained cells. CD45+ cells were selected and further separated into discrete populations of high, medium, and low based on fluorescence intensity. For macrophages/microphages, after CD45+ positive only cells were selected, an initial gate was scaled to select discrete populations that were positive for both Iba1 and CD11b. For all further analysis, a quadrant system was created so that 99% of the unstained cells were in the third quadrant to determine phenotype and receptor expression. For Tregs, only CD45 high positive cells were used for analysis. An initial gate was scaled to select discrete population positive for CD4. For all further analysis, a quadrant system was created using CD25 and FoxP3 fluorescence so that 99% of the unstained cells were in the third quadrant to determine phenotype and receptor expression.

4.3.14. ELISA Assays

4.3.14.1. Serum GFAP

Concentrations of circulating glial fibrillary acidic protein (GFAP) in serum were determined by ELISA (R&D Systems), according to manufacturer's instructions.

Briefly, standards, controls, and aliquots of serum samples were loaded into a 96-well plate precoated with antibodies specific for GFAP and incubated at room temperature for 2 hours. With intervening washes, plates were sequentially incubated with 100 µL of conjugate for 2 hours, and 100 µL of substrate solution for 30 minutes. The color reaction was stopped by an equal volume of stop solution and read at 450 nm in a microplate reader (Bio-Tek, VT). Standard curves were established from optical densities of wells containing known dilutions of standard (1.56 – 100 ng/mL) using KC3 software (Bio-Tek), and sample measurements were interpolated from standard curves. The intraassay coefficient of variation was 1.30%.

4.3.14.2. Multiplex Cytokine Kit

Tissue expression for a panel of cytokine/chemokine was measured in the ischemic and non-ischemic hemisphere and serum of rAAV5-GFAP-hIGF-1 and rAAV5-GFAP-control animals, using a multiplexed magnetic bead immunoassay (Milipore Corp., MA) following manufacturer's instructions. Briefly, the filter plate was blocked with assay buffer for 10 min and decanted. Standards and samples was added into appropriate wells, followed by addition of premixed beads and incubated for 2 hour at room temperature on a plate shaker. Wells were washed 2 times, 25 µL of detection antibody was added, incubated for 1 hour incubation at RT and followed by 30 min incubation with addition of 25 µL of streptavidin-phycoerythrin per well. After 2 washes, beads were resuspended in 150 µL of sheath fluid and a minimum of 50 beads per analyte was analysed in a Bio-Plex suspension array system (Bio-Rad Laboratories, CA). Cytokine/chemokine levels were normalized to total protein content. The following chemokines and cytokines were assessed: Granulocyte colony stimulating factor (G-CSF), eotaxin, GM-CSF, interleukin (IL)-1α, leptin, macrophage inflammatory protein (MIP)-1a, MIP2, IL-4, IL1-b, IL-2, IL-6, EGF, IL-13, IL-10, IL-12 phosphorylated 70 KDa (IL-12-p-70), Interferon (IFN)-γ, IL-5, IL-17A, IL-18, Chemokine C-motif Ligand (CCL2), Interferon gamma induced protein (IP)-10, Growth related oncogene/Keratinocyte derived chemokine (GRO/KC), VEGF, Fractalkine, Lipoploysacharide-induced CXC (LIX) chemokine, MIP-2, Tumor necrosis factor (TNF)- α, RANTES (regulated on activation, normal T cell expressed and secreted).

4.3.15. Statistical analyses

Group size was determined using power analyses. Power analyses was computed based on effect sizes seen in previous data and pilot studies. In order to achieve power of 0.8 (1-β) and Type 1 error rate $\alpha=0.05$, the minimum sample size is 4. For these studies, most group sizes ranged from 5 to 8. The Kaplan Maier test was used for survival analysis. For behavioral tests, a paired t-test was used for each group, comparing the values obtained pre- and post-stroke. For all other tests, an unpaired t-test was performed. Group differences were considered significant at $p<0.05$ in each case. The statistical package SPSS (v. 21, IBM) was used for these analyses.

4.4. Results

4.4.1. Characterization of AAV5 Integration

AAV5 integration was assessed by a combination of histological and molecular techniques. Brain sections from animals injected stereotaxically with either the control (rAAV5-GFAP-hIGF-1; Figure 4-1A) or the IGF-1 (rAAV5-GFAP-control; Figure 4-1B) construct were visualized by fluorescent microscopy for the mCherry reporter. The mCherry reporter gene was located downstream of the constitutively expressed cytomegalovirus (CMV) promoter (see Figure 4-1), hence mCherry expression was widely distributed in neuronal and non-neuronal cells of the cortex (Figure 4-2Ai) and striatum (Figure 4-2Aii). mCherry expression was also localized to GFAP-immunolabeled cells (Figure 4-2B), indicating that the viral construct was internalized to astrocytes. To assess whether the AAV5-GFAP-hIGF-1 construct was functional, sections from AAV5 injected animals were processed for hIGF-1

immunohistochemistry. No hIGF-1 positive cells were seen in animals injected with rAAV5-GFAP-control (Figure 4-2Ci), while hIGF-1 label (green; Figure 4-2Cii) was co-localized to mCherry positive cells (red) in the rAAV5-GFAP-hIGF-1 treatment. Many of these double-labeled cells were located around blood vessels.

Expression of hIGF-1 was further confirmed by qRT-PCR in whole brain homogenates and astrocyte homogenates. Astrocytes were collected by GLAST-positive selection by magnetic beads, using our previous procedures that results in a virtually pure astrocyte population (Chisholm et al. 2015). As expected, hIGF-1 was undetectable by qRT-PCR in whole hemisphere homogenates (Figure 4-2Di) and astrocytes homogenates (Figure 4-2Dii) from either the ischemic or non-ischemic hemisphere of animals injected with rAAV5-GFAP-control. In contrast, hIGF-1 was highly expressed in whole brain and astrocyte homogenates of the ischemic hemisphere of animals that were injected with AAV-GFAP-hIGF-1, with virtually no hIGF-1 gene expression in the non-ischemic hemisphere. There was no difference in the amount of rat IGF-1 expression in tissue lysates and astrocytes regardless of hemisphere or treatment (Figure 4-2Diii and 4-2Div). qRT-PCR of astrocyte homogenates used in these analyses show strong expression of GFAP, and virtually undetectable levels of PECAM (endothelial cell marker) and Iba1 (microglial specific marker) (Figure 4-2E), indicating an enriched astrocyte population.

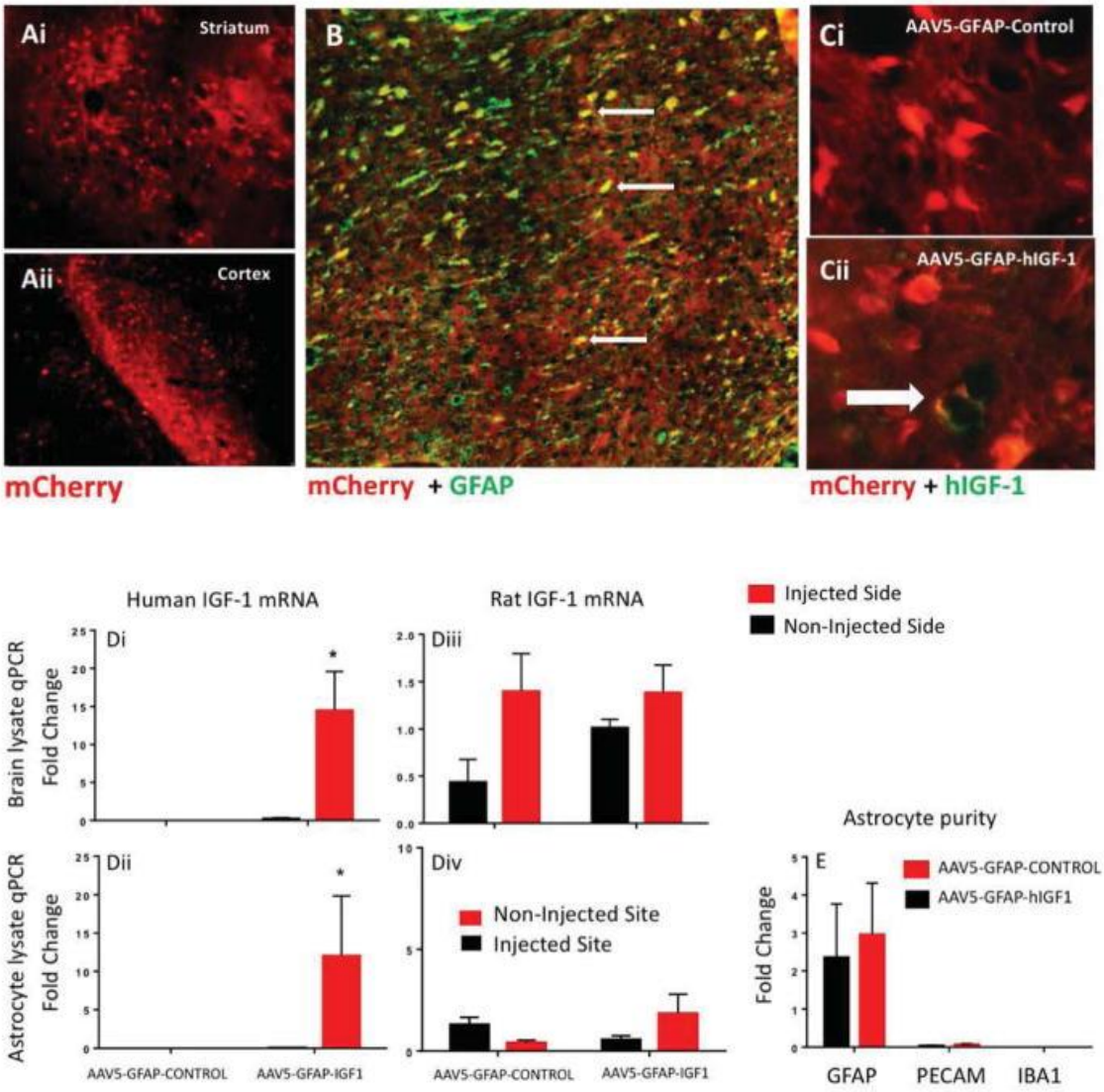

Figure 4-2: Integration of the AAV5 in the brain.
AAV5 uptake into cells was detected by the mCherry reporter. A) At the striatal (Ai) and cortical (Aii) injection sites, both glial and neuronal cells were labeled by the mCherry reporter. B) Immunohistochemical labeling of GFAP in green and AAV5 mCherry reporter in red. Arrows indicate cells that are double labeled for AAV5 mCherry reporter and the glia marker GFAP. C) Immunohistochemistry for hIGF1 in green and AAV5 mCherry reporter in red. hIGF-1 positive cells were seen in animals injected with

AAV5-GFAP-hIGF-1 (Cii) but not the AAV5-GFAP-control injected animals (Ci). hIGF-1 positive cells were colocalized to mCherry-labeled cells and mainly seen around blood vessels. D) mRNA expression of human and rat IGF-1 in harvested astrocytes. mRNA hIGF-1 expression was significantly only increased in the injected hemisphere site in whole brain (Di) and in harvested astrocytes (Dii). (N=5–8). No differences were seen in rat IGF-1 mRNA in whole brain lysates (N=4) (Diii) or astrocyte mRNA (N=6–8) (Div). Magnetically harvested astrocytes produced a virtually pure population (E). ($F(2, 18) = 7.132$ $P = 0.0052$ Two-way ANOVA) (All graphs represent mean ± SEM).

4.4.2. Post-Ischemic Survival

Two doses of AAV5-GFAP-Control and AAV5-GFAP-hIGF-1 were injected into the striatum and cortex, a low dose of 2.5 × 1011 VP/mL and a high dose of 2.5 × 1012 VP/mL. After 6–8 weeks post injection, all animals were subject to MCAo. In the high dose treatment, post-stroke mortality was higher in animals injected with the AAV5-GFAP-control as compared with AAV5-GFAP-hIGF-1 treated animals ($p<0.0001$; Figure 4-3A). High dose AAV5-GFAP-control animals did not survive more than 24 hours post-stroke, while high dose AAV5-GFAP-hIGF-1 treated animals survived 5 days, the predetermined termination point for this study.

Animals that received the low dose AAV5 treatment did not show any differences in post-stroke mortality (Figure 4-3B; $p = 0.8311$). Both rAAV5-GFAP-control and AAV5-GFAP-hIGF-1 groups survived until the predetermined termination point of the study at 5 days. Therefore, all subsequent studies were performed with the low dose AAV5.

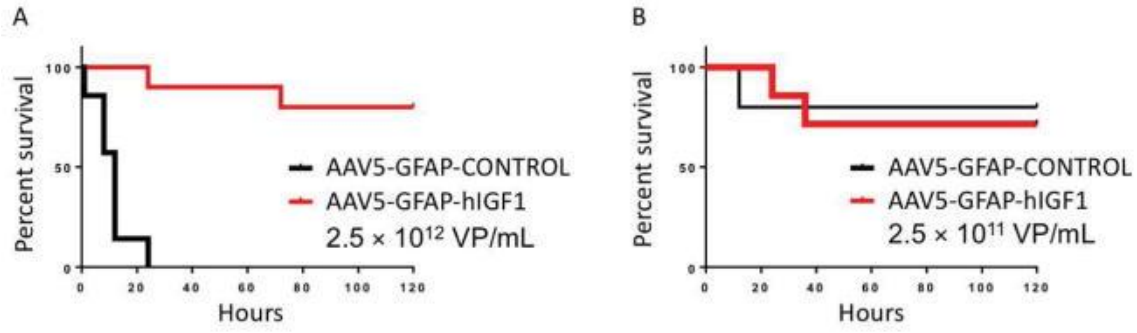

Figure 4-3: Post-ischemic survival

Kaplan–Meier Survival Analysis for High Dose and Lose Dose. A) Animals who received the high dose AAV5-GFAP-hIGF-1 had significant survival post-stroke over 120 hours (5 days) compared to high dose AAV5-GFAP-control ($p<0.0001$; n =7–10) B) Animals that received the lose dose AAV5-GFAP-hIGF-1 or AAV5-GFAP-control construct did not show differences in post-stroke survival over 120 hours ($p=0.8311$) (N= 4 – 5)

4.4.3. Physiological measures affected by MCAo at the early acute period (2 days) post-stroke

Physiological measures affected by MCAo at the early acute period (2 days) post-stroke

Animals injected with AAV5-GFAP-control and rAAV5-GFAP-hIGF-1 were subject to ischemic stroke for 90 mins followed by reperfusion. Both groups experienced approximately 10% weight loss at 2 days post-stroke, which is commonly seen after stroke, however there was no difference in the extent of weight loss between the two groups (Figure 4-4A). Systolic blood pressure was also monitored pre- and post-stroke. Pre-stroke, AAV5-GFAP-control animals had a mean systolic blood pressure of 141.8

mmHg, and AAV5-GFAP-hIGF-1 animals averaged 133.9 mmHg. Post-stroke, the mean systolic blood pressure for AAV5-GFAP-control animals significantly decreased 24% to 99.1 mmHg ($p = 0.0098$). The AAV-GFAP-hIGF-1 animals maintained a mean systolic blood pressure of 129.2 mmHg (Figure 4-4B).

Infarct volume: Infarction was localized largely to the striatum, with smaller cortical infarcts. Infarct volume, assessed at 2 days post stroke, however, was similar between AAV5-GFAP-control and AAV5-GFAP-hIGF-1 groups ($p = 0.3927$; Figure 4-4C).

The neurological score, an indicator of motor disability, was significantly worse in AAV5-GFAP-control as compared to AAV5-GFAP-hIGF-1treated animals. Post-stroke, AAV5-GFAP-control animals showed impaired mobility, righting reflex, grasping and pronounced circling behavior resulting in an average neurological score of 3.86±0.89, which is typical of the post stroke disability observed in middle-aged female rats. 4. In contrast, AAV5-GFAP-hIGF-1 animals had significantly less impairment with an average neurological score of 2+1.0 ($p = 0.0033$; Figure 4-4D).

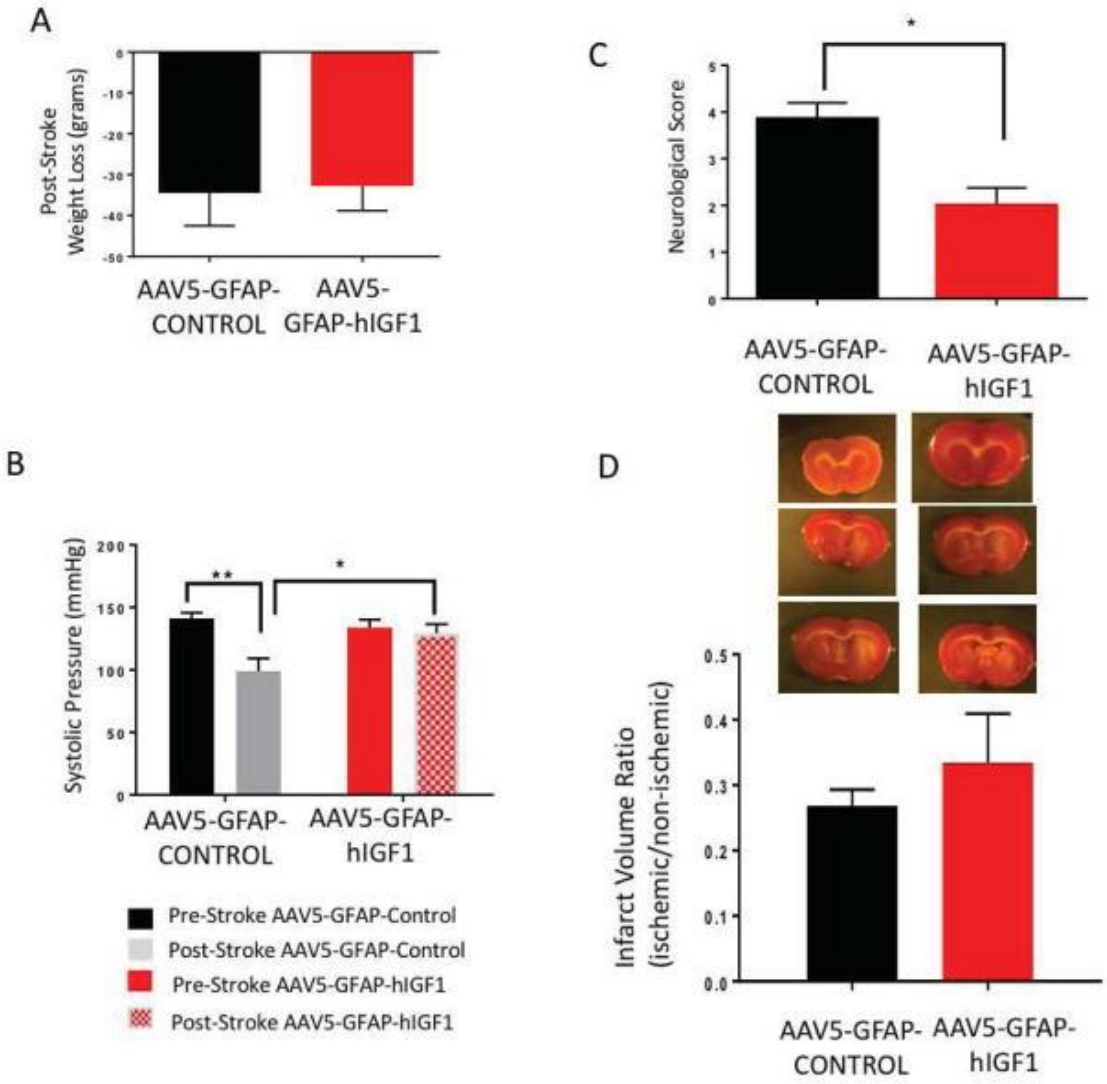

Figure 4-4: Low dose post-ischemic outcomes
A) No differences were seen between AAV5-GFAP-hIGF-1 and AAV5-GFAP-control treated animals in weight loss after stroke. (Unpaired t test; p=0.8675) B) AAV5-GFAP-hIGF-1 treatment preserved systolic blood pressure. (F (1, 12) = 6.012, P = 0.0305; post hoc t-test for pre- and post-AAV5-GFAP-Control p = 0.0042). C) Neurological deficits were significantly decreased in the AAV5-GFAP-hIGF-1 animals as compared to the controls (unpaired t test; p = 0.0033). D) No differences found in infarct volumes

between groups (unpaired t test; p = 0.3927) (N= 7 – 8). All graphs represent mean ± SEM.

4.4.4. Post-stroke sensory-motor behavioral outcomes

To assess the effect of AAV5 treatment on sensory motor function post-stroke, the vibrissae evoked-forelimb placing task performance was assessed at 2 days (early acute phase) and 5 days (late acute phase) after MCAo. Consistent with other reports, sensory motor performance improved as animal progressed from the acute phase to the late phase. For the rAAV5-GFAP-control group, there was no response (NR) to either the same side or cross-midline test on the side contralateral to the ischemic side (contralesional) during the early acute phase (Figure 4-5Ai). In the AAV5-GFAP-hIGF-1 group, during the early acute phase (2d post stroke), post-stroke performance was impaired compared to the pre-stroke performance, however animals in this group were still able to maintain about 45% of their pre-stroke responses to the vibrissae stimulation, unlike the AAV5-GFAP-Control group ($F(3,24)=3.44$; $p=0.0359$; Figure 4-5Ai).

Similarly, on the ipsilesional side for the early acute phase, AAV5-GFAP-control had no responses to the same side test, while the AAV5-GFAP-hIGF-1 group maintained 40% of their pre-stroke responses ($F(3, 24) = 13.84$; $p<0.0001$), although these were lower than the pre-stroke levels ($F(1, 24) = 50.28$; $p<0.0001$; Figure 4-5Aii). No loss of response was seen on the cross-midline task on the ipsilesional side.

During the late acute phase (5 days post-stroke), improvement was noted in both groups, however performance in the AAV5-GFAP-control group was significantly

worse than pre-stroke levels (F(1, 14)=15.79; p = 0.0014). Specifically, AAV5-GFAP-Control animals had lower responses on the same side (54%, p = 0.0294) and cross midline (42%, p = 0.0059) task on the paw contralateral to the infarct (Figure 4-5Bi). In contrast, performance of the AAV5-GFAP-hIGF-1 group was statistically no different from the pre-stroke performance (p = 0.9; Figure 4-5Bi and 4-5 Bii), indicating an improved rate of recovery.

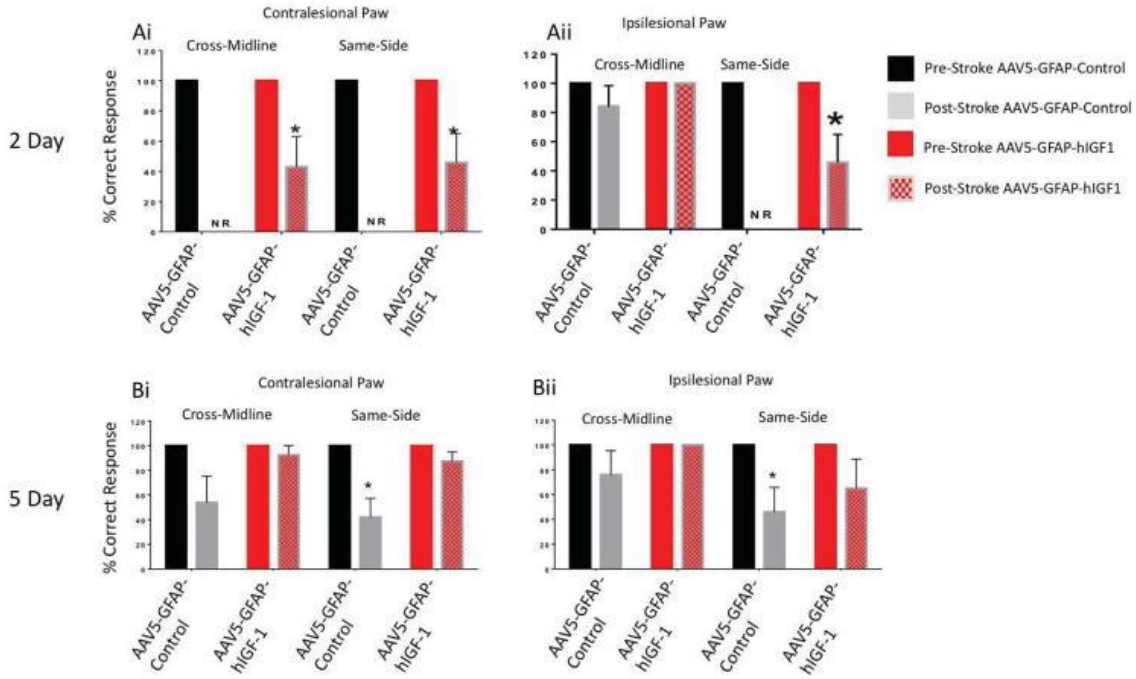

Figure 4-5: Vibrissae-Evoked Forelimb Placing Test
Sensory motor performance was evaluated by vibrissae-evoked forelimb placing task at 2 days (Ai and Aii) and 5 days (Bi and Bii) after stroke. Histogram depicts percent (+SEM) correct responses over 10 trials for tests of the contralesional (Ai and Bi) and ipsilesional (Aii and Bii) paw. NR: No Response; *: p<0.05), n= 7–8 for 2d post stroke, n=4–5 at 5d post stroke.

4.4.5. Blood brain barrier permeability

Circulating levels of GFAP were analyzed as a surrogate measure of blood brain barrier permeability function (Marchi et al. 2004) from serum samples collected pre-stroke, during the early acute and late acute phases of stroke. As shown in Figure 4-6A, GFAP was detected in all samples, however there was a main effect of stroke (pre and post-stroke) and treatment (AAV-GFAP-Control vs AAV-GFAP-IGF-1). GFAP levels were significantly elevated in both groups after stroke ($F(1,27)= 7.32$, $p<0.05$), and also significantly elevated by treatment ($F(1,27)= 7.72$, $p<0.05$) such that animals with AAV-GFAP-hIGF-1 had significantly lower levels of GFAP. Planned comparisons showed that while the groups were no different at baseline, the AAV5-GFAP-hIGF-1 group had almost 50% lower levels of circulating GFAP as compared to the AAV5-GFAP-control group, indicative of decreased blood brain barrier permeability.

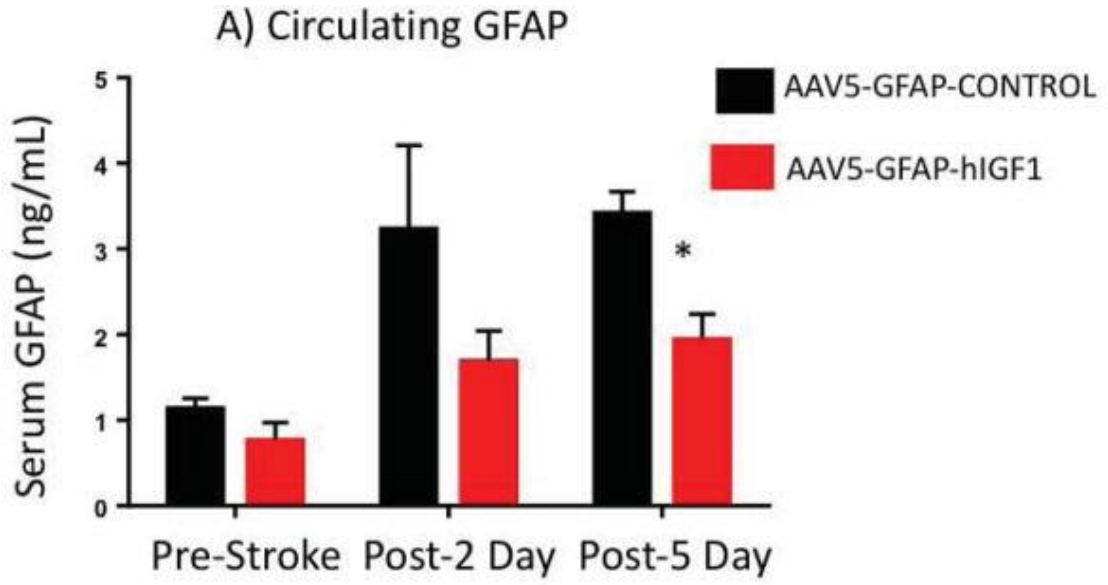

Figure 6B

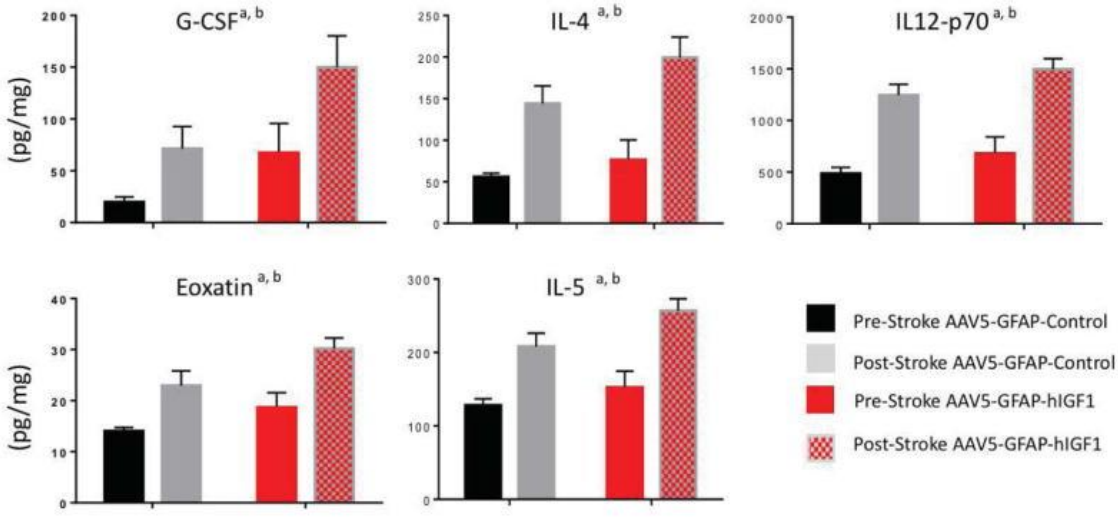

Figure 4-6: Serum Analysis

A) GFAP serum levels measured pre-stroke and at 2d and 5d post stroke in samples from AAV5-GFAP-control and AAV5-GFAP-hIGF-1 animals. a: main effect of AAV treatment; b: main effect of stroke, *: $p>0.05$; n=6–7. B) Cytokine levels of AAV5-GFAP-control and AAV5-GFAP-hIGF-1 animals in serum samples taken pre-stroke and

2 days post stroke for G-CSF, IL-4, IL-12-p70, Eotaxin, and IL-5. (a: main effect of treatment; b: main effect of stroke) All graphs represent mean ± SEM. N = 6–7 in each group.

4.4.6. Stroke-induced Inflammation

4.4.6.1. Serum Cytokines and Chemokines

A panel of cytokines and chemokines were examined in serum at 2 days after MCAo for AAV5 treated animals. Almost all cytokines and chemokines were elevated after ischemia, while a subset were also affected by IGF-1 gene transfer. Compared to the rAAV5-control group (Figure 4-6B), the AAV5-GFAP-hIGF-1 groups showed elevated levels of G-CSF (main effect of treatment, $p = 0.0048$, and stroke, $p = 0.0331$), IL-4 (main effect of treatment, $p = 0.0332$, and stroke, $p = 0.0005$), IL-5 (main effect of treatment, $p = 0.0216$, and stroke, $p = 0.0004$), Eotaxin (main effect of treatment, $p = 0.0160$, and stroke, $p = 0.0011$), and IL12-P70 (main effect of treatment, $p = 0.0232$, and stroke, $p < 0.0001$).

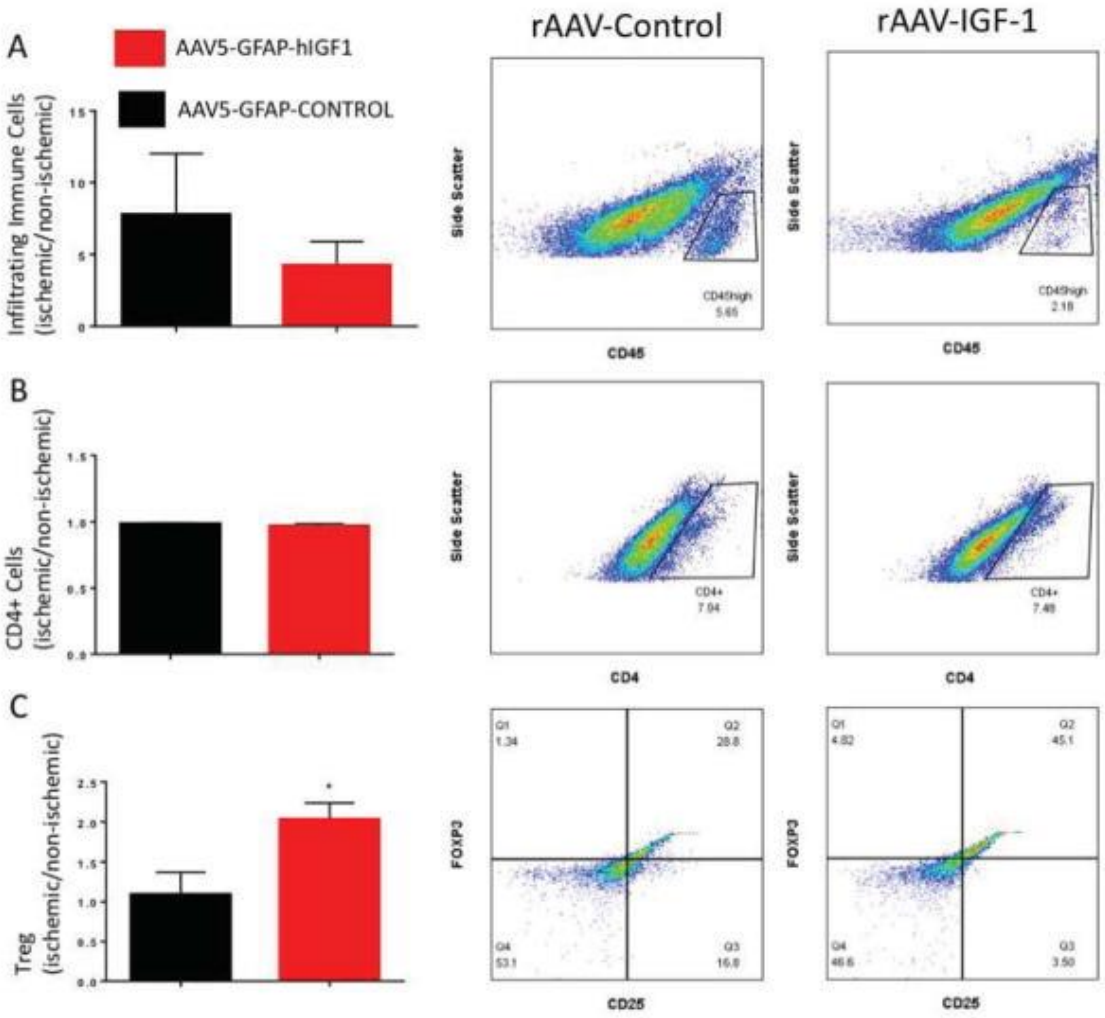

Figure 4-7: Infiltrating regulatory T-cell Analysis
A) Proportion of (CD45high) infiltrating immune cells detected in AAV5-GFAP-control and AAV5-GFAP-hIGF-1 treated animals (p = 0.4008). B) Proportion of CD4+ cells in AAV5-GFAP-control and AAV5-GFAP-hIGF-1 treated animals (p = 0. 0.3950). C) Proportion of infiltrating regulatory T-cells (CD45high, CD4/CD25/FoxP3) in AAV5-GFAP-control and AAV5-GFAP-hIGF-1 treated animals (p = 0.0219). All graphs represent mean ± SEM, n = 5–6 in each group.

4.4.6.2. Trafficking of peripheral immune cells

Flow cytometry was used to determine whether AAV5-GFAP-hIGF-1 affected the cohort of immune cells trafficked to the ischemic hemisphere. Mononuclear cells were harvested from the brain 2 days post-stroke and sorted for cell markers for infiltrating cells. The proportion of infiltrating immune cells identified by high CD45 expression was no different between the AAV5-GFAP-control and AAV5-GFAP-hIGF-1 groups ($p = 0.4008$; Figure 4-7A). Similarly, there were no group differences between CD4 positive cells ($p = 0.3950$; Figure 4-7B), however the proportion of infiltrating regulatory T-cells, identified as CD45high/CD4/CD25/FoxP3 cells, was significantly elevated in the ischemic hemisphere of AAV5-GFAP-hIGF-1 treated animals as compared to AAV5-GFAP-control animals ($p =0.0219$; Figure 4-7C).

In the case of infiltrating macrophages, identified by CD45high/CD11b/Iba1, there were no differences in the proportion of these invading cells in the AAV5-GFAP-control and AAV5-GFAP-hIGF-1 groups ($p = 0.2280$; Figure 4-8A). However, infiltrating macrophages differed in the extent of M1 and M2 cohorts seen in each group. As shown in Fig 8B, the proportion of infiltrating macrophages labeled with CD68/CD86 (M1 phenotype) was decreased by 62% in AAV5-GFAP-IGF-1 treated animals as compared to AAV5-GFAP-control treated animals ($p = 0.0485$). In contrast, the proportion of infiltrating macrophages labeled with CD163/CD206 (M2 phenotype) was increased by 57% in AAV5-GFAP-hIGF-1 treated animals as compared to AAV5-GFAP-control treated animals ($p =0.0248$; Figure 4-8C).

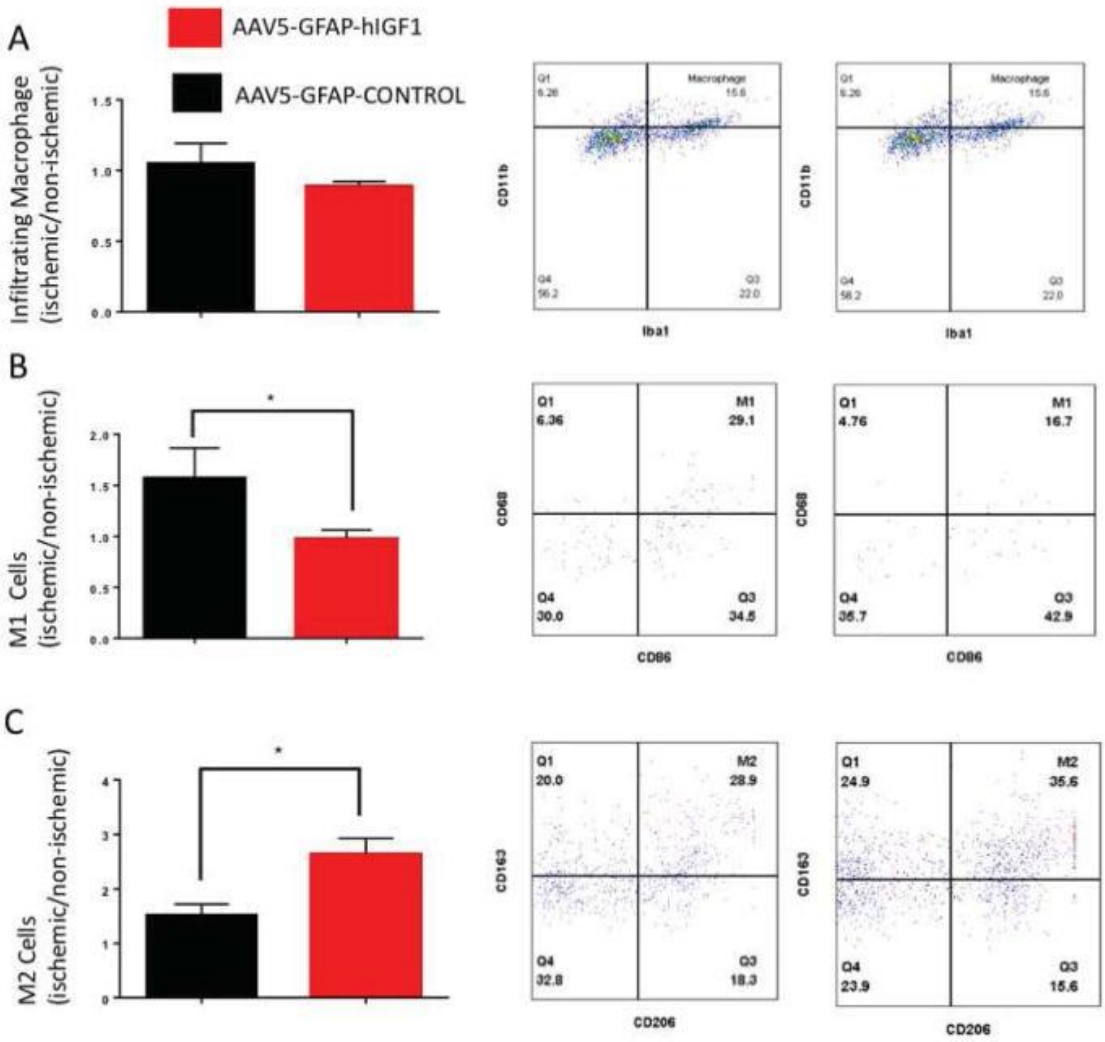

Figure 4-8: Infiltrating M1/M2 Macrophage Analysis
A) Proportion of CD45high/CD11b/Iba1 stained cells (infiltrating macrophages) in AAV5-GFAP-control and AAV5-GFAP-hIGF-1 treated animals (p = 0.2280). B) Proportion of infiltrating M1 macrophages (CD45high/CD11b/Iba1/CD68/CD86 stained cells) in AAV5-GFAP-control and AAV5-GFAP-hIGF-1 treated animals (*: p = 0.0485) and infiltrating M2 macrophages (CD45high/CD11b/Iba1/CD163/CD206) (*: p = 0.0248). All graphs represent mean ± SEM, n = 5–6 in each group.

4.4.7. Impact of rAAV5-GFAP-hIGF-1 in a permanent ischemia model

In view of the perivascular location of rAAV-GFAP-hIGF-1 cells, we next determined whether replenishing astrocytic IGF-1 would be effective in a permanent ischemic model (i.e., no reperfusion). As shown in Figure 4-9, AAV5-GFAP-hIGF-1 treatment had no effect on any of the measures tested. Similar to the transient MCAo, animals lost weight after stroke, and there were no group effects on weight loss (Figure 4-9A). In case of the neurological score, AAV5-GFAP-control animals were significantly impaired after permanent MCAo (Figure 4-9B), averaging a score of 4 for both groups, similar to the deficiency seen in the transient MCAo for AAV5-GFAP-control group (compare with Figure 4-4C). However, in the pMCAo condition, AAV5-GFAP-hIGF-1 treatment had no effect on the neurological score ($p = 0.9769$). Infarct volume (Figure 4-9C; $p = 0.7721$) was also no different between the two groups, although mean infarct volume was much higher in this model than the transient ischemic model (Figure 4-4D). The vibrissae evoked forelimb placing task showed that both groups were severely impaired (Figure 4-4 Ei and Eii), and performance was not improved by AAV5-GFAP-hIGF-1. Overall, AAV5-GFAP-hIGF-1 had no protective effect on the permanent MCAo model.

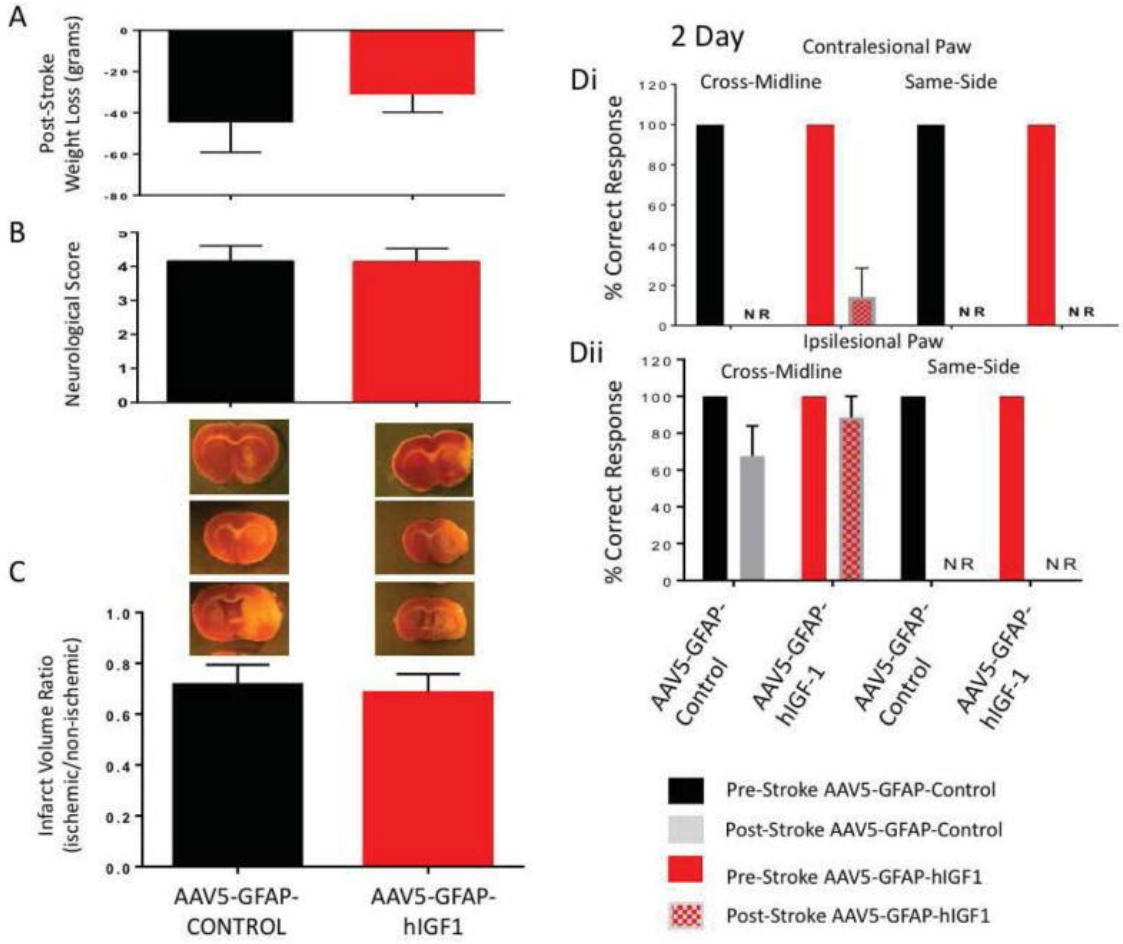

Figure 4-9: Permanent MCAo Model

A) Weight loss due to stroke in AAV5-GFAP-control and AAV5-GFAP-hIGF-1 treated animals. B) Neurological score assessed 2days after stroke in in AAV5-GFAP-control and AAV5-GFAP-hIGF-1 treated animals. C) Infarct volume measured 5d after stroke in AAV5-GFAP-control and AAV5-GFAP-hIGF-1 treated animals. Di and Dii) Sensory-motor performance measured by vibrissae evoked forelimb placing task in AAV5-GFAP-control and AAV5-GFAP-hIGF-1 treated animals. All graphs represent mean ± SEM. n = 5–6 in each group. No significant differences were seen in any of these measures.

4.5. Discussion

These data support the hypothesis that elevating IGF-1 expression in astrocytes significantly improves stroke outcomes after transient ischemia-reperfusion in middle-aged female SD rats. AAV5 mediated-expression of hIGF-1 in astrocytes reduced stroke-induced motor impairment, improved sensory motor performance and preferential transmigration of immune cells associated with protective or anti-inflammatory actions. Additionally, systolic blood pressure was stable after transient MCAo in animals with replenished astrocyte IGF-1, while controls experienced a decrease in systolic blood pressure after stroke, which is associated with poorer clinical outcomes and increased mortality in stroke patients (Lin et al. 2015; Okin et al. 2015) especially in the acute period of stroke (Wohlfahrt et al. 2015). These novel findings are in accordance with a growing body of evidence that functional modifications of astrocytes yields major benefits for neurodegenerative diseases (Bajenaru et al. 2002; Furman et al. 2012; Furman et al. 2016).

Age-regulated decreases in the functional capacity of astrocytes may increase the severity of neurological diseases. Aging astrocytes display decreased glucose uptake, GLUT1 expression, and glutathione (GSH) content (Souza et al. 2015), increased levels of intermediate glial fibrillary acidic protein and cytokine secretion (Capilla-Gonzalez et al. 2014; Salminen et al. 2011). Moreover, with age, astrocytes are less sensitive to the anti-inflammatory cytokine IL-10, which results in prolonged neuroinflammation due to persistent microglial activation (Norden et al. 2016). Our previous studies show that, compared to astrocytes from younger female rats, astrocytes from middle-aged females

have significantly reduced capacity for glutamate clearance, elevated expression of chemokines and increased ability to recruit PBMC in co-cultures (Lewis et al. 2012). More recent studies show that astrocytes from middle aged females have epigenetic modifications that cause transcriptional repression (Chisholm et al. 2015). This decline in astrocytic functional capacity coincides with an increase in infarct volumes and worsening post-stroke recovery in our model. Whether astrocyte dysfunction is the cause or the result of disease progression has yet to be elucidated. Nevertheless, astrocyte replacement by neural progenitor cells and glial-restricted precursors is reported to have some benefit in acute injury models such as spinal cord injury (Haas and Fischer 2013; van Gorp et al. 2013).

Targeted modification of astrocyte proteins has been used in several neural injury models with success. In Huntington's disease, AAV2/5 mediated restoration of Kir4.1, a rectifying potassium channel, in striatal astrocytes increased longevity and improved motor performance on the rotorad test, footprint analysis, and paw clasp test (Dvorzhak et al. 2016). In spinal cord injury, AAV8-mediated overexpression of Glutamate transporter 1, a protein found primarily in astrocytes, increased diaphragm dysfunction, affected breathing, and increased forelimb dysfunction six weeks after contusion (Li et al. 2014). In hippocampal ischemic injury, heat shock protein (Hsp)70 or superoxide dismutase (SOD) targeted for expression in astrocytes reduced cell death (Xu et al. 2010) in vivo, while virally-mediated astrocyte specific expression of the excitatory amino acid transporter (EEAT2) decreased cell death in hippocampal cultures exposed to moderate oxygen glucose deprivation (OGD) (Weller et al. 2008). Interestingly,

enhanced expression of EEAT2 was only neuroprotective against moderate levels of OGD but not severe OGD (Weller et al. 2008). This was also seen in the present study where AAV5-mediated IGF-1 in astrocytes improved sensory motor function after stroke in transient MCA (Figure 4-5) but not permanent MCAo, which results in a much larger infarct volume (Figure 4-9) and is considered a more severe ischemic injury. In transient focal ischemia, suppression of CD38 in astrocytes reduced transfer of mitochondria, resulting in worse neurological outcomes. (Hayakawa, et. al., 2016). The unique finding of this study is that while non-cell specific viral-mediated transfer of IGF-1 either prior (Zhu et al. 2008) or after (Zhu et al. 2009) MCAo promotes neovascularization and neurogenesis, the present study is first demonstration that astrocyte targeted IGF-1 improves motor outcomes post-stroke.

Surprisingly, while virally-mediated increase in astrocyte IGF-1 improved neurological scores and sensory motor performance and barrier function, it did not lead to reduction of infarct volume. While some studies have shown a significant correlation between increased infarct volume and worse neurological scores and motor impairment (Rogers et al. 1997), other studies showed no correlation between behavioral impairment and infarct volume (Wahl et al. 1992). Clinically, infarct volumes are not the strongest predictor of long-term prognosis unless combined with NIHSS scores (Baird et al. 2001), as well as involvement of white matter tracts and cerebral blood supply (Heiss and Kidwell 2014). Furthermore, several other growth factors therapies also improve behavior independent of infarct volume. In SD rats, fibroblast growth factor treatment initiated 1 day after MCAo improved behavioral recovery but had no effect on infarct

volume (Kawamata et al. 1996). Similarly, rats infused with brain-derived neurotrophic factor after MCAo showed less functional deficit at 28 days after treatment than controls but lesion size measured by T2-MRI did not show differences at 7 and 28 days (Ramos-Cejudo et al. 2015). Additionally, blocking ephrin-A5 signaling, an important pathway for axonal sprouting in premotor and prefrontal motor circuits, in reactive astrocytes after MCAo also improved motor function recovery without a significant change in infarct volume (Overman et al. 2012).

The current studies also reveal a clear difference between the neuroprotective effects of intracerebroventricular (ICV) infusions of hIGF-1 versus AAV5-mediated astrocyte expression of hIGF-1. In middle-aged SD rats, intracerebroventricular (ICV) delivery of hIGF-1 after stroke significantly decreases infarct volume and reduces blood brain barrier permeability (Bake et al. 2014). Furthermore, ICV hIGF-1 treatment decreased trafficking of CD4+ cells and T regulatory cells into the ischemic hemisphere, consistent with the idea that IGF-1 reduces hyperpermeability at the blood brain barrier (Bake et al. 2016). In contrast, astrocyte-derived hIGF-1, did not improve infarct volume although barrier properties were improved as evidenced by serum GFAP levels. Furthermore, astrocyte hIGF-1 did not reduce overall immune trafficking into the ischemic hemisphere, but altered the cohort of immune subtypes. Thus, while there was no difference in the proportion of M1/M2 phenotype resident microglia, infiltrating regulatory T cells and infiltrating M2 macrophages were elevated, indicating that astrocyte-derived hIGF-1 altered immune cell transmigration to favor neuro-supportive and anti-inflammatory cells (Li et al. 2013; Liesz et al. 2015; Won et al. 2015). The

difference between the actions of ICV delivery of IGF-1 versus astrocyte mediated hIGF-1 could be due to differences in the amount of IGF-1 available via each method or due to the fact that virally-induced astrocyte hIGF-1 constitutes a 'pretreatment' while ICV-hIGF-1 is a post stroke treatment. Overall, our previous and current data support the hypothesis that the poorer stroke outcomes in older females is associated with age-related decreases in this peptide hormone.

Despite its central location, AAV5-mediated astrocyte hIGF-1 expression has striking effects on the peripheral physiological milieu, as seen by regulation of peripheral cytokines as well as maintenance of systolic blood pressure post-stoke. Astrocytic hIGF-1 elevated circulating levels of granulocyte colony-stimulating factor (GCSF), which is reported to be neuroprotective (Bath and Sprigg 2007; Fan et al. 2015; Shin and Cho 2016), as well as IL-4 and IL-5, which are associated with the Th2 immune response and correlates with reduction in infarct volume (Luo et al. 2015). Peripheral inflammation in stroke patients, usually caused by infection, worsens stroke outcomes (Grau et al. 1999). LPS treatment after stroke, for example, increases macrophage infiltration and caused a prolonged impairment of hindlimb function (Langdon et al. 2010). Thus behavioral improvement seen in AAV-GFAP-hIGF-1 infected animals may be mechanistically linked to a modification of the inflammatory environment.

Astrocytes are the most abundant cell in the brain, outnumbering neurons by at least five to one (Cotrina and Nedergaard 2002; Sofroniew and Vinters 2010). Despite their abundance, stroke research has been mostly neurocentric, aimed towards

developing interventions focused on neuronal survival after ischemic injury (Barreto et al. 2011a; Lo et al. 2004), an approach that has not led to successful drug development (Barreto et al. 2011b). The recent trend towards targeting single genes in astrocyte shows promise as a therapy, although most studies have focused on young animal models. Our study is the first to show that correcting a growth factor deficiency in astrocytes in older animals can improve stroke outcomes. In conjunction with refinement of cell based stroke therapies, our data suggest that targeted elevation of IGF-1 in glial-restricted precursors may enhance stroke recovery in older or more susceptible patient populations.

4.6. Main Points

There are two major points of this study: 1) Ischemia-induced damage and disability is worse in middle-aged female rats than young female rats; and 2)Astrocyte-specific gene transfer of IGF-1 improves the immunological response and motor sensory recovery after stroke in middle-aged females.

4.7. References

Abbott NJ, Ronnback L, Hansson E. Astrocyte-endothelial interactions at the blood-brain barrier. *Nat Rev Neurosci*. 2006;7:41–53.

Allaman I, Belanger M, Magistretti PJ. Astrocyte-neuron metabolic relationships: for better and for worse. *Trends Neurosci*. 2011;34:76–87.

Ayadi AE, Zigmond MJ, Smith AD. IGF-1 protects dopamine neurons against oxidative stress: association with changes in phosphokinases. Exp Brain Res. 2016;234:1863–73.

Badan I, Buchhold B, Hamm A, Gratz M, Walker LC, Platt D, Kessler C, Popa-Wagner A. Accelerated glial reactivity to stroke in aged rats correlates with reduced functional recovery. J Cereb Blood Flow Metab. 2003;23:845–54.

Baird AE, Dambrosia J, Janket S, Eichbaum Q, Chaves C, Silver B, Barber PA, Parsons M, Darby D, Davis S, et al. A three-item scale for the early prediction of stroke recovery. *Lancet.* 2001;357:2095–9

Bajenaru ML, Zhu Y, Hedrick NM, Donahoe J, Parada LF, Gutmann DH. Astrocyte-specific inactivation of the neurofibromatosis 1 gene (NF1) is insufficient for astrocytoma formation. *Mol Cell Biol.* 2002;22:5100–13.

Bake S, Okoreeh AK, Alaniz RC, Sohrabji F. Insulin-Like Growth Factor (IGF)-I Modulates Endothelial Blood-Brain Barrier Function in Ischemic Middle-Aged Female Rats. *Endocrinology.* 2016;157:61–9.

Bake S, Selvamani A, Cherry J, Sohrabji F. Blood Brain Barrier and Neuroinflammation Are Critical Targets of IGF-1-Mediated Neuroprotection in Stroke for Middle-Aged Female Rats. *PLoS ONE.* 2014;9:e91427.

Bano D, Young KW, Guerin CJ, Lefeuvre R, Rothwell NJ, Naldini L, Rizzuto R, Carafoli E, Nicotera P. Cleavage of the plasma membrane Na+/Ca2+ exchanger in excitotoxicity. *Cell.* 2005;120:275–85.

Barreto G, White RE, Ouyang Y, Xu L, Giffard RG. Astrocytes: targets for neuroprotection in stroke. *Cent Nerv Syst Agents Med Chem.* 2011a;11:164–73.

Barreto GE, Gonzalez J, Torres Y, Morales L. Astrocytic-neuronal crosstalk: implications for neuroprotection from brain injury. *Neurosci Res.* 2011b;71:107–13.

Bath PM, Sprigg N. Colony stimulating factors (including erythropoietin, granulocyte colony stimulating factor and analogues) for stroke. *Cochrane Database Syst Rev.* 2007:Cd005207.

Bhat R, Crowe EP, Bitto A, Moh M, Katsetos CD, Garcia FU, Johnson FB, Trojanowski JQ, Sell C, Torres C. Astrocyte senescence as a component of Alzheimer's disease. *PLoS One.* 2012;7:e45069.

Bondy CA, Cheng CM. Signaling by insulin-like growth factor 1 in brain. *Eur J Pharmacol.* 2004;490:25–31.

Buga AM, Sascau M, Pisoschi C, Herndon JG, Kessler C, Popa-Wagner A. The genomic response of the ipsilateral and contralateral cortex to stroke in aged rats. *J Cell Mol Med.* 2008;12:2731–53.

Capilla-Gonzalez V, Cebrian-Silla A, Guerrero-Cazares H, Garcia-Verdugo JM, Quinones-Hinojosa A. Age-related changes in astrocytic and ependymal cells of the subventricular zone. *Glia.* 2014;62:790–803.

Cekanaviciute E, Buckwalter MS. Astrocytes: Integrative Regulators of Neuroinflammation in Stroke and Other Neurological Diseases. *Neurotherapeutics.* 2016;13:685–701.

Chisholm NC, Henderson ML, Selvamani A, Park MJ, Dindot S, Miranda RC, Sohrabji F. Histone methylation patterns in astrocytes are influenced by age following ischemia. *Epigenetics.* 2015;10:142–52.

Chisholm NC, Sohrabji F. Astrocytic response to cerebral ischemia is influenced by sex differences and impaired by aging. *Neurobiol Dis.* 2016;85:245–53.

Cotrina ML, Nedergaard M. Astrocytes in the aging brain. *J Neurosci Res.* 2002;67:1–10.

Dienel GA, Hertz L. Astrocytic contributions to bioenergetics of cerebral ischemia. *Glia.* 2005;50:362–88.

Dvorzhak A, Vagner T, Kirmse K, Grantyn R. Functional Indicators of Glutamate Transport in Single Striatal Astrocytes and the Influence of Kir4.1 in Normal and Huntington Mice. *J Neurosci.* 2016;36:4959–75.

Fan ZZ, Cai HB, Ge ZM, Wang LQ, Zhang XD, Li L, Zhai XB. The Efficacy and Safety of Granulocyte Colony-Stimulating Factor for Patients with Stroke. *J Stroke Cerebrovasc Dis.* 2015;24:1701–8.

Furman JL, Sama DM, Gant JC, Beckett TL, Murphy MP, Bachstetter AD, Van Eldik LJ, Norris CM. Targeting astrocytes ameliorates neurologic changes in a mouse model of Alzheimer's disease. *J Neurosci.* 2012;32:16129–40.

Furman JL, Sompol P, Kraner SD, Pleiss MM, Putman EJ, Dunkerson J, Mohmmad Abdul H, Roberts KN, Scheff SW, Norris CM. Blockade of Astrocytic Calcineurin/NFAT Signaling Helps to Normalize Hippocampal Synaptic Function and Plasticity in a Rat Model of Traumatic Brain Injury. *J Neurosci.* 2016;36:1502–15.

Grau AJ, Buggle F, Schnitzler P, Spiel M, Lichy C, Hacke W. Fever and infection early after ischemic stroke. *J Neurol Sci.* 1999;171:115–20.

Haas C, Fischer I. Human astrocytes derived from glial restricted progenitors support regeneration of the injured spinal cord. *J Neurotrauma.* 2013;30:1035–52.

Hayakawa K, Esposito E, Wang X, Terasaki Y, Liu Y, Xing C, Ji X, Lo EH. Transfer of mitochondria from astrocytes to neurons after stroke. *Nature.* 2016;535:551–5.

Heiss WD, Kidwell CS. Imaging for prediction of functional outcome and assessment of recovery in ischemic stroke. *Stroke.* 2014;45:1195–201

Jezierski MK, Sohrabji F. Neurotrophin expression in the reproductively senescent forebrain is refractory to estrogen stimulation. *Neurobiol Aging.* 2001;22:309–19.

Karki P, Smith K, Johnson J, Jr, Lee E. Astrocyte-derived growth factors and estrogen neuroprotection: role of transforming growth factor-alpha in estrogen-induced upregulation of glutamate transporters in astrocytes. *Mol Cell Endocrinol.* 2014;389:58–64.

Kawamata T, Alexis NE, Dietrich WD, Finklestein SP. Intracisternal basic fibroblast growth factor (bFGF) enhances behavioral recovery following focal cerebral infarction in the rat. *J Cereb Blood Flow Metab.* 1996;16:542–7.

Langdon KD, MacLellan CL, Corbett D. Prolonged, 24-h delayed peripheral inflammation increases short- and long-term functional impairment and histopathological damage after focal ischemia in the rat. *Journal of Cerebral Blood Flow and Metabolism: Official Journal of the International Society of Cerebral Blood Flow and Metabolism.* 2010;30:1450–1459.

Latour A, Grintal B, Champeil-Potokar G, Hennebelle M, Lavialle M, Dutar P, Potier B, Billard JM, Vancassel S, Denis I. Omega-3 fatty acids deficiency aggravates glutamatergic synapse and astroglial aging in the rat hippocampal CA1. *Aging Cell.* 2013;12:76–84.

Lewis DK, Thomas KT, Selvamani A, Sohrabji F. Age-related severity of focal ischemia in female rats is associated with impaired astrocyte function. *Neurobiol Aging.* 2012;33:1123, e1–16.

Li K, Nicaise C, Sannie D, Hala TJ, Javed E, Parker JL, Putatunda R, Regan KA, Suain V, Brion JP, et al. Overexpression of the astrocyte glutamate transporter GLT1 exacerbates phrenic motor neuron degeneration, diaphragm compromise, and forelimb motor dysfunction following cervical contusion spinal cord injury. *J Neurosci.* 2014;34:7622–38.

Li P, Gan Y, Sun BL, Zhang F, Lu B, Gao Y, Liang W, Thomson AW, Chen J, Hu X. Adoptive regulatory T-cell therapy protects against cerebral ischemia. *Ann Neurol.* 2013;74:458–71.

Liesz A, Hu X, Kleinschnitz C, Offner H. Functional role of regulatory lymphocytes in stroke: facts and controversies. *Stroke.* 2015;46:1422–30.

Lin MP, Ovbiagele B, Markovic D, Towfighi A. Systolic blood pressure and mortality after stroke: too low, no go? *Stroke.* 2015;46:1307–13.

Lo EH, Broderick JP, Moskowitz MA. tPA and proteolysis in the neurovascular unit. *Stroke*. 2004;35:354–6.

Lo EH, Dalkara T, Moskowitz MA. Mechanisms, challenges and opportunities in stroke. *Nat Rev Neurosci.* 2003;4:399–415.

Luo Y, Zhou Y, Xiao W, Liang Z, Dai J, Weng X, Wu X. Interleukin-33 ameliorates ischemic brain injury in experimental stroke through promoting Th2 response and suppressing Th17 response. *Brain Res.* 2015;1597:86–94.

Madathil SK, Carlson SW, Brelsfoard JM, Ye P, D'Ercole AJ, Saatman KE. Astrocyte-Specific Overexpression of Insulin-Like Growth Factor-1 Protects Hippocampal

Neurons and Reduces Behavioral Deficits following Traumatic Brain Injury in Mice. *PLoS One.* 2013;8:e67204.

Manwani B, Liu F, Xu Y, Persky R, Li J, McCullough LD. Functional recovery in aging mice after experimental stroke. *Brain Behav Immun.* 2011;25:1689–700.

Marchi N, Cavaglia M, Fazio V, Bhudia S, Hallene K, Janigro D. Peripheral markers of blood–brain barrier damage. *Clinica Chimica Acta.* 2004;342:1–12.

Mozaffarian D, Benjamin EJ, Go AS, Arnett DK, Blaha MJ, Cushman M, de Ferranti S, Després J-P, Fullerton HJ, Howard VJ, et al. *Heart Disease and Stroke Statistics—2015 Update. A Report From the American Heart Association.* 2015;131:e29–e322.

Norden DM, Trojanowski PJ, Walker FR, Godbout JP. Insensitivity of astrocytes to interleukin 10 signaling following peripheral immune challenge results in prolonged microglial activation in the aged brain. *Neurobiol Aging.* 2016;44:22–41.

Okin PM, Kjeldsen SE, Devereux RB. Systolic Blood Pressure Control and Mortality After Stroke in Hypertensive Patients. *Stroke.* 2015;46:2113–8.

Olsen ML, Sontheimer H. Functional implications for Kir4.1 channels in glial biology: from K(+) buffering to cell differentiation. *Journal of Neurochemistry.* 2008;107:589–601.

Overman JJ, Clarkson AN, Wanner IB, Overman WT, Eckstein I, Maguire JL, Dinov ID, Toga AW, Carmichael ST. A role for ephrin-A5 in axonal sprouting, recovery, and activity-dependent plasticity after stroke. *Proc Natl Acad Sci* U S A. 2012;109:E2230–9.

Panickar KS, Norenberg MD. Astrocytes in cerebral ischemic injury: morphological and general considerations. *Glia*. 2005;50:287–98.

Posada-Duque RA, Barreto GE, Cardona-Gomez GP. Protection after stroke: cellular effectors of neurovascular unit integrity. *Front Cell Neurosci.* 2014;8:231.

Ramos-Cejudo J, Gutiérrez-Fernández M, Otero-Ortega L, Rodríguez-Frutos B, Fuentes B, Vallejo-Cremades MT, Hernanz TN, Cerdán S, Díez-Tejedor E. Brain-Derived Neurotrophic Factor Administration Mediated Oligodendrocyte Differentiation and Myelin Formation in Subcortical Ischemic Stroke. *Stroke.* 2015;46:221–228.

Ridet JL, Malhotra SK, Privat A, Gage FH. Reactive astrocytes: cellular and molecular cues to biological function. *Trends Neurosci.* 1997;20:570–7.

Rogers DC, Campbell CA, Stretton JL, Mackay KB. Correlation Between Motor Impairment and Infarct Volume After Permanent and Transient Middle Cerebral Artery Occlusion in the Rat. *Stroke*. 1997;28:2060–2066.

Rossi DJ, Brady JD, Mohr C. Astrocyte metabolism and signaling during brain ischemia. *Nat Neurosci.* 2007;10:1377–1386.

Salminen A, Ojala J, Kaarniranta K, Haapasalo A, Hiltunen M, Soininen H. Astrocytes in the aging brain express characteristics of senescence-associated secretory phenotype. *Eur J Neurosci.* 2011;34:3–11.

Selvamani A, Sohrabji F. The neurotoxic effects of estrogen on ischemic stroke in older female rats is associated with age-dependent loss of IGF-1. *The Journal of Neuroscience: the official journal of the Society for Neuroscience.* 2010;30:6852–6861.

Shin YK, Cho SR. Exploring Erythropoietin and G-CSF Combination Therapy in Chronic Stroke Patients. *Int J Mol Sci.* 2016;17:463.

Sofroniew MV, Vinters HV. Astrocytes: biology and pathology. *Acta Neuropathol.* 2010;119:7–35.

Souza DG, Bellaver B, Raupp GS, Souza DO, Quincozes-Santos A. Astrocytes from adult Wistar rats aged in vitro show changes in glial functions. *Neurochem Int.* 2015;90:93–7.

Topp KS, Faddis BT, Vijayan VK. Trauma-induced proliferation of astrocytes in the brains of young and aged rats. *Glia.* 1989;2:201–11.

Utada K, Ishida K, Tohyama S, Urushima Y, Mizukami Y, Yamashita A, Uchida M, Matsumoto M. The combination of insulin-like growth factor 1 and erythropoietin protects against ischemic spinal cord injury in rabbits. *J Anesth.* 2015;29:741–8.

van Gorp S, Leerink M, Kakinohana O, Platoshyn O, Santucci C, Galik J, Joosten EA, Hruska-Plochan M, Goldberg D, Marsala S, et al. Amelioration of motor/sensory dysfunction and spasticity in a rat model of acute lumbar spinal cord injury by human neural stem cell transplantation. *Stem Cell Res Ther.* 2013;4:57.

Wahl F, Allix M, Plotkine M, Boulu RG. Neurological and behavioral outcomes of focal cerebral ischemia in rats. *Stroke.* 1992;23:267–72.

Weller ML, Stone IM, Goss A, Rau T, Rova C, Poulsen DJ. Selective Over Expression Of EAAT2 In Astrocytes Enhances Neuroprotection From Moderate But Not Severe Hypoxia-Ischemia. *Neuroscience.* 2008;155:1204–1211.

Wohlfahrt P, Krajcoviechova A, Jozifova M, Mayer O, Vanek J, Filipovsky J, Cifkova R. Low blood pressure during the acute period of ischemic stroke is associated with decreased survival. *J Hypertens.* 2015;33:339–45.

Won S, Lee JK, Stein DG. Recombinant tissue plasminogen activator promotes, and progesterone attenuates, microglia/macrophage M1 polarization and recruitment of microglia after MCAO stroke in rats. *Brain Behav Immun.* 2015;49:267–79.

Woodlee MT, Asseo-Garcia AM, Zhao X, Liu SJ, Jones TA, Schallert T. Testing forelimb placing "across the midline" reveals distinct, lesion-dependent patterns of recovery in rats. *Exp Neurol.* 2005;191:310–7.

Xie L, Yang SH. Interaction of astrocytes and T cells in physiological and pathological conditions. *Brain Res.* 2015;1623:63–73.

Xu L, Emery JF, Ouyang YB, Voloboueva LA, Giffard RG. Astrocyte targeted overexpression of Hsp72 or SOD2 reduces neuronal vulnerability to forebrain ischemia. *Glia.* 2010;58:1042–9.

Zhu W, Fan Y, Frenzel T, Gasmi M, Bartus RT, Young WL, Yang GY, Chen Y. Insulin growth factor-1 gene transfer enhances neurovascular remodeling and improves long-term stroke outcome in mice. *Stroke.* 2008;39:1254–61.

Zhu W, Fan Y, Hao Q, Shen F, Hashimoto T, Yang G-Y, Gasmi M, Bartus RT, Young WL, Chen Y. Postischemic IGF-1 gene transfer promotes neurovascular regeneration after experimental stroke. *Journal of cerebral blood flow and metabolism: official journal of the International Society of Cerebral Blood Flow and Metabolism.* 2009;29:1528–1537.

5. CONCLUSIONS

5.1. Insulin-like Growth Factor-1 Protects the Blood Brain Barrier

Insulin-like growth factor-1, a neuroprotective peptide hormone for our aging female model (Bake, Selvamani, Cherry, & Sohrabji, 2014), is secreted each cell of the neurovascular unit: astrocytes, endothelial cells, neurons, microglial cells, and pericytes (Fernandez & Torres-Aleman, 2012; Nishijima et al., 2010; Sohrabji, Bake, & Lewis, 2013; Zhu et al., 2008). Previous studies have shown that IGF-1 decreases post-stroke inflammation and infarct volumes (Bake et al., 2014). This research approaches the benefits and mechanisms of IGF-1 post-stoke neuroprotection in our aging female model by focusing on non-neuronal cell types and endothelial cells with the hope of implementing IGF-1 as a possible post-stroke treatment, particularly in females.
The research within this dissertation tests the hypothesis that insulin-like growth factor-1 reduces brain infarction acts by preserving the integrity of the blood brain barrier after ischemia in females.

The research presented within this dissertation repeatedly provides evidence supporting this hypothesis by using both in vivo and in vitro methodology. In the first study, post-stroke IGF-1 treatment, in vivo, decreases two surrogate markers of blood brain barrier permeability, both CD4+ and Treg cells that are harvested from ischemic middle-aged female rat brain. The study goes further to understand the molecular details by harvesting brain microvascular endothelial cells (BMEC)s from middle-aged female rats and subjecting them to stroke-like conditions (OGD), in vitro. IGF-I treatment to

these BMECs significantly reduces the transfer of fluorescently labeled BSA across a BMEC monolayer and reduces ischemia-induced morphological changes in BMECs. These data suggest that, in our female aging model, IGF-1 supports blood brain barrier function and integrity after ischemia, specifically, by acting on brain microvascular endothelial cells.

Building on the results from the first study, the second study also applies in vivo and in vitro methodologies to further investigate the neuroprotective effects of IGF-1 on the female BBB during ischemia, honing in on brain microvascular endothelial cells. The architecture of post-stroke microvascular in our aging model was analyzed to determine if the BMEC morphology changes seen in vitro in the first study translated in vivo. Post-stroke IGF-1 treatment prevented microvascular collapse. In addition, Post-stroke IGF-1 preserved vinculin, an important protein which anchors vessels to the basement membrane. Both findings suggests that post-stroke IGF-1 preserves BBB integrity. In vitro, IGF-1 reduced ischemic-induced stress fiber formation in female BMECs, correlating F-actin formation to the morphological changes seen in BMEC from the first study. All together these data strongly suggests that BMECs are a major target of post-stroke IGF-1 neuroprotection in our aging female model and that IGF-1 mitigates the ischemia-induced morphological and molecular responses of BMECs which results in increased BBB permeability and neurotoxic inflammation.

The third study approaches the dissertation overall hypothesis by targeting a cell that is intimately associated with BBB, the astrocyte, a cell of neurovascular unit (Abbott, 2002; Abbott & Friedman, 2012; Abbott, Ronnback, & Hansson, 2006). Gene

transfer of IGF-1 specifically in astrocytes prior to ischemic improves post-stroke outcomes and decreased BBB permeability, as assessed by serum GFAP, a surrogate marker (Marchi et al., 2003; Park & Sohrabji, 2016). This study, unlike when IGF-1 is provided ICV, demonstrates that targeted treatment to the microvasculature post-stroke is enough to improve recovery, further suggesting IGF-1 act at the level of the BBB to improve post-stroke outcomes.

Taken together, this data implies that insulin-like growth factor-1 acts by preserving the integrity of the blood brain barrier after ischemia in females and is a likely candidate for the stroke therapy in women. Though these studies in this dissertation are limited to the acute phase of stroke recovery, in other studies, our laboratory has shown that early post-stroke IGF-1 treatment improves outcomes several months after injury.

As previously mentioned, stroke is an extremely deadly, debilitating disease, particularly for women, with very few interventions. The work presented here further suggests that IGF-1 is poised to address the dire need for neurovascular treatments. IGF-1 has great promise in providing an improved treatment option for older women. Compared to tPA, IGF-1 is likely to have a wider therapeutic window than 4.5 hour after onset (Davis & Donnan, 2009), allowing IGF-1 to serve a wider proportion of stroke patients, and IGF-1 is likely not to have the acute life-threatening risk associated with tPA, e.g. hemorrhage (J. Zhang, Yang, Sun, & Xing, 2014).

5.2. Further Work and Challenges

To translate IGF-1 from benchtop to bedside, more research on its neuroprotective effects is needed. Though the work presented here furthers our understanding of the effects of IGF-1 on the ischemic brain, the precise mechanisms and parameters of IGF-1 are poorly understood. Critical research issues follow.

5.2.1. The Therapeutic Window of IGF-1

A major result from the second study was that IGF-1 treatment after stroke resulted in significant biological changes in the early stages of stroke recovery, however these effects waned over time. But despite the lack of biological differences between vehicle and IGF-1 treatment at the later time points, IGF-1 improved long-term assessments of sensory motor function in the middle-aged female animal model. However, it is unknown how long after a stroke IGF-1 can be provided with a significant benefit in the middle-aged female model.

Stroke patients are not always able to come to a medical facility rapidly after the onset of stroke (Fields & Levine, 2005). This often means that they are not eligible for tPA treatment, which can only be administered 3-4.5 h after stroke. It would be important to determine if IGF-1 treatment is neuroprotective if given at progressively longer times after stroke. This would include hours to days after the onset of stroke. As these studies show, both morphological, biochemical and behavioral assessments should be used. If IGF-1 is still beneficial 24 hours after stroke, it will be a significant advancement over other current therapies including tPA. Though the effect may not be

as dramatic as early treatment, any improvement seen at the later treatment-onset time point would have a significant clinical impact.

5.2.2. The Long Term Effects & Toxicity of IGF-1

All the studies in this thesis have focused on recovery in the acute phase of stroke, such as neurological score and sensory motor deficits. However, stroke also results in long term disability, and other psychiatric conditions such as post-stroke depression (Thomas et al., 2016), post-stroke epilepsy (Kim, Park, Choi, & Lee, 2016), and changes in addictive behaviors (Abdolahi et al., 2015a, 2015b; Brust & Richter, 1976). Future studies need to focus on the effect of long term recovery, using a variety of outcome measures.

An important issue that also needs to be addressed in preclinical studies is the toxicity of the IGF-1. As a growth hormone, there is some concern that the systemic injections of IGF-1 would lead to an increased risk of cancer. Long term studies therefore need to also include full body histopathology to exclude the possibility of tumor development. Due the short time period of IGF-1 treatment post-stroke, we believe it is unlikely that IGF-1 will be a reliable cause of cancer.

Another concern in the clinical application of IGF-1 is hypoglycemia. As an anabolic agent, IGF-1 can decrease glucose level when provided intravenously (Di Cola, Cool, & Accili, 1997; Kovacs et al., 1999). In rats, this effect has rapid-onset and is dose-dependent. Again, it is unlikely to occur at the low doses needed for neuroprotection, but such effects would have to be tested in the aged female model before human testing. Also, in the presence of others metabolic disorders, such diabetes

which is a risk factor for stroke, the detrimental metabolic effects of IGF-1 may be amplified.

5.2.3. Molecular Pathways of IGF-1

To translate IGF-1 to the clinic, we need a more thorough understanding of IGF-1's neuroprotective mechanism of action, to better predict drug interactions. In this context in vitro studies would be most effective in understanding signaling pathways, using a combination of gene silencing techniques or pharmacological tools. As the second study shows, the effect of IGF-1 in vitro can mirror events that occurred in vivo, suggesting in vitro modeling is a useful tool to assess the mechanism of IGF-1. The in vitro model would also be useful in investigating the delayed effects of IGF-1.

In the brain, all cells of the neurovascular unit secrete IGF-1 and provides both autocrine and paracrine input (Bassil, Fernagut, Bezard, & Meissner, 2014). Once released IGF-1 binds to IGF-1R, this binding activates the tyrosine kinase domains on the β subunits of IGF-1R (the major target of JB-1, our IGF-1 antagonist), leading to the activation of the canonical PI3K/mTOR/AKT and MAPK/ERK pathways, two important signaling cascades proliferation, cell cycle, and survival within the brain (Alonso & Gonzalez, 2012). Our laboratory has shown that post-stroke IGF-1 treatment does increase expression of phosphorylated of AKT and ERK expression (Bake et al., 2014). In addition, other researchers have connected to the endothelial stress response to IGF-1 signaling (Panganiban & Day, 2013; Yentrapalli et al., 2013).

Since it known which pathways is most consequence for IGF-1 neuroprotection, the next step could be to knock down loci on the PI3K/mTOR/AKT and MAPK/ERK

pathways in separate experiments with OGD. The PI3K/mTOR/AKT pathway can be targeted using Wortmannin which targets PI3K (Wang et al., 2016), rapamycin which targets mTOR (C. Y. Li et al., 2015), or MK-2206 2HCl which targets (L. Zhang et al., 2015). The MAPK/ERK pathway can be targeted using SB203580 which targets MAPK (Dong et al., 2014) and SCH772984 which targets ERK (Abravanel et al., 2015). After knocking down, to further confirm the role each of these loci, the members of the pathway can be upregulated by gene transfer in presence of JB-1 plus IGF-1 to determine if the stress responses to OGD are reduced. Rho GTPases inhibitors can also be used to investigate stress fiber formation. Using these pharmacological agents, a stronger understanding of the neurological protective pathway of IGF-1 can be achieved.

5.2.4. Interaction of Endothelial Cells and Astrocytes

Thorough the three studies in the dissertation, endothelial cells and astrocytes, two important of glial cells of NVU, were shown to be affected by our treatments. In vivo, our data suggest that astrocyte derived IGF-1 affects the blood brain barrier presumably by acting on endothelial cells. However, this interaction between glia and endothelial cells was not directly tested. To more accurately replicated BBB in vitro, IGF-1's effects should be examined in co-culture of astrocytes and endothelial cells. Studies in this dissertation show that the early morphological BMEC changes are receptor mediated, which is not surprising. However, more mechanistic details are needed to better understand the post stroke vascular collapse seen in vivo. One approach to investigate this would be to systemically knock down loci in the canonical PI3K/mTOR/AKT and MAPK/ERK pathways cascade specifically and conditionally in

endothelial cells. This can be done in vivo using knockout mice or CRISPR/Cas9 technology and in vitro using siRNA.

5.2.5. Stem Cell Therapy

The most exciting result of this research was showcasing that restoring the secretion of one peptide hormone (IGF-1) by a single CNS cell type (astrocyte) can have significant consequences for stroke recovery in an aged female model. This result invites the question: Will introducing cells with increased IGF-1 secretion post-stroke improve outcomes and recovery?

Steps towards approaching this question having already in progress. Bone marrow-derived mesenchymal stem cells (BMDSC) are being used in stroke with moderate success (Steinberg et al., 2016). There is a phase 1/2a trial with eighteen patients that were provided post-stroke BMDSCs treatment for chronic stroke. After 12 month after treatment, these patients showed improvement in European Stroke Scale, National Institutes of Health Stroke Scale, and Fugl-Meyer total score (Steinberg et al., 2016). However, the BMDSC did not show any improvement in the modified Rankin Scale, the most widely used clinical measure of global neurological function and behavior after stroke during any time points after treatment (Harrison, McArthur, & Quinn, 2013). We have showed IGF-1 improves behavior well after post-stroke treatment, implying that IGF-1 would be a suitable supplement to this stem cell treatment. This implies the current BMDSC have also shown great promise in the other acute CNS injury models, such as spinal cord injury (Yousefifard et al., 2016) and traumatic brain injury (Jiang, Bu, Liu, & Cheng, 2012). The research presented here

suggests that priming BMDSC with increased IGF-1 secretion using gene transfer before post-stroke injection would be more efficacious than the currently unmodified BMDSC, increasing patient recovery and behavioral health. This type of strategy is already being explored in other research areas (M. Li et al., 2010; Tao et al., 2016).

There are potential pitfalls to address. Introducing a cell into the CNS that continuously produces IGF-1 would likely increase the opportunity for unwanted cell growth. AAV5 typically does not integrate into the host genome, thus gene transfer is loss after replication. This may cause some moderate issues in cell culture, however it may be advantageous once the stem cells are activated in the brain. As these cells divide and differentiate in the brain, the level of IGF-1 overexpression should decrease exponentially over time. This would be advantageous since long term IGF-1 replenishment poses a risk for cancer and there is building evidence that suggests IGF-1 treatment would be most beneficial in the early phases of stroke recovery.

5.3. Final Words

Stroke is a markedly expensive U.S. health concern that does not have a clear sign of waning as life spans expands, as food deserts swell thorough the heartland and the wealth inequality continues to stifle the majority of Americans from making responsible food choices and health decisions. Stroke particularly affects the lives of women, both in terms of mortality and increased disability. The studies in this thesis make a strong case for IGF-1 as a neuroprotectant for women's health.

5.4. References

Abbott, N. J. (2002). Astrocyte-endothelial interactions and blood-brain barrier permeability. *J Anat, 200*(6), 629-638.

Abbott, N. J., & Friedman, A. (2012). Overview and introduction: the blood-brain barrier in health and disease. *Epilepsia, 53 Suppl 6*, 1-6. doi:10.1111/j.1528-1167.2012.03696.x

Abbott, N. J., Ronnback, L., & Hansson, E. (2006). Astrocyte-endothelial interactions at the blood-brain barrier. *Nat Rev Neurosci, 7*(1), 41-53. doi:10.1038/nrn1824

Abdolahi, A., Williams, G. C., Benesch, C. G., Wang, H. Z., Spitzer, E. M., Scott, B. E., van Wijngaarden, E. (2015a). Damage to the insula leads to decreased nicotine withdrawal during abstinence. *Addiction, 110*(12), 1994-2003. doi:10.1111/add.13061

Abdolahi, A., Williams, G. C., Benesch, C. G., Wang, H. Z., Spitzer, E. M., Scott, B. E., van Wijngaarden, E. (2015b). Smoking cessation behaviors three months following acute insular damage from stroke. *Addict Behav, 51*, 24-30. doi:10.1016/j.addbeh.2015.07.001

Abravanel, D. L., Belka, G. K., Pan, T. C., Pant, D. K., Collins, M. A., Sterner, C. J., & Chodosh, L. A. (2015). Notch promotes recurrence of dormant tumor cells following HER2/neu-targeted therapy. *J Clin Invest, 125*(6), 2484-2496. doi:10.1172/JCI74883

Alonso, A., & Gonzalez, C. (2012). Neuroprotective role of estrogens: relationship with insulin/IGF-1 signaling. *Front Biosci (Elite Ed), 4*, 607-619.

Bake, S., Selvamani, A., Cherry, J., & Sohrabji, F. (2014). Blood brain barrier and neuroinflammation are critical targets of IGF-1-mediated neuroprotection in stroke for middle-aged female rats. *PLoS One, 9*(3), e91427. doi:10.1371/journal.pone.0091427

Bassil, F., Fernagut, P. O., Bezard, E., & Meissner, W. G. (2014). Insulin, IGF-1 and GLP-1 signaling in neurodegenerative disorders: targets for disease modification? *Prog Neurobiol, 118*, 1-18. doi:10.1016/j.pneurobio.2014.02.005

Brust, J. C., & Richter, R. W. (1976). Stroke associated with addiction to heroin. *J. Neurol Neurosurg Psychiatry, 39*(2), 194-199.

Davis, S. M., & Donnan, G. A. (2009). 4.5 hours: the new time window for tissue plasminogen activator in stroke. *Stroke, 40*(6), 2266-2267. doi:10.1161/STROKEAHA.108.544171

Di Cola, G., Cool, M. H., & Accili, D. (1997). Hypoglycemic effect of insulin-like growth factor-1 in mice lacking insulin receptors. *J Clin Invest, 99*(10), 2538-2544. doi:10.1172/JCI119438

Dong, H. J., Shang, C. Z., Peng, D. W., Xu, J., Xu, P. X., Zhan, L., & Wang, P. (2014). Curcumin attenuates ischemia-like injury induced IL-1beta elevation in brain microvascular endothelial cells via inhibiting MAPK pathways and nuclear factor-kappaB activation. *Neurol Sci, 35*(9), 1387-1392. doi:10.1007/s10072-014-1718-4

Fernandez, A. M., & Torres-Aleman, I. (2012). The many faces of insulin-like peptide signalling in the brain. *Nat Rev Neurosci, 13*(4), 225-239. doi:10.1038/nrn3209

Fields, M. C., & Levine, S. R. (2005). Patient page. Clot-busting therapy helps stroke victims--but only if they get treatment in time. *Neurology, 64*(2), E1-2.

Harrison, J. K., McArthur, K. S., & Quinn, T. J. (2013). Assessment scales in stroke: clinimetric and clinical considerations. *Clin Interv Aging, 8*, 201-211. doi:10.2147/CIA.S32405

Jiang, J., Bu, X., Liu, M., & Cheng, P. (2012). Transplantation of autologous bone marrow-derived mesenchymal stem cells for traumatic brain injury. *Neural Regen Res, 7*(1), 46-53. doi:10.3969/j.issn.1673-5374.2012.01.008

Kim, H. J., Park, K. D., Choi, K. G., & Lee, H. W. (2016). Clinical predictors of seizure recurrence after the first post-ischemic stroke seizure. *BMC Neurol, 16*(1), 212. doi:10.1186/s12883-016-0729-6

Kovacs, G. T., Worgall, S., Schwalbach, P., Steichele, T., Mehls, O., & Rosivall, L. (1999). Hypoglycemic effects of insulin-like growth factor-1 in experimental uremia: can concomitant growth hormone administration prevent this effect? *Horm Res, 51*(4), 193-200. doi:23357

Li, C. Y., Li, X., Liu, S. F., Qu, W. S., Wang, W., & Tian, D. S. (2015). Inhibition of mTOR pathway restrains astrocyte proliferation, migration and production of inflammatory mediators after oxygen-glucose deprivation and reoxygenation. *Neurochem Int, 83-84*, 9-18. doi:10.1016/j.neuint.2015.03.001

Li, M., Jayandharan, G. R., Li, B., Ling, C., Ma, W., Srivastava, A., & Zhong, L. (2010). High-efficiency transduction of fibroblasts and mesenchymal stem cells by tyrosine-mutant AAV2 vectors for their potential use in cellular therapy. *Hum Gene Ther, 21*(11), 1527-1543. doi:10.1089/hum.2010.005

Marchi, N., Rasmussen, P., Kapural, M., Fazio, V., Kight, K., Mayberg, M. R., . . . Janigro, D. (2003). Peripheral markers of brain damage and blood-brain barrier dysfunction. *Restor Neurol Neurosci, 21*(3-4), 109-121.

Nishijima, T., Piriz, J., Duflot, S., Fernandez, A. M., Gaitan, G., Gomez-Pinedo, U., Torres-Aleman, I. (2010). Neuronal activity drives localized blood-brain-barrier transport of serum insulin-like growth factor-I into the CNS. *Neuron, 67*(5), 834-846. doi:10.1016/j.neuron.2010.08.007

Panganiban, R. A., & Day, R. M. (2013). Inhibition of IGF-1R prevents ionizing radiation-induced primary endothelial cell senescence. *PLoS One, 8*(10), e78589. doi:10.1371/journal.pone.0078589

Park, M. J., & Sohrabji, F. (2016). The histone deacetylase inhibitor, sodium butyrate, exhibits neuroprotective effects for ischemic stroke in middle-aged female rats. *J Neuroinflammation, 13*(1), 300. doi:10.1186/s12974-016-0765-6

Sohrabji, F., Bake, S., & Lewis, D. K. (2013). Age-related changes in brain support cells: Implications for stroke severity. *Neurochem Int, 63*(4), 291-301. doi:10.1016/j.neuint.2013.06.013

Steinberg, G. K., Kondziolka, D., Wechsler, L. R., Lunsford, L. D., Coburn, M. L., Billigen, J. B., . . . Schwartz, N. E. (2016). Clinical Outcomes of Transplanted Modified Bone Marrow-Derived Mesenchymal Stem Cells in Stroke: A Phase 1/2a Study. *Stroke, 47*(7), 1817-1824. doi:10.1161/STROKEAHA.116.012995

Tao, K., Frisch, J., Rey-Rico, A., Venkatesan, J. K., Schmitt, G., Madry, H., . . . Cucchiarini, M. (2016). Co-overexpression of TGF-beta and SOX9 via rAAV gene transfer modulates the metabolic and chondrogenic activities of human bone marrow-derived mesenchymal stem cells. *Stem Cell Res Ther, 7*, 20. doi:10.1186/s13287-016-0280-9

Thomas, S. A., Coates, E., das Nair, R., Lincoln, N. B., Cooper, C., Palmer, R., . . . Drummond, A. E. (2016). Behavioural Activation Therapy for Depression after Stroke (BEADS): a study protocol for a feasibility randomised controlled pilot trial of a psychological intervention for post-stroke depression. *Pilot Feasibility Stud, 2*, 45. doi:10.1186/s40814-016-0072-0

Wang, Z., Ye, Z., Huang, G., Wang, N., Wang, E., & Guo, Q. (2016). Sevoflurane Post-conditioning Enhanced Hippocampal Neuron Resistance to Global Cerebral Ischemia Induced by Cardiac Arrest in Rats through PI3K/Akt Survival Pathway. *Front Cell Neurosci, 10*, 271. doi:10.3389/fncel.2016.00271

Yentrapalli, R., Azimzadeh, O., Sriharshan, A., Malinowsky, K., Merl, J., Wojcik, A., . . . Tapio, S. (2013). The PI3K/Akt/mTOR pathway is implicated in the premature senescence of primary human endothelial cells exposed to chronic radiation. *PLoS One, 8*(8), e70024. doi:10.1371/journal.pone.0070024

Yousefifard, M., Nasirinezhad, F., Shardi Manaheji, H., Janzadeh, A., Hosseini, M., & Keshavarz, M. (2016). Human bone marrow-derived and umbilical cord-derived mesenchymal stem cells for alleviating neuropathic pain in a spinal cord injury model. *Stem Cell Res Ther, 7*, 36. doi:10.1186/s13287-016-0295-2

Zhang, J., Yang, Y., Sun, H., & Xing, Y. (2014). Hemorrhagic transformation after cerebral infarction: current concepts and challenges. *Ann Transl Med, 2*(8), 81. doi:10.3978/j.issn.2305-5839.2014.08.08

Zhang, L., Zhang, S., Yao, J., Lowery, F. J., Zhang, Q., Huang, W. C., Yu, D. (2015). Microenvironment-induced PTEN loss by exosomal microRNA primes brain metastasis outgrowth. *Nature, 527*(7576), 100-104. doi:10.1038/nature15376

Zhu, W., Fan, Y., Frenzel, T., Gasmi, M., Bartus, R. T., Young, W. L., Chen, Y. (2008). Insulin growth factor-1 gene transfer enhances neurovascular remodeling and improves long-term stroke outcome in mice. *Stroke, 39*(4), 1254-1261. doi:10.1161/STROKEAHA.107.500801